UNIVERSITY OF OKLAHOMA

GRADUATE COLLEGE

EXPERT SYSTEM FOR EVALUATION OF NUTRIENT POLLUTION POTENTIAL IN GROUNDWATER FROM LAND APPLICATION OF MANURE

A Dissertation

SUBMITTED TO THE GRADUATE FACULTY

in partial fulfillment of the requirements for the

degree of

Doctor of Philosophy

By

ABU NOMAN M. AHSANUZZAMAN
Norman, Oklahoma
2004

Downloaded from SHAREOK. Persistent Handle URL: https://hdl.handle.net/11244/724

UMI Number: 3122308

INFORMATION TO USERS

The quality of this reproduction is dependent upon the quality of the copy submitted. Broken or indistinct print, colored or poor quality illustrations and photographs, print bleed-through, substandard margins, and improper alignment can adversely affect reproduction.

In the unlikely event that the author did not send a complete manuscript and there are missing pages, these will be noted. Also, if unauthorized copyright material had to be removed, a note will indicate the deletion.

UMI®

UMI Microform 3122308

Copyright 2004 by ProQuest Information and Learning Company.

All rights reserved. This microform edition is protected against unauthorized copying under Title 17, United States Code.

ProQuest Information and Learning Company
300 North Zeeb Road
P.O. Box 1346
Ann Arbor, MI 48106-1346

© Copyright by ABU NOMAN M. AHSANUZZAMAN 2004

All Rights Reserved.

EXPERT SYSTEM FOR EVALUATION OF NUTRIENT POLLUTION POTENTIAL IN GROUNDWATER FROM LAND APPLICATION OF MANURE

A DISSERTATION APPROVED FOR THE
SCHOOL OF CIVIL ENGINEERING
AND
ENVIRONMENTAL SCIENCE

By

Md. Musharraf Zuzzaman 05/05/04
Musharraf Zaman, Committee Chair

Keith A. Strevett, Co-Chair

Randall L. Kolar, Member

Robert Knox, Member

May Yuan, Member

Acknowledgement

I wish to express my profound appreciation to all of those who contributed to my dissertation. Dr. M. Zaman, chairman of my dissertation committee, was a great mentor who gave me valuable assistance and encouragement throughout the preparation of my dissertation. His optimistic vision in research inspired me on many occasions. Dr. K. Strevett, my co-advisor, provided me enormous support in preparing the dissertation prospectus and in developing the expert systems. I sincerely acknowledge him for his heartfelt support during my research. Dr. R. L. Kolar, member of my dissertation committee, provided unlimited help to me throughout my dissertation. I am extremely thankful to him for his valuable suggestions and guidance toward completion of my dissertation, and for supporting me no less than as my advisors. For their support, assistance and encouragement, I would like to acknowledge the remaining members of my dissertation committee, Dr. R. Knox, and Dr. M. Yuan. I am especially grateful to Dr. Knox for encouraging me to develop an expert system for the farmers and regulators instead of a complex numerical model. Most importantly, I would like to thank my companion for life, Nipa and my lovely little son, Raeed for the hardship and sacrifice they made throughout the journey for my dissertation. My parents, siblings, and my other family members deserve the deepest appreciation for constantly motivating me and for always keeping me in their prayers. Finally, I am thankful to the almighty Allah for his merciful support in all phases of my life.

Disclaimer

Neither the developers of the expert systems nor the University of Oklahoma assume any legal liability or responsibility for the accuracy, completeness, or usefulness of any information, product, or process disclosed in this dissertation.

Preface

In recent years, groundwater contamination from animal husbandries has become a growing concern for the regulatory agencies and farmers. The animal husbandries usually dispose off the manure produced in the facility to the adjacent land. This manure serves as a supplemental nutrient source for the crops, as it contains considerable amount of nitrogen and phosphorous. Inefficient application of manure could result in leaching of nutrients to the groundwater, and thus, become a potential health risk to the downgradient recipients. Recent studies show that the number of counties at risk of groundwater contamination from nutrients has increased due to the application of excessive manure than the potential uptake by plants. This is particularly significant for nitrogen, as the nitrification process very quickly converts the ammonium nitrogen in the manure into highly mobile nitrate. Currently, regulators and farmers are in need of a decision support tool that can evaluate the groundwater pollution potential from land application of manure. The evaluation would help them in developing an environmental-friendly management practice by optimizing the number and type of animals, selecting suitable crop(s) and by finding optimum land area for manure disposal at a given site.

This study presents a tool, in the form of an expert system, to evaluate the groundwater pollution potential from land application of manure. Expert systems are useful decision support tools, as they are simple to use, require minimum input data, limit the need for skilled individuals to run the simulation, and are comparatively cost-effective as compared to numerical modeling. The expert system presented herein could be used to optimize the management practices for an existing animal husbandry and to

aid in locating suitable sites for building new facilities. A window-based software for the expert system, named NPATH, is also developed. Effort has been given to make the software as user-friendly as possible so that people with limited skill with groundwater modeling can take advantage of the expert system. Several databases are also incorporated into the software to suggest default values for input parameters.

Two levels of analyses are included in the expert system. These are named simple expert system and advanced expert system. The simple expert system requires fewer input parameters, simulation time, and skill than the advanced expert system, while the latter uses advanced modeling techniques. The simple expert system consists of five modules: surface loading, sorption, vadose zone transport, saturated zone transport and final module. It evaluates the pollution potential in two steps. In the first step, rating values are evaluated for the selected modules. A set of expert system rules is assigned to evaluate the rating values. In the second step, the groundwater pollution potential is evaluated based on another set of rules. The groundwater pollution potential is rated in five levels: very low, low, medium, high, and very high. Chapter 1 presents detailed discussions on the simple expert system.

Chapter 2 is an effort toward improving the modeling technique used in the saturated zone transport module of the simple expert system. A series of three-dimensional analytical models for instantaneous point and finite sources is presented in this chapter. Analytical models are derived for a pollution source at the water table of semi-infinite and finite aquifers. Existing analytical models for instantaneous point sources consider injection of mass in an infinite domain i.e., in the middle of an infinitely thick aquifer, while the expert system requires a model that considers source at the water

table of a finite aquifer. The analytical models for instantaneous source are more important than the continuous source models, as the former could be used for transient mass input to the saturated zone. Superposition of the instantaneous point sources in time and space to represent a transient non-point source is also verified in this chapter.

Chapter 3 presents a set of regression models to characterize the breakthrough curve for drainage from the vadose zone to the groundwater. As the hydraulic characteristics of unsaturated soils are highly variable with time, numerical modeling would be most appropriate for estimating drainage through the vadose zone. However, a simple model would be useful for a preliminary level assessment. It is found that the existing empirical, semi-empirical, or analytical models estimate the infiltration rate at the soil surface instead of the breakthrough curve for drainage to the groundwater. The lag time between surface application and initial breakthrough at the groundwater table, and the breakthrough time for recession following cessation of surface application have been overlooked in the past. Moreover, existing models are often limited to constant and uniform initial soil water content profiles within the vadose zone, while in reality the water content varies with depth. The regression models developed herein are capable of estimating the lag and recession times, and are also applicable to handling a variable initial moisture content distribution in the soil profile.

Chapter 4 presents the advanced expert system. In the simple expert system, it is assumed that the surface loading module directly inputs the nutrient mass to the saturated zone transport module. To simplify the system, advection and equilibrium sorption with no dispersion are assumed in evaluation of solute transport through the vadose zone. This limitation is overcome in the advanced expert system by incorporating a numerical model

to evaluate the solute transport through the vadose zone. In the advanced expert system, all modules are sequentially interconnected from the source to the receptor. The surface loading module contributes nutrient mass to the vadose zone transport module, and the latter inputs mass to the saturated zone transport module. The pollution potential in the advanced expert system is evaluated at the final stage based on the predicted nutrient concentration at the receptor well and the possible health risk from exposure. Additional advancement in the advanced expert system is achieved by using the non-point source model for the saturated zone transport module instead of the point source model. The advanced expert system requires more input parameters, simulation time, and skilled personnel than the simple expert system.

In addition to the four chapters, six appendices are included in this study. Appendices A and B represent manure nutrient contents for different animals, and nutrient uptake rates for different crops, respectively. Appendix C presents the regression models for Theis well-function, which is used for assessing the effect of pumping at a downgradient receptor well. A criterion for determining the limiting source dimensions of the instantaneous point source model is presented in Appendix D. Appendix E discusses the results of a comparison between the Green-Ampt and Richards based models for estimating the distance traveled by a wetting front due to application of water at the soil surface. Appendix F contains information on availability of the software, NPATH.

Table of Contents

Acknowledgement iv
Disclaimer v
Preface vi
List of Figures xii
List of Tables xiii
Chapter 1: Simple Expert System 1
Abstract 1
1.1. Introduction 2
1.2. Structure of the Expert System 3
1.3. Surface Loading 4
1.4. Sorption 8
1.4.1 Nitrate Sorption 8
1.4.2 Phosphate Sorption 10
1.5. Vadose Zone Transport 12
1.5.1 Estimating the Distance Traveled by the Wetting Front 14
1.6. Saturated Zone Transport 23
1.7. Final Module 28
1.8. Case Studies 30
1.9. Sensitivity Analyses 37
1.10. Advantages and Limitations of the Simple Expert System 40
1.11. Conclusions and Recommendations 41
Reference 43
Chapter 2: Analytical Models for Instantaneous Point and Finite Sources 46
Abstract 46
2.1. Introduction 46
2.2. Advection-Dispersion Equation for Solute Transport 49
2.3. Analytical Model for Instantaneous Point Source in an Infinite Domain 50
2.4. Analytical Model for Instantaneous Finite Source in an Infinite Domain 51
2.5. Superposition of Point Sources to Represent Non-Point Sources 53
2.6. Transient Concentration Sources 54
2.7. Analytical Model for Instantaneous Point Source in a Semi-Infinite Domain . 57
2.8. Instantaneous Point and Finite Source Models for Finite Aquifer Thickness .. 59
2.8.1 Numerical Model Setup 61
2.8.2 Adjustment of grid spacing in the Numerical Model 63
2.8.3 Verification of Analytical Models for Finite Aquifer 67
2.9. Conclusions 69
References 71
Chapter 3: Regression Model for Estimating Flow Through the Vadose Zone 73
Abstract 73
3.1. Introduction 74
3.2. Materials and Methods 76
3.2.1 Flow through Unsaturated Soil 76
3.2.2 Numerical Model 79
3.2.3 Conceptual Model for Flow through the Vadose Zone 80

3.2.4 Model Simulation 81
3.3. Results and Discussion 83
3.3.1 Development of the Regression Equations 83
3.3.2 Validation of the Regression Models 93
3.3.3 Assumptions and Limitations of the Regression Model 97
3.4. Application of the Regression Model to Variable Surface Inflow Rates 98
3.5. Conclusions 101
References 103
Chapter 4: Advanced Expert System 105
Abstract 105
4.1. Introduction 105
4.3. General Information Module 107
4.4. Sorption 108
4.5. Surface Loading 109
4.6. Vadose Zone Transport 109
4.7. Saturated Zone Transport 111
4.8. Health Effect 113
4.9. Decision Module 115
4.10. Case Study 116
4.11. Advantages and Limitations of the Advanced Expert System 119
4.12. Concluding Remarks 119
References 121
APPENDICES 122
Appendix A: Manure Nutrient Content 123
Appendix B: Nutrient Application Rates for Crops, Hays and Forages 124
Appendix C: Well Function 128
Appendix D: Limiting Source Dimensions for Analytical Point Source Model 130
Appendix E: Performance of the Green-Ampt Model in Estimating Flow through the Vadose Zone 134
Abstract 134
E.1. Introduction 134
E.2. Materials and Methods 135
E.3. Results and Discussion 138
E.4. Conclusion and Recommendation 139
References 142
Appendix F: Software Availability 143

List of Figures

Figure 1.1. Structure of the simple expert system 5
Figure 1.2. Cumulative rainfall distribution. 17
Figure 1.3. HYDRUS output for clay loam for different rainfall conditions. 18
Figure 1.4. HYDRUS output for sand for different rainfall conditions. 18
Figure 1.5. Distance traveled by the wetting-front in a year for different USDA soils. 19
Figure 1.6. Distance traveled by the wetting-front in 90 days for different USDA soils. 21
Figure 1.7. Potentiometric surface map for RS1 on July 1998. 34
Figure 1.8. Nitrate concentration at MW4 and MW9 of RS1 36
Figure 1.9. Sensitivity of the vadose zone transport module rating for different water table depths, rainfall amounts, and soil types. 39
Figure 1.10. Sensitivity of the saturated zone transport module ratings for the swine CAFO (original conditions). 40
Figure 2.1. Comparison between the instantaneous finite source (FS) model and superposition of a point source (PS) model. 55
Figure 2.2. Comparison between the continuous source models and superposition in time of an instantaneous point source model. 57
Figure 2.3. Comparison between the instantaneous point source (PS) and finite source (FS) models for a semi-infinite domain. 59
Figure 2.4. Comparison between the numerical and analytical models for uniform grid spacing. 64
Figure 2.5. Maximum concentration ratio (CR) along the direction of flow 66
Figure 2.6. Comparison between the selected numerical (GC1) and analytical models. . 67
Figure 2.7. Verification of analytical model for finite aquifer thickness 69
Figure 3.1. Conceptual model for flow through the vadose zone. 80
Figure 3.2. Initial conditions used in dataset-1 82
Figure 3.3. Scatter plot and linear regression model for Phase-1. 85
Figure 3.4. Logarithmic plot and regression model for Phase-1 86
Figure 3.5. Logarithmic plot and regression model for Phase-2 87
Figure 3.6. Recession curve for Phase-4 and trend line for Q_{10}. 89
Figure 3.7. Recession curve for Phase-4 and trend line for Q_{30}. 89
Figure 3.8. Regression model with all data for Phase-4. 91
Figure 3.9. Regression model for soil with high Ks (Phase-4). 91
Figure 3.10. Regression model for soil with low Ks (Phase-4) 93
Figure 3.11. Validation of the regression model for Phase-1. 95
Figure 3.12. Validation of the regression model for Phase-2. 95
Figure 3.13. Variable surface application rate used to demonstrate the application of the regression models 99
Figure 4.1. Structure of the advanced expert system 108
Figure C.1. Regression equation of Theis well function for $1e\text{-}8 < u \leq 0.2$ 128
Figure C.2. Regression equation of Theis well function for $0.2 < u < 1$ 128
Figure C.3. Regression equation of Theis well function for $1 \leq u \leq 9$. 129
Figure E.1. Piston-type wetting-front for GA model 136

List of Tables

Table 1.1. RF as a function of pH and nitrate concentrations..... 9
Table 1.2. RF as a function of pH and nitrate concentrations used in the expert system. 10
Table 1.3. Values for phosphate sorption. 11
Table 1.4. Average suction potentials and Van Genuchten parameters for each soil class. 16
Table 1.5. Rules for evaluating groundwater pollution potential. 28
Table 1.6. Recommendations for the groundwater pollution potential levels. 30
Table 1.7. Expert system input for the two case studies. 31
Table 1.8. Pollution potential from the Expert System for the two case studies. 33
Table 2.1. Non-uniform grid configurations. 66
Table 2.2. Statistical evaluations of the concentration ratio. 66
Table 3.1. Unsaturated soil hydraulic properties for different USDA soil classes. 79
Table 3.2. Datasets used in simulating HYDRUS for developing the regression model. 82
Table 3.3. Regression model for Phase-1 86
Table 3.4. Regression model for Phase-2 87
Table 3.5. Datasets used in simulating HYDRUS for validating the regression model ... 94
Table 3.6. Statistics for validation of the regression model for Phase-4 96
Table 3.7. Hydraulic properties of the soils used for further validation. 96
Table 3.8. Comparison between the regression models and HYDRUS outputs 97
Table 3.9. Application of the regression models. 101
Table 4.1. Input parameters for RS1 for compiling the advanced expert system. 117
Table A.1. Nitrogen and phosphorus content in manure for different animals. 123
Table B.1. Nutrient application rates for common crops 126
Table B.2. Nitrogen and phosphorus application rates for common hays and forages .. 127
Table E.1. Unsaturated soil hydraulic parameters of clay loam and sand 140
Table E.2. Comparison between GA model and HYDRUS for sand 140
Table E.3. Comparison between GA model and HYDRUS for clay loam 141

Chapter 1: Simple Expert System

Abstract

An expert system for the evaluation of groundwater pollution potential due to leaching of nutrients from land application of manure is developed in this study. The expert system consists of five modules: surface loading, sorption, vadose zone transport, saturated zone transport and final module. The expert system evaluates the pollution potential in two steps. In the first step, rating values are evaluated for the selected modules. A set of expert system rules is assigned to evaluate the rating value for each selected module. In the second step, the pollution potential is evaluated by calculating the weighted average rating of the selected modules. Two case studies are presented to validate the expert system. The advantages of the expert system include its user-friendliness, requirement of easily-available input data, and faster evaluation time. Also, the expert system allows individuals with minimum skills in related fields to evaluate the pollution potential. The expert system is recommended to farmers for improving their management practices. Regulatory agencies can also use the expert system to identify the most vulnerable existing sites, and to find suitable locations for building new facilities.

1.1. Introduction

The waste generated from a Concentrated Animal Feeding Operation (CAFO), often called manure, is commonly used as supplemental nutrients (e.g., nitrogen and phosphorus) for plants and crops. The manure from most of the CAFOs, except swine, is usually applied to cultivated land without any treatment. For swine CAFOs, the manure is stabilized in lagoon(s) prior to land application. Even after stabilization, lagoon effluent can contain high concentrations of nutrients and fecal bacteria (e.g., fecal coliforms and fecal streptococci) (Barker, 1996). Inefficient application of this waste could result in leaching of nutrients to groundwater and could become a potential health risk to the downgradient users. Leaching of fecal bacteria through irrigated land from manure application is not likely, as colloidal fecal bacteria would be restrained by filtration (Bitton et al., 1976). Moreover, heat from sunlight and low moisture content during dry seasons would adversely affect the survival of bacteria.

Kellogg and Lander (1999) reported that potential of groundwater pollution by nutrients due to land application of manure has increased over the years. In 1992, 114 counties in the United States, as opposed to 28 counties in 1949, were at high risk of groundwater pollution by nutrients (Kellogg and Lander, 1999). Thus, it has become a growing concern for regulatory agencies and the existing CAFO owners to assess the groundwater pollution potential from land application of manure. Currently, there is need for a tool that can evaluate groundwater pollution potential from land application of manure. So far, effort has been given to develop expert systems for evaluating groundwater contamination from pesticide leaching (Crowe and Mutch, 1992, 1994; Arora and McTernan, 1994). But none of those expert systems considered manure

application. Although the USEPA (1997) developed a methodology to evaluate overall environmental risks from swine CAFOs, it does not address land application and subsequent groundwater pollution potential.

Here the study focus is on developing a simple expert system that can evaluate the groundwater pollution potential at a downgradient well from land application of manure. By naming it 'simple', it is emphasized that the expert system developed in this study is simple to use and requires easily-available inputs. Expert systems have some advantages over numerical models: they are simple to use, do not require highly skilled personnel to run, are relatively cost effective and require less data. The expert system developed herein is designed to aid farmers in developing operational practices for land application of manure and in selecting sites suitable for building new CAFOs. The proposed expert system would also be useful as a preliminary assessment tool for regulatory agencies in identifying the most vulnerable sites.

1.2. Structure of the Expert System

The expert system considers manure as the source of nutrients and a downgradient well as the receptor. The exposure pathway for nutrients is from the soil surface through the vadose and saturated zones to the receptor well. Based on the nutrient transport pathway, three modules are included in the expert system. These are surface loading, vadose zone transport, and saturated zone transport modules. The surface loading module evaluates the impact from a nutrient source. The vadose and saturated zone transport modules address the impact of nutrient transport from the source to the receptor. Two additional modules, named sorption and final modules, are included in the expert system.

The sorption module addresses retardation of nutrient transport due to chemical adsorption and the final module evaluates the overall pollution potential for the site.

First, a rating value between 1 and 5 (5 being the most critical) is evaluated for the surface loading, vadose zone transport, and saturated zone transport modules. Rating values are assessed based on a set of rules suggested by a panel of experts in the field of hydrogeology and environmental engineering. Figure 1.1 shows the structure of the simple expert system. The surface loading module evaluates a rating value based on the nutrient content in the manure and crop uptake. It passes the excess nutrient mass to the saturated zone, which evaluates the rating by applying analytical solute transport models. In order to avoid using a complex solute transport model, only the flow parameters are used in evaluating the rating value for the vadose zone transport module. To this end, no connection between the vadose zone transport and surface loading modules is shown. The sorption module approximates the retardation factor based on user input and passes that to the vadose and saturated zone transport modules. No rating value is assigned to the sorption module. The final module evaluates the groundwater pollution potential from individual rating values of the surface loading, vadose zone transport, and saturated zone transport modules. The weighted average rating (WAR) is also calculated from the rating scores of individual modules and the relative weights assigned to respective modules. A detail discussion of each module is presented in the following sections.

1.3. Surface Loading

The surface-loading module evaluates the impact from the nutrient source. In addition to assigning a rating value, the surface-loading module passes the excess nutrient

mass following crop uptake to the saturated zone module. The rating value is assigned by comparing the effective nutrient mass from manure and fertilizer to the potential nutrient uptake rates by the harvested crop(s).

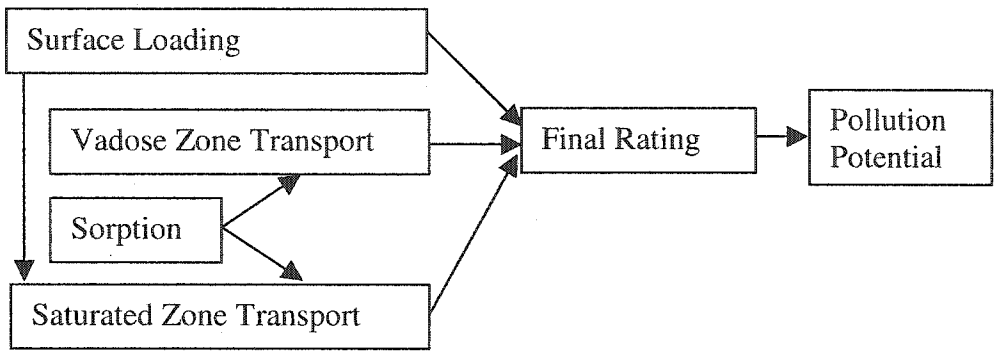


Figure 1.1. Structure of the simple expert system

The surface loading module first calculates the total recoverable waste (TRW) generated in the animal husbandry from Equation 1.1.

$$\text{TRW (tons)} = \sum_{i=1}^{at} (M_m \times R_f \times N_a / C_{au}) \qquad (1.1)$$

where, *at* is the number of animal types, M_m is the mass of manure produced per animal unit (tons/AU), R_f is the manure recovery factor for each animal type (unitless), N_a is the number of animals in each type, and C_{au} is the factor used to convert the number of animals to animal unit (animals/AU).

The database presented by Lander et al. (1998) is used to obtain the manure produced (M_m), manure recovery factor (R_f), and conversion factor (C_{au}) for each selected animal type (see Table A.1 in Appendix A). M_m is the mass of manure produced 'as excreted' by an animal, R_f is the factor used to obtain the recoverable manure from that excreted. It should be noted that the term 'animal unit' (AU) is commonly used to

represent all animal types in one common unit. After estimating the TRW value, the nutrient concentration in the manure (N_{man}) is calculated from Equation 1.2.

$$N_{man}\ (\text{lbs/ton}) = \sum_{i=1}^{n} \{(M_m \times R_f \times N_a / C_{au}) \times N_{cf} / TRW\} \qquad (1.2)$$

where, N_{cf} is the manure nutrient conversion factor (lbs/ton), which is the mass of each nutrient available in the recoverable manure.

Lander et al. (1998) present the N_{cf} value for both nitrogen and phosphorus (see Table A.1 in Appendix A). It should be noted that the database by Lander et al. (1998) presents the nutrient content after losses, which in turn could be considered as the nutrient available for plant uptake. Total nutrient available per acre land (N_{app}) in a cultivation season from manure, fertilizer, and soil (as background) is calculated from Equation 1.3.

$$N_{app}\ (\text{lbs/acre}) = N_{man} \times L_m + N_{fer} + N_{soil} \times 5.3 \qquad (1.3)$$

where, L_m is the mass of manure applied per acre land (tons/acre), N_{fer} is the nutrient from fertilizer (lbs/acre), and N_{soil} is the background concentration of the nutrient in the soil (mg/kg), and 5.3 is the factor used for converting the unit from mg per kg of soil to pounds per acre of land with the assumption that the root zone depth is 18 inches and the bulk density of soil is 1.3 gm/cc.

Potential crop nutrient uptake is obtained from commonly used nutrient application rates in the United States. Lander and Moffitt (1996) present the maximum, average, and minimum nutrient application rates for thirty-six crops (see Table B.1 in Appendix B). Nutrient application rates for hays and forages are obtained from USDA's National Agricultural Statistic Service (USDA-NASS, 2000) and from different USDA extension services (see Table B.2 in Appendix B). It should be noted that for crops with

no reported phosphorus application rates, approximate values are calculated by dividing the respective nitrogen application rates by 7.2, which is the stochiometric mass ratio of nitrogen and phosphorus in plant biomass (Nultsch, 1971). In addition to the minimum, average, and maximum application rates, an additional application rate, named 'critical application rate' is used in the expert system. The critical application rate (CrN_{cp}) is defined as the nutrient application required, in addition to the maximum application rate ($MaxN_{cp}$), to elevate the nutrient concentration of the aquifer to the threshold limit (C_{th}), which is 10 mg/L for nitrate and is 5 mg/L for phosphate (USEPA, 1999). Equation 1.4 is used for calculating the critical nutrient application rates.

$$CrN_{cp}\ (\text{lbs/acre}) = MaxN_{cp}(\text{lbs/acre}) + C_{th}\ (\text{mg/L}) \times n_p \times H_{aq}\ (\text{ft}) \times 2.72(\text{lbs·L/mg/acre/ft}) \quad (1.4)$$

where, H_{aq} is the aquifer thickness in ft, and n_p is the porosity.

The rating value for the surface loading module is assigned based on the following five rules.

Rule #1: If the amount of nutrient applied is less than the minimum nutrient application rate ($MinN_{cp}$), then the rating is 1.

If $N_{app} \leq MinN_{cp}$ Then Rating = 1

Rule #2: If the amount of nutrient applied is between the minimum and average nutrient application rates ($AvgN_{cp}$), then the rating is between 1 and 2.

$$\text{If } MinN_{cp} < N_{app} \leq AvgN_{cp} \text{ Then Rating} = \frac{N_{app} - MinN_{cp}}{AvgN_{cp} - MinN_{cp}} + 1$$

Rule #3: If the amount of nutrient applied is between the average and maximum nutrient application rates, then the rating is between 2 and 3.

$$\text{If } AvgN_{cp} < N_{app} \leq MaxN_{cp} \text{ Then Rating} = \frac{N_{app} - AvgN_{cp}}{MaxN_{cp} - AvgN_{cp}} + 2$$

Rule #4: If the amount of nutrient applied is between the maximum and critical nutrient application rates, then the rating is between 3 and 5.

$$\text{If } MaxN_{cp} < N_{app} \leq CrN_{cp} \text{ Then Rating} = \frac{N_{app} - MaxN_{cp}}{CrN_{cp} - MaxN_{cp}} \times 2 + 3$$

Rule #5: If the amount of nutrient applied is more than the critical nutrient application rates, then the maximum rating is assigned.

$$\text{If } N_{app} > CrN_{cp} \text{ Then Rating} = 5$$

1.4. Sorption

The sorption module estimates the retardation factor (RF) for the nutrient of interest (i.e., either nitrate or phosphate) and passes that value to the vadose zone transport and saturated zone transport modules. Unlike the other modules, the sorption module does not provide any rating for sorption. An extensive literature survey was conducted to find model(s) for the RF of each nutrient. Unfortunately, no model as a function of the factors affecting sorption was found in the literature. Based on the information available in the literature, the expert system sets up rules to approximate the RF value of each nutrient. It should be noted that the RF value approximated by the expert system is the default value for evaluation. The user has the option to change the default RF value, if necessary.

1.4.1 Nitrate Sorption

Factors affecting nitrate sorption are pH, AEC (Anion Exchange Capacity) of soil and concentration and ionic strength of the adsorbate chemical (Bellini et al., 1996;

Qafoku et al., 2000a). After studying nitrate and chloride leaching through a soil column, Bellini et al. (1996) concluded that retardation of anions is a function of AEC of the soil. To further validate the study done by Bellini et al. (1996), which was limited to analysis on only one soil, Qafoku et al. (2000a) conducted nitrate and chloride leaching for 16 different soils from different regions in the world. In addition to the column leaching tests, soil minerals were also studied for all those soils. Qafoku et al. (2000a) concluded that nitrate leaching is significantly influenced by pH and concentration of the leaching solution. Some of the results from Qafoku et al. (2000a) for nitrate retardation factors (RF) at different pH values are presented in Table 1.1. Qafoku et al. (2000a) also proposed a correlation between AEC and RF value for any soils at their native pH and for nitrate concentration in water of 70 mg/L as N (Equation 1.5).

$$RF = 3.267 \times AEC + 0.547 \quad (1.5)$$

Table 1.1. RF as a function of pH and nitrate concentrations.

pH	Nitrate concentrations (mg/L)$^{\Psi}$			
	70	140	280	420
4.21	3.86	2.96	1.87	1.58
4.45	3.19	2.39	1.69	1.32
5.47	2.24	1.81	1.64	1.55
6.47	1.92	1.32	1.32	1.49

Source: Qafoku et al. (2000a);
$^{\Psi}$For, AEC = 1.15 cmol/kg, bulk density = 1.13 gm/cc, porosity = 0.4

Based on the data presented in Table 1.1 and Equation 1.5, a set of rules has been proposed for estimating the RF value for nitrate. Table 1.2 is used to estimate the RF value if both soil pH and nitrate concentration in the groundwater are known. Table 1.2 is derived from Table 1.1 by taking a conservative approach, i.e., considering less retardation. If either the soil pH or the nitrate concentration in water is not known, the RF

value is assumed to be one, which is commonly used for nitrate transport. Equation 1.5 is used only if AEC of soil is known. If all input parameters are known, the average of the RF values obtained from Table 1.2 and Equation 1.5 is used. It should be noted that the expert system sets the lower limit for the RF value from Equation 1.5 to one.

Table 1.2. RF as a function of pH and nitrate concentrations used in the expert system.

pH	RF at different nitrate concentrations (mg/L)				
	< 70	70 - 140	140 - 280	280 - 420	> 420
< 4.2	3.86	2.96	1.87	1.58	1
4.2 - 4.5	3.19	2.39	1.69	1.32	1
4.5 - 5.5	2.24	1.81	1.64	1.55	1
5.5 - 6.5	1.92	1.32	1.32	1.49	1
> 6.5	1	1	1	1	1

1.4.2 Phosphate Sorption

Factors affecting phosphate sorption are soil pH (Naidu et al., 1990), aluminum and iron oxides in the soil (Parfitt, 1978; Borggaard, 1983; Borggaard et al., 1990; Van der Zee and Van Riemsdijk, 1986), calcium content (Naidu et al., 1990) and organic matter in the soil (Borggaard et al., 1990). Although a number of studies have been conducted on phosphorous sorption, an equation for estimating the RF value for phosphate transport was not available. The primary objective of previous studies on phosphorus sorption was to develop methodology for estimating phosphorous availability for crop growth rather than transport through the subsurface. Bottani et al. (1993) studied phosphorous sorption capacity of three different soils, named C2, R3 and LP. Table 1.3 shows the textural classification and adsorption parameters for the three soils. A Langmuir type model was considered as the adsorption isotherm for the soils (Equation 1.6).

$$C_s = \frac{K_l b C}{1 + K_l C} \tag{1.6}$$

where, C_s is the mass of the sorbed chemical per unit mass of the soil (mg/kg), C is the dissolved concentration of the chemical (mg/L), K_l is Langmuir constant (L/mg), and b is mass of phosphorous required to saturate a unit mass of soil i.e., the maximum sorption capacity (mg/kg). The retardation factor (RF) is defined as,

$$RF = 1 + \frac{\rho}{n}\frac{\partial C_s}{\partial C} \tag{1.7}$$

where, ρ is the bulk density of soil (kg/L), and n is the porosity.

From Equation 1.6,

$$\frac{\partial C_s}{\partial C} = \frac{K_l b}{(1 + K_l C)^2} \tag{1.8}$$

Therefore, the retardation factor (RF) for the Langmuir model is,

$$RF = 1 + \frac{\rho}{n}\frac{bK_l}{(1 + K_l C)^2} \tag{1.9}$$

Table 1.3. Values for phosphate sorption.

Soil	C2	R3	LP
Clay (%)*	40.6	17	18
Silt (%)*	40.2	60.5	61
Sand (%)*	19.2	22.5	21
pH (1:1)*	5.9	7.4	5.8
Organic mater (%)*	5.1	6.2	3.41
TKN (%)*	0.23	0.34	0.21
Extractable Phosphate (mg/L)*	23	11.2	16.4
Ca (mmol/kg)*	118	107	41
K_l (L/mg)*	0.102	1.271	1.259
b (mg/kg)*	274.9	261.4	258.3
Specific Surface Area (m^2/gm)*	31.73	28.74	10.55
C (mg/L) †	5 10 50	5 10 50	5 10 50
RF†	41 22 3.4	21 7 1.3	21 7 1.3

* Bottani et al. (1993); †Calculated herein

The expert system uses the Langmuir model for estimating phosphate sorption. Input values of the parameters in Equation 1.9 are selected by taking a conservative approach, i.e., to estimate a lower value of RF. The conservative values of K_l and b from Table 1.3 are 1.27 L/mg and 258 mg/kg, respectively. ρ and n are assumed to be 1.3 gm/cc and 0.4, respectively. To get the RF value for phosphate, the users need to input the value for C in mg/L. The user may input C as the average phosphate concentration in the groundwater from the source to the sink. It should be noted that it is conservative to assume a higher value for C, as RF is inversely proportional to C (see Equation 1.9) (and the lower the RF, the more mobile the contaminant). The expert system sets the upper limit for the RF value to 20, which is obtained from Equation 1.9 for 5 mg/L of phosphate. The phosphate concentration of 5 mg/L was chosen because it is the maximum allowable concentration in drinking water (USEPA, 1999).

1.5. Vadose Zone Transport

The vadose zone transport module evaluates the impact of nutrient (nitrogen or phosphorus) transport through the vadose zone. To simplify the system, advection and equilibrium sorption with no dispersion are assumed in evaluating the impact of nutrient transport. The expert system approximates the distance traveled by the nutrient within a given time and compares that with the water table depth to assign the rating for this module. The input parameters selected for the vadose zone transport module are soil type (USDA), water table depth (D_{wt}), rainfall, and retardation factor. With the input of soil type and rainfall data, the expert system estimates the distance traveled by the wetting front from regression equations, derived in this study. The distance traveled by the

nutrient is equal to the distance traveled by the wetting front divided by the retardation factor (RF). The RF value for each nutrient is obtained from the sorption module. It should be noted that the expert system does not consider cracking (or expansive) soils or the effects of fingering. The effects of cracking and fingering could be ignored in land applications, if nutrients are applied following plowing and when the soil is wet.

A rating for the vadose zone transport module is assigned by calculating the distance traveled by the nutrient in 90 (D_{90}) and 365 (D_{365}) days. These durations are chosen because nutrient application usually follows a cycle of either a minimum of one cultivation season (90 days) or a maximum of one year (365 days). The rating for the vadose zone module is assigned based on the following four rules.

Rule #1: If the nutrient reaches the water table in 90 days, then the maximum rating (5) is applied.

$$\text{If } D_{90} \geq D_{wt} \text{ Then Rating} = 5$$

Rule #2: If the nutrient reaches the water table in 365 days, then the rating is 4.

$$\text{If } D_{365} = D_{wt} \text{ Then Rating} = 4$$

Rule #3: Between 90 and 365 days, then the rating varies linearly between 4 and 5.

$$\text{If } D_{90} < D_{wt} \text{ and } D_{wt} \leq D_{365} \text{ Then Rating} = 4 + \frac{D_{365} - D_{wt}}{D_{365} - D_{90}}$$

Rule #4: If the nutrient reaches the water table in more than 365 days, then the rating varies between 1 and 4 according to the following equation.

$$\text{If } D_{wt} > D_{365} \text{ Then Rating} = 1 + 3 \times \frac{D_{365}}{D_{wt}}$$

1.5.1 Estimating the Distance Traveled by the Wetting Front

The HYDRUS model (Simunek et al., 1998) was used to develop the regression equations for estimating the distance traveled by the wetting front. HYDRUS is a Galerkin linear finite element model, developed by US Salinity Laboratory, for simulating water, heat and solute transport in one-dimensional variably saturated media. One-dimensional flow through vadose zone is considered based on the assumption that manure is applied uniformly on a flat land and thus lateral dispersion should be minimal due to low concentration gradients in that direction. HYDRUS solves the Richard's equation for variably saturated water flow and advection-dispersion equations for heat and solute transport. Richard's equation of soil moisture flow through the vadose zone is based on the Darcy's law combined with the equation of continuity. Equation 1.10 presents the Richard's equation for flow in vertical direction.

$$\frac{\partial \theta}{\partial t} = \frac{\partial}{\partial z}\left(K(\theta)\frac{\partial h(\theta)}{\partial z}\right) - \frac{\partial (K(\theta))}{\partial z} \qquad (1.10)$$

where, θ is volumetric water content and $K(\theta)$ and $h(\theta)$ are unsaturated hydraulic conductivity and suction potential as function of θ, respectively.

The factors affecting water flow through the vadose zone are soil hydraulic properties, initial soil moisture content or matric potential, and rainfall. Van Genuchten's (1980) model is used to characterize the unsaturated soil hydraulic properties. This model has five parameters: saturated hydraulic conductivity (K_s), saturated volumetric moisture content (θ_s), residual moisture content (θ_r), and two constants (α and n). Since soil testing for Van Genuchten's parameters is highly sophisticated and cannot be conducted in an ordinary soil laboratory, it would be difficult for the users to input such parameters in the expert system. Alternatively, published values of the hydraulic parameters can be

obtained from Carsel and Parrish (1988) with the input of USDA soil type (see Table 1.4). The USDA soil classification is relatively simple and can be conducted in any soil laboratory. Therefore, USDA soil types are considered as a variable input in the HYDRUS simulation.

Initial soil matric potential (h_0) is assumed to be constant throughout the soil profile. The h_0 value for each USDA soil type is estimated from the annual average field values of soil suction potentials. The field values are obtained from the Oklahoma Mesonet, which has 110 stations throughout Oklahoma (Mesonet, 2004). Soil suction potentials at 5, 25, 60, and 75 cm depths are measured at each Mesonet station. The USDA soil classification for each station and a year-long data (1997-98) at 5 cm depth (chosen based on data availability) are used to calculate the average suction potential for each USDA soil type. For the soil types missing in the Oklahoma Mesonet stations (e.g., clay, sandy clay loam, and silt loam), the average suction potentials are obtained from the soils having close K_s values and neighbors in the USDA soil classification triangle. Table 1.4 shows the initial h_0 value for each USDA soil type and the corresponding moisture content (θ_i), as obtained from applying the Van Genuchten model.

Rainfall is considered as the top boundary for HYDRUS compilation, while free drainage is considered for the bottom end of the soil profile. Since actual (real time) daily rainfall distribution is highly variable, it would be extremely difficult to generalize the distribution. Moreover, inputting the actual daily rainfall for an entire year would be tedious for the users and thus, defy the objective of the simple expert system. To simplify the input of rainfall, the distance traveled by the wetting-front for three different rainfall conditions were compared. These are actual daily, monthly average (per day), and annual

average (per day) rainfalls. Figure 1.2 shows the cumulative rainfall distribution for the three conditions. HYDRUS was compiled for all rainfall conditions considering two different soils: (i) sand with very high hydraulic conductivity (713 cm/d), and (ii) clay loam with very low hydraulic conductivity (6.24 cm/d). Hydraulic parameters for both sand and clay loam are obtained from Carsel and Parrish (1988) (see Table 1.4). Figures 1.3 and 1.4 show the distance traveled by the wetting-front for clay loam and sandy soils, respectively. Between the two averages, the monthly average rainfall is the best, as it shows less than 1 percent error after one year when compared with the same for the actual daily rainfall distribution. The annual average rainfall shows less than 2 percent error after one year for both soils. Although the monthly average rainfall distribution shows better result than the annual average rainfall, the latter is used in the expert system for simplicity.

Table 1.4. Average suction potentials and Van Genuchten parameters for each soil class.

Soil Type	θ_r [Ψ]	θ_s [Ψ]	n [Ψ]	α [Ψ] (cm^{-1})	K_s [Ψ] (cm/d)	h_0 (cm)	θ_i
Clay	0.068	0.38	1.09	0.008	4.8	6720	0.286
Clay Loam	0.095	0.41	1.31	0.019	6.24	6720	0.165
Loam	0.078	0.43	1.56	0.036	25	2950	0.104
Loamy Sand	0.057	0.41	2.28	0.124	350	2300	0.057
Sand	0.045	0.43	2.68	0.145	713	245	0.046
Sandy Clay	0.1	0.38	1.23	0.027	2.88	1220	0.225
Sandy Clay Loam	0.1	0.39	1.48	0.059	31.4	1220	0.137
Sandy Loam	0.065	0.41	1.89	0.075	106	1460	0.070
Silt	0.034	0.46	1.37	0.016	6.0	2500	0.143
Silt Loam	0.067	0.45	1.41	0.02	10.8	2130	0.149
Silty Clay	0.07	0.36	1.09	0.005	0.48	714	0.324
Silty Clay Loam	0.089	0.43	1.23	0.01	1.68	2500	0.251

[Ψ]Carsel and Parrish (1988)

To develop the regression equations for the distance traveled by the wetting front in a year, HYDRUS was compiled for hydraulic properties of each USDA soil type and

annual average rainfalls from 15 to 60 inches in 5-inch increments. Similarly, HYDRUS was compiled for 90-day rainfall totals from 5 to 17 inches with a 3-inch increment to develop regression equations for estimating distance traveled by the wetting-front in 90 days. The outputs generated from HYDRUS and corresponding regression equations are listed in Figures 1.5 and 1.6. It should be noted that for silty clay type soil, the HYDRUS simulation could not be converged for large rainfall values due to very low K_s value of the soil. The regression equations for silty clay loam are used to represent silty clay, as these soils have the closest hydraulic conductivity values (see Table 1.4) and are neighbors in the USDA soil classification triangle. This assumption would estimate faster solute transport for silty clay soils than the actual value. However, cracks in the soil surface, which are common for soils with low hydraulic conductivity, would somewhat counteract this overestimation.

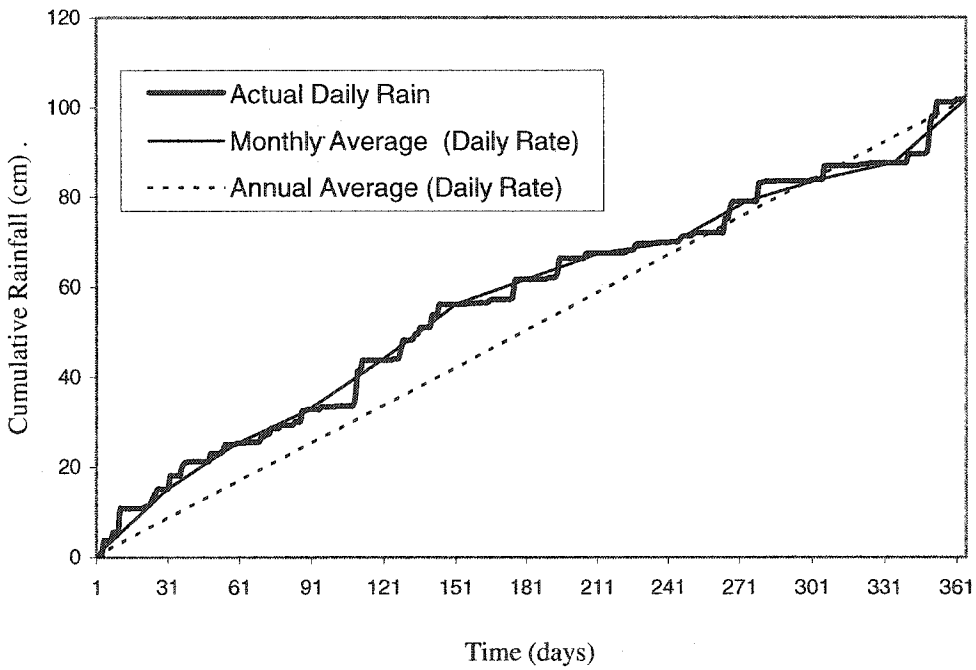


Figure 1.2. Cumulative rainfall distribution.

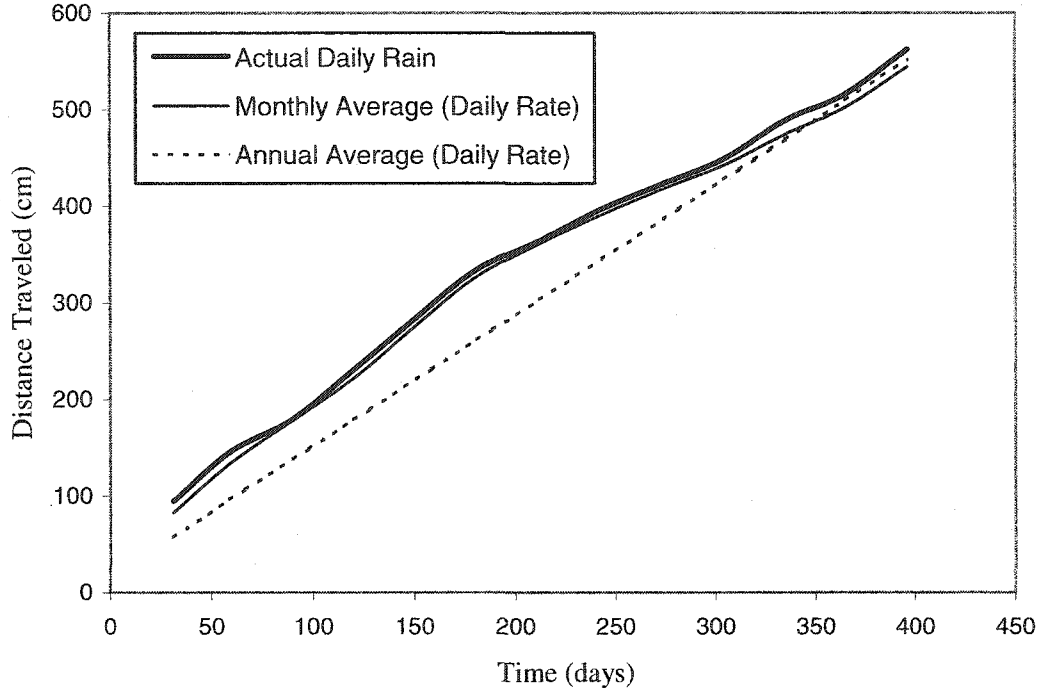


Figure 1.3. HYDRUS output for clay loam for different rainfall conditions.

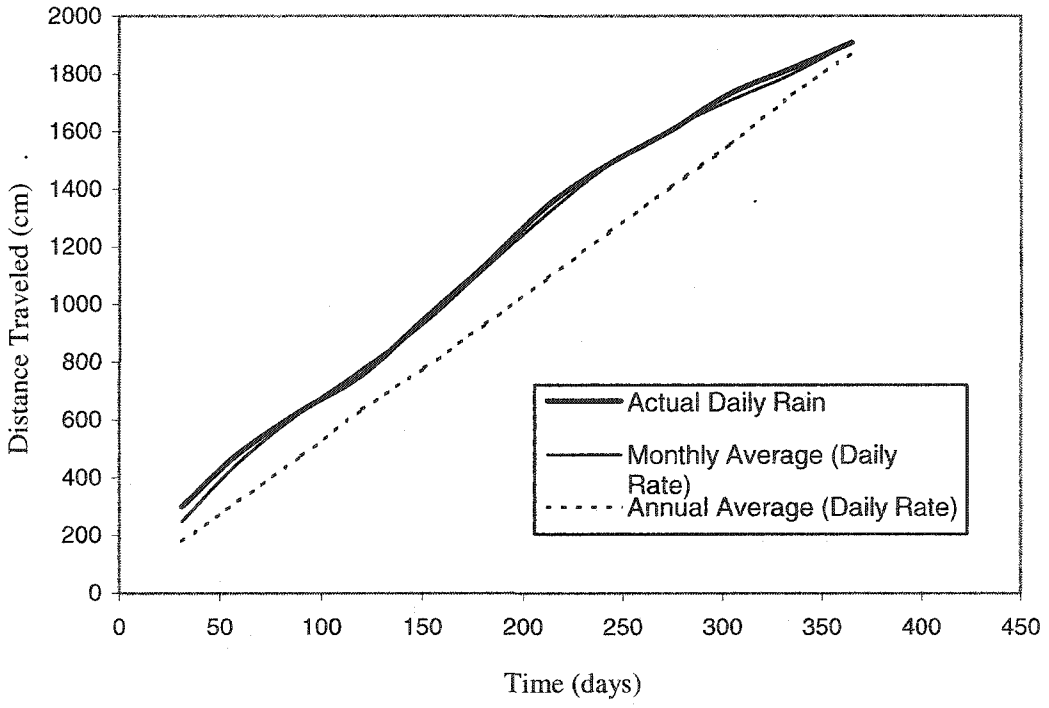


Figure 1.4. HYDRUS output for sand for different rainfall conditions.

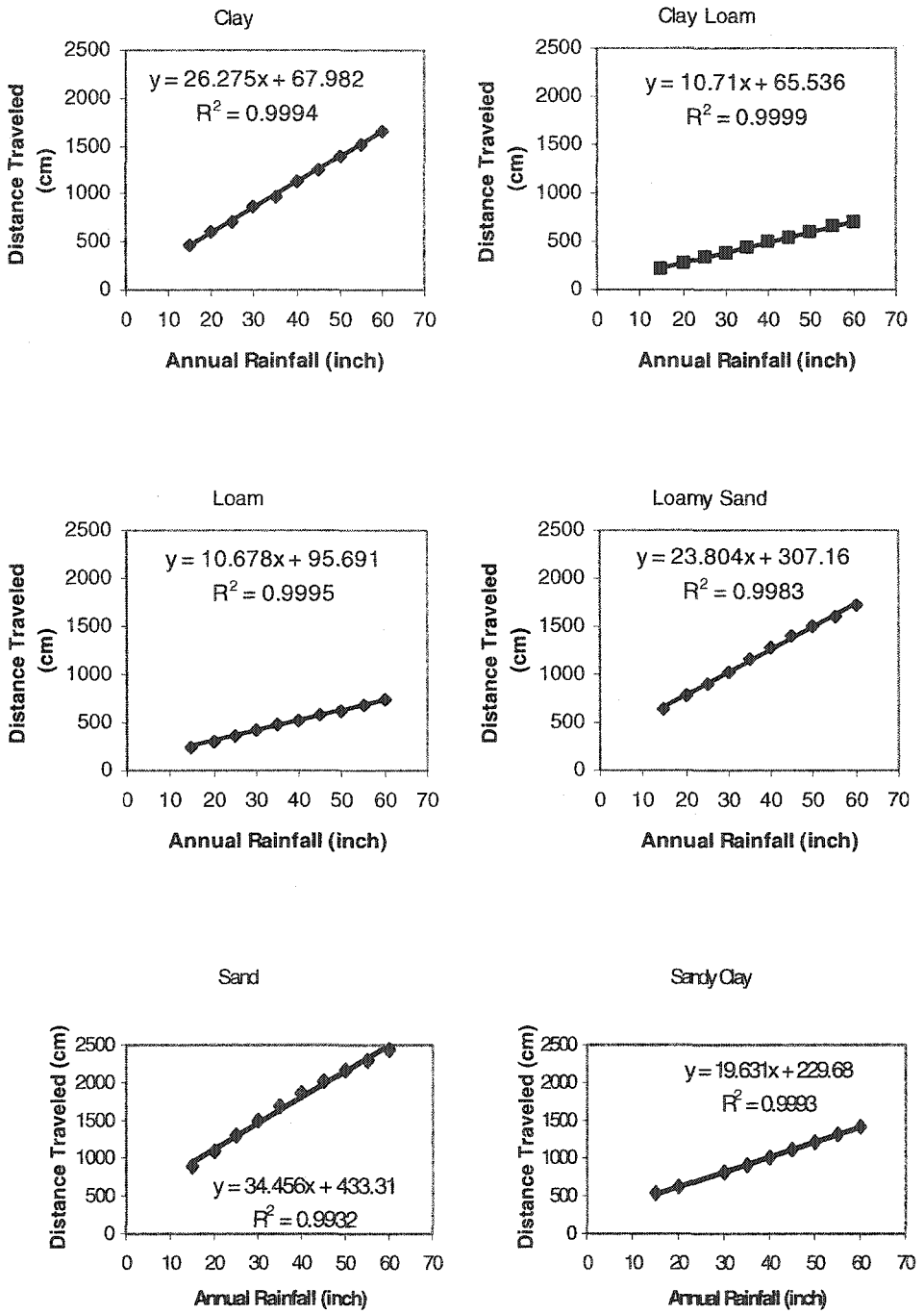


Figure 1.5. Distance traveled by the wetting-front in a year for different USDA soils.

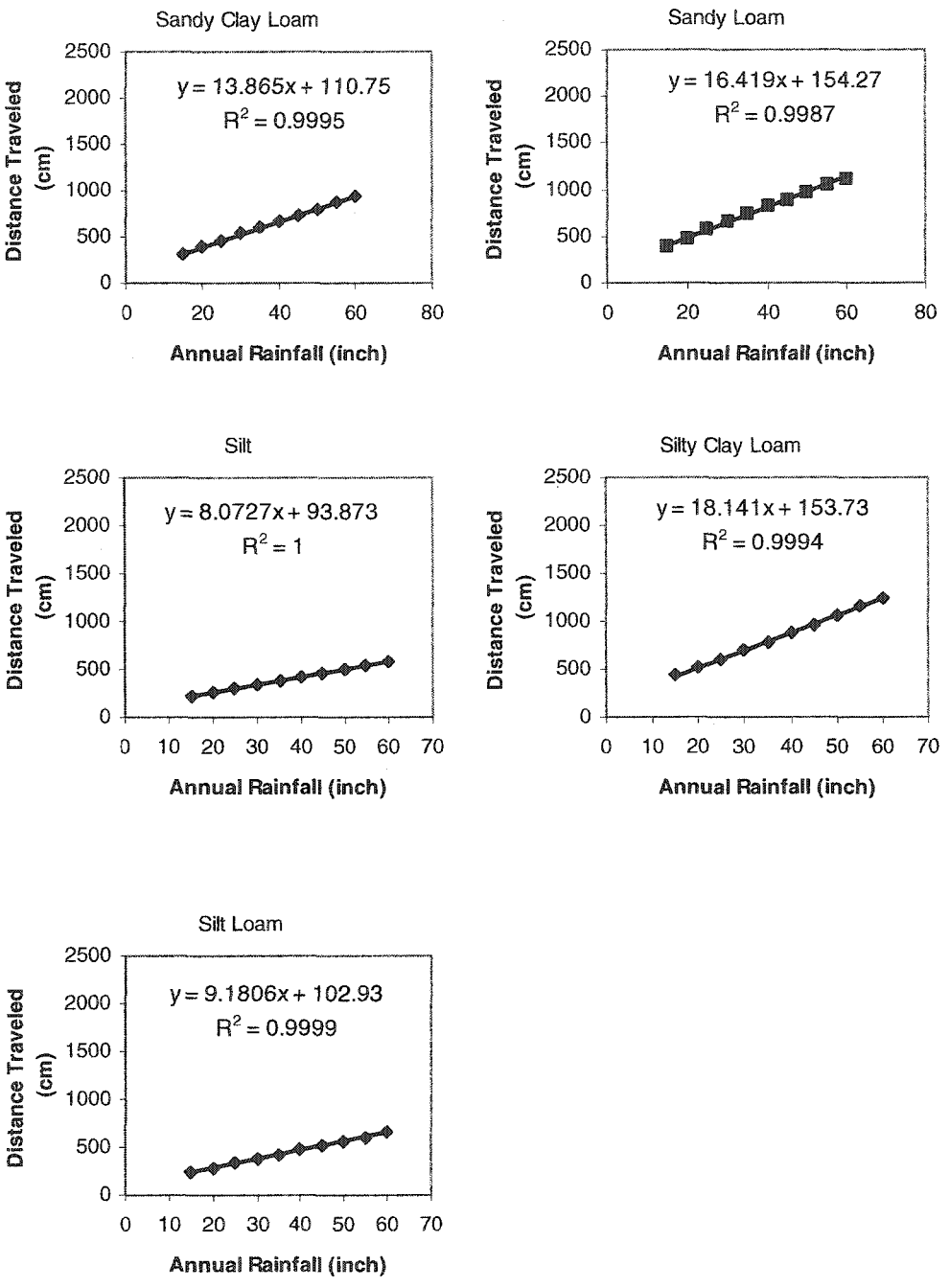


Figure 1.5 (Cont.). Distance traveled by the wetting-front in a year for different USDA soils.

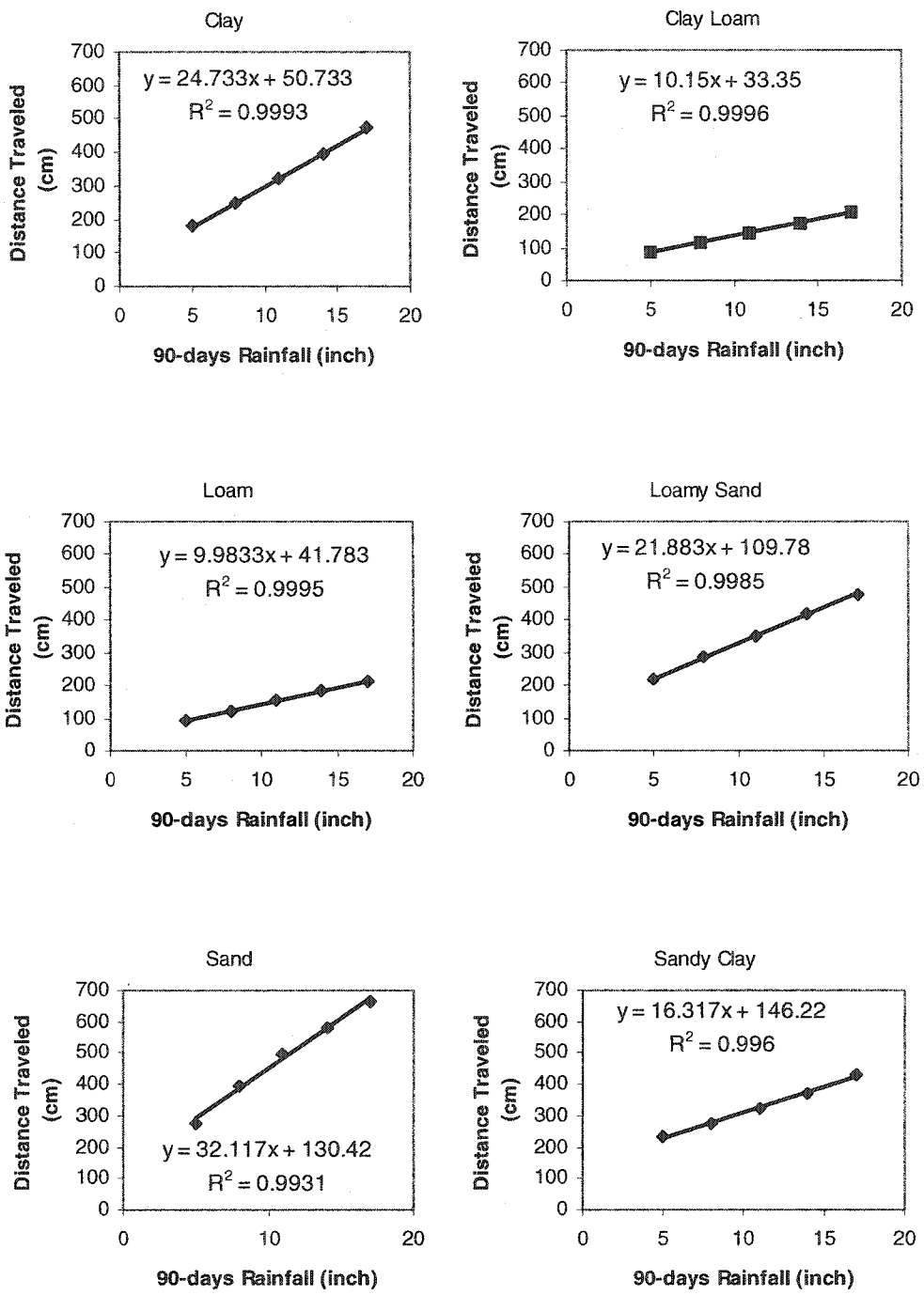


Figure 1.6. Distance traveled by the wetting-front in 90 days for different USDA soils.

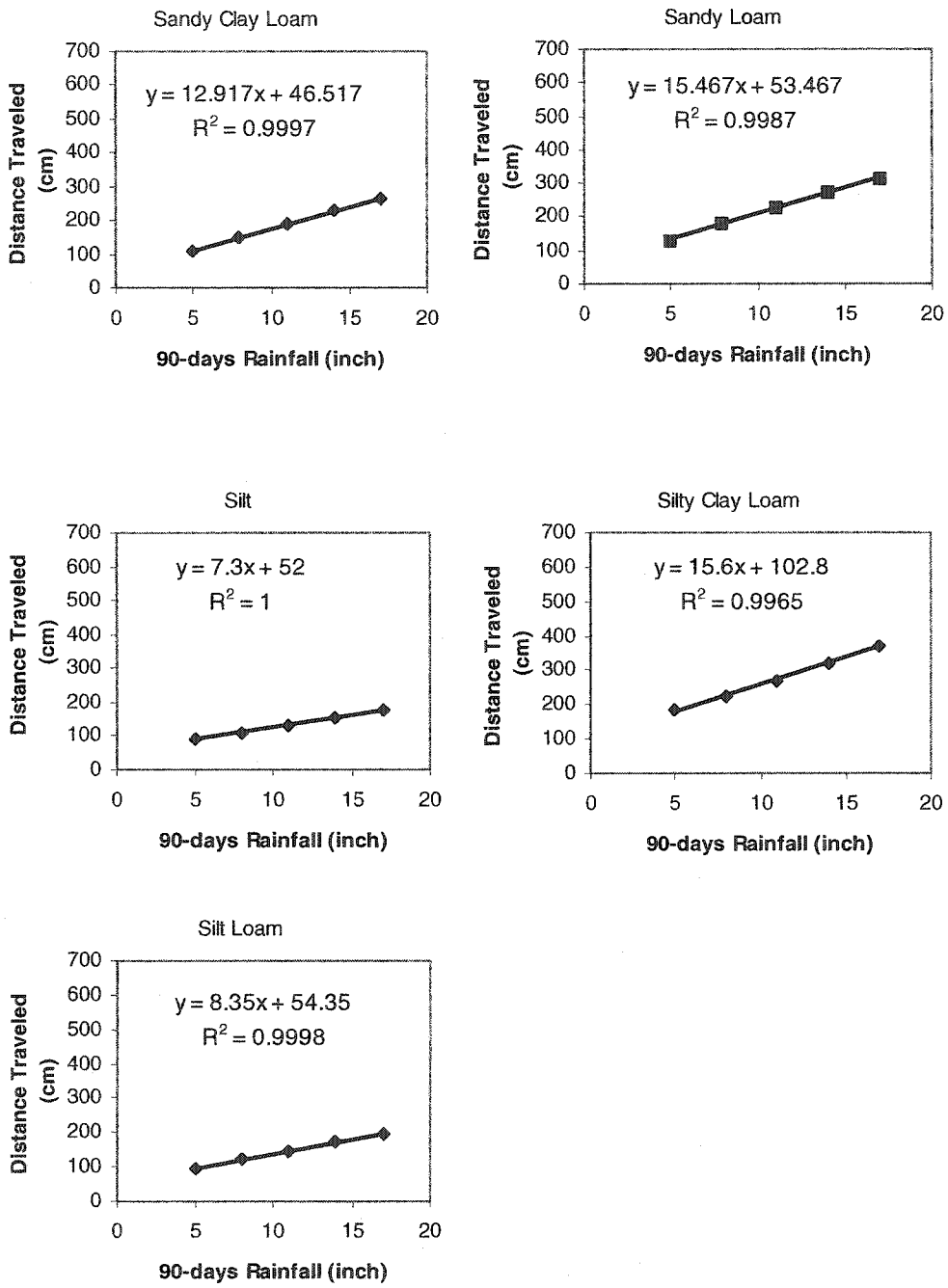


Figure 1.6 (Cont.).Distance traveled by the wetting-front in 90 days for different USDA soils.

As seen, an excellent correlation exists between the distance traveled by the wetting-front and rainfall rate. For the annual rainfall condition, R^2-values vary between 0.9932 and 1. A comparable correlation is obtained for the 90-day average daily rainfall condition as well (R^2-values between 0.9931 and 1). The almost perfect linear correlation between the rainfall rate and distance traveled by the wetting-front is most likely a result of the assumption of constant initial moisture content (θ_i) in the soil profile and constant continuous rainfall rate at the top. With the advancement of the wetting-front, the soil above the wetting-front remains saturated. At the same time, the water required to saturate the soil ahead of the wetting-front (i.e., θ_s - θ_i) remains the same, as both θ_s and θ_i are constants. Therefore, suction potential ahead of the wetting-front remains unchanged at any time, irrespective of the rainfall rate. As a result, advancing of the wetting-front parallels the rainfall rate. Consequently, the drainage rate at the wetting-front is proportional to the rainfall rate, as dictated by a simple mass balance on the system. Therefore, a linear correlation between the distance traveled by the wetting-front and rainfall rate could be expected.

1.6. Saturated Zone Transport

The saturated zone transport module evaluates the effect of nutrient (nitrogen or phosphorus) transport through groundwater. The objective of this module is to provide a rating value for the saturated zone by using a simple evaluation technique under conservative conditions. The aquifer is assumed to be homogeneous and isotropic with uniform hydraulic gradient. Denitrification of nitrate is ignored, as the process is limited to anaerobic conditions (Tesoriero et al., 2000), which are rare in most shallow aquifers.

The input parameters selected for this module are saturated hydraulic conductivity of the aquifer (K_s), porosity (n), hydraulic gradient (I_g), distance of the nearest well (D_w), pumping rate (Q), duration of pumping (t), number of years of manure application (T_m), and retardation factor (RF). The default value of K_s can be obtained from the input of the aquifer soil type (see Table 1.4). Also, the saturated volumetric moisture content (θ_s) value in Table 1.4 can be used as the default value for soil porosity. The default value for hydraulic gradient is assumed to be 0.007, which is the regional average for the Central Oklahoma Aquifer (Christenson, 1992). The users have the option to change the default value(s) of hydraulic conductivity, porosity, or hydraulic gradient, if site-specific values are known. Using the hydraulic conductivity, porosity, hydraulic gradient and RF, the effective groundwater seepage velocity (V_e) is calculated from Equation 1.11.

$$V_e = \frac{K_S \times I_g}{n \times RF} \tag{1.11}$$

The expert system has the option to incorporate the effect of pumping at the well. Pumping at the well could cause considerably faster movement of groundwater. It is assumed that the well is directly downgradient of the source along the direction of flow in order to obtain the maximum effect from pumping. Nodes are assigned between the well and the source at 0.10 feet intervals for the first 10 feet from the well, and at 1 feet intervals for the rest of the distance (D_w). The shorter intervals near the well are chosen to better approximate the sharp gradient near the well. Drawdown (D_d) values due to pumping are calculated at all nodes using the methodology developed by Theis (1935) (Equations 1.12 and 1.13).

$$u = \frac{r^2 S}{4Tt} \tag{1.12}$$

$$D_d = \frac{QW(u)}{4\pi T} \tag{1.13}$$

where, W(u) is the well function, r is the distance of the node from the well center, S is the storage coefficient, T is the transmissivity, t is the duration of pumping. The storage coefficient is assumed to be 0.0001, which is within the range specified by Freeze and Cherry (1979). The well function is approximated from the following set of regression equations (see Appendix C).

$$W(u) = -0.9967 * \text{Log}(u) - 0.532, \; u \leq 0.2$$

$$W(u) = 1.6128 * \text{Exp}(-2.0634 * u), \; 0.2 < u < 1$$

$$W(u) = 0.7079 * \text{Exp}(-1.2476 * u), \; 1 \leq u \leq 9$$

$$W(u) \approx 0, \; u > 9 \tag{1.14}$$

Groundwater velocity at each nodal interval is calculated using Equation 1.11. It is assumed that the gradient between two consecutive nodes used for groundwater velocity calculation is the sum of the gradient due to pumping and the regional gradient. Finally, the average effective groundwater velocity due to pumping (V_a) is calculated from Equation 1.15.

$$V_a = \frac{D_w}{\sum_{i=1}^{N-1} \frac{L_i}{V_i}} \tag{1.15}$$

where, L_i and V_i are the nodal interval and the groundwater velocity between node i and (i+1), and N is the number of nodes between the well and the source.

The rating for the saturated zone transport module is assigned by calculating the distance traveled by the solute center-of-mass, i.e., the plume center (D_t), and the solute concentration at the well (C_w) at time T_m. D_t is calculated from multiplying V_a by T_m. C_w

is obtained from the analytical solution of the two-dimensional advection-dispersion equation with equilibrium sorption (Equation 1.16).

$$RF\frac{\partial C}{\partial t}=-\left(v_x\frac{\partial C}{\partial x}\right)+\left(D_x\frac{\partial^2 C}{\partial x^2}+D_z\frac{\partial^2 C}{\partial z^2}\right) \tag{1.16}$$

where, C is the solute concentration, v_x is the average groundwater velocity in the x directions, D_x and D_z are the hydrodynamic dispersion coefficients in the x and z directions, respectively, and RF is the retardation factor

Lateral dispersion is ignored in Equation 1.16 based on the assumption that uniform application of manure over a large area would result in low concentration gradient in the lateral direction. The solution for Equation 1.16, considering instantaneous injection of solute mass as a line source at the water table, is given by Equation 1.17 (Sun, 1996).

$$C(x,z,t)=\frac{m/n}{2(\pi t)\sqrt{D_{ex}D_{ez}}}\exp\left\{-\frac{(x-v_{ex}t)^2}{4D_{ex}t}-\frac{z^2}{4D_{ez}t}\right\} \tag{1.17}$$

where, C(x,z,t) is the solute concentration at a point (x, z) at time t, m is the mass of solute injected instantaneously along the y-axis at t = 0, v_{ex} is the effective groundwater velocity in the x direction, and D_{ex} and D_{ez} are the effective hydrodynamic dispersion coefficients in the x and z directions, respectively.

The effective groundwater velocity (v_{ex}) is equal to V_a, and the effective hydrodynamic dispersion coefficients are equal to the respective hydrodynamic dispersion coefficients divided by RF. The longitudinal hydrodynamic dispersion coefficient is calculated from Equation 1.18.

$$D_i = \alpha_i \times V_a + D_m \tag{1.18}$$

where, D_i and α_i are hydrodynamic dispersion coefficient and dispersivity in i-direction, respectively, and D_m is molecular diffusion in the porous media.

The expert system assumes that longitudinal dispersivity (α_x) is 10% of the flow length (D_t) (Gelhar, 1986). Vertical dispersion (α_z) is assumed to be 1% of α_x, which is the default value used in Visual MODFLOW (WHI, 1999). The molecular diffusion (D_m) for nitrate is assumed to be 1.90×10^{-5} cm^2/sec (Cussler, 1997). The molecular diffusion (D_m) for phosphate could not be found from the literature. It is assumed that the D_m value for phosphate is equal to that of nitrate. Typically, D_m is much smaller than the advective-dispersion term ($\alpha_x \times Va$). However, for soils with very low hydraulic conductivity, D_m could become greater than the advective-dispersion.

The rating for the saturated zone module is assigned based on the following two rules.

Rule #1: If the center of the plume (COP) passes the well, then the rating is between 1 and 5.

$$\text{If } D_t \geq D_W \text{ Then Rating} = 5 \times \frac{C_M}{C_{th}} \text{ and } 1 \leq \text{Rating} \leq 5.$$

where, C_{th} is the limiting concentration of the nutrient, which is 10 mg/L for nitrate or 5 mg/L for phosphate and C_M is the maximum nutrient concentration when the COM reaches the well. C_M is calculated from Equation 1.17, where m is the mass of nutrient applied in excess of the maximum crop uptake rate (obtained from the surface loading module), and t is equal to the time to reach the well at an average effective groundwater velocity (V_a).

Rule #2: If COP does not reach the well, then the rating is between 1 and 5. Here, the actual concentration of the solute in the well at time T_m (C_w) is used in place of the maximum concentration (C_M) in Rule #1.

$$\text{If } D_t \le D_w \text{ Then Rating} = 5 \times \frac{C_w}{C_{th}} \text{ and } 1 \le \text{Rating} \le 5.$$

1.7. Final Module

The groundwater pollution potential (GWPP) is evaluated in the final module. Two types of ratings for the GWPP are provided by the expert system. One is the qualitative rating and the other is the number rating. The qualitative rating is grouped into four levels: 'Very Low to Low', 'Low to Medium', 'Medium to High', and 'High to Very High'. The rating is estimating based on the rules stated in Table 1.5, which are combinations of the minimum, average, and maximum rating values for each module (i.e., 1, 3, and 5, respectively). It is evident that the rules in Table 1.5 provide the highest emphasis on the surface-loading module, as it is associated with the nutrient source.

Table 1.5. Rules for evaluating groundwater pollution potential.

Rule No.	Surface Loading	Vadose Zone Transport	Saturated Zone Transport	GWPP
1	5	> 3	> 3	High to Very High
2	≥ 3	5	5	High to Very High
3	5	>1 and < 3	>1 and < 3	Medium to High
4	3	≥ 3 and < 5	≥ 3 and < 5	Medium to High
5	3	>1 and < 3	> 1 and < 3	Low to Medium
6	1	≥ 3 and < 5	≥ 3 and < 5	Low to Medium
7	<3	1	1	Very Low to Low
8	1	>1 and < 3	>1 and < 3	Very Low to Low

The number rating is estimated from the weighted average rating (WAR) value. The WAR is calculated from the rating and relative weight of each module. The set of

rules in Table 1.5 and the following four rules are used to select the relative weight for each module.

Rule # 1: If WAR < 2 Then GWPP = Very Low to Low

Rule # 2: If WAR ≥ 2 and WAR < 3 Then GWPP = Low to Medium

Rule # 3: If WAR ≥ 3 and WAR < 4 Then GWPP = Medium to High

Rule # 4: If WAR ≥ 4 Then GWPP = High to Very High

Three sets of relative weights are tested to satisfy the rules. These are {5, 2, 3}, {4, 3, 3}, and {4, 2, 4}, which are in the order of the surface loading, vadose zone transport, and saturated zone transport modules, respectively. Of the three sets, the first set satisfies all the rules in Table 1.5; hence, selected as the relative weight for the respective modules.

Table 1.6 provides the recommended course of actions for each GWPP level. Severe risk for water quality is anticipated for the 'high to very high' level. At this level, all modules have a higher than average rating of 3. Also, either the source or transport modules have the maximum possible rating (see rules 1 and 2 in Table 1.5). As the simple expert system is based on limited site-specific information and is proposed for site screening or preliminary site assessment, an extensive site assessment must be done before enforcing any drastic decision, e.g., site closure. At the 'medium to high' level, the surface loading (SL) module has higher than the average rating value, but the transport modules have ratings between 1 and 5 (see rules 3 and 4 in Table 1.5). As the source (SL) is at the high end, this level is considered at high risk. The next level, i.e., 'low to medium', is expected to have a moderate risk for water quality. At this level, either the source or transport modules have a higher than average rating (see rules 5 and 6 in Table

1.5). So, there is some potential for water pollution at the 'low to medium'. Finally, the 'very low to low' level is not expected to have any negative impact on water quality, as all modules have lower than the average rating. It should be noted that further refinement of the interpretations might be needed to incorporate any specific recommendations from the regulatory agencies.

Table 1.6. Recommendations for the groundwater pollution potential levels.

GWPP level	Recommendation
High to Very High	Severe risk for water quality. Requires immediate attention. Must conduct extensive site assessment. May require site closure.
Medium to High	High risk for water quality. Requires immediate attention. Extensive site assessment is recommended. Substantial source control is recommended for lowering the GWPP level.
Low to Medium	Moderate risk for water quality. No immediate attention is required. Extensive site assessment is not recommended. Any increase in animal units is not recommended.
Very Low to Low	No risk for water quality. No immediate attention is required. Extensive site assessment is not recommended. Animal units could be increased if desired.

1.8. Case Studies

Two case studies were conducted to evaluate the expert system. Table 1.7 shows the input parameters for the case studies. The first case study is for a large swine CAFO in Oklahoma. The farm was restricted by the court from application of manure over 450 acres of land. After an extensive evaluation, the farm was recommended by the court to purchase an additional 600 acres of land to obtain the permit. The evaluation was conducted by a group of experts in environmental engineering. The simple expert system is used to evaluate the pollution potential for both the original (450 acres) and recommended (1050 acres) land areas. The results are then compared with those of the experts.

Table 1.7. Expert system input for the two case studies.

Surface Loading Module	**Swine CAFO**	**RS1**
Animal types and numbers	Hogs-breeding: 27,000	Hogs-breeding: 1,520 Hogs-feed: 960
Types and numbers of crops	corn, wheat	wheat
Thickness of the aquifer (ft)	200	20
Land area for manure application (acres)	450 (original); 1,050 (recommended)	80
Nitrogen in fertilizer (lb/acre)	-	-
Nitrogen in soil (mg/kg)	-	-
Sorption Module		
Nitrate Sorption:		
pH	-	6.6
Nitrate in water (mg/L as N)	-	15.2
AEC (cmol/kg)	-	1.1
Retardation factor (RF)	1.0	1.0
Phosphate Sorption:		
Phosphate in water (mg/L as P)	-	0.6
Retardation factor (RF)	20.0	20.0
Vadose Zone Transport Module		
Depth of water table (ft)	150	6.3
Annual rainfall (in)[!]	24	36
Seasonal rainfall (in)[!]	7	12
USDA soil class	clay loam	clay
Saturated Zone Transport		
Distance to the well (ft),	300	1,070
Hydraulic gradient (ft/ft),	0.007	0.0056
USDA soil class	-	-
Hydraulic conductivity (ft/d)	150	8.5
Effective porosity	0.30	0.20
Years of operation	1	3
Pumping rate at the well (gpd)	-	0
Pumping period (days/year)	-	-

[!]<http://climate.ocs.ou.edu/rainfall_update.html>

The farm was raising 27,000 swine annually and was growing corn and winter wheat. The input parameters for the expert system were obtained from soil explorations, soil and water quality analysis and from a hydrogeologic atlas (Morton and Goemaat, 1973). The aquifer thickness is considered to be 200 ft (Morton and Goemaat, 1973). The RF values for nitrate (N) and phosphate (P) are approximated to be 1 and 20, respectively. The vadose zone soil is clay loam. Average annual and seasonal (highest)

rainfalls are 24 and 7 inches, respectively. Rainfall data is obtained from the Oklahoma Climatological Survey (OCS). The depth of the water table (150 ft) is obtained from soil explorations. Hydraulic conductivity and porosity for the saturated zone soil are 150 ft/day and 0.30, respectively. The distance to the well is assumed to be 300 ft, which is the minimum distance for a non-pumping well from a CAFO, according to the Oklahoma regulations (USDA, 1998). Since the evaluation is performed on an annual basis, the year of operation is assumed to be one.

The final ratings from the expert system are presented in Table 1.8. It is found that before purchasing additional land (original), the farm had 'medium to high' pollution potentials for both nitrate (N) and phosphate (P). After increasing land area to 1,050 acres for manure application (permit requirements), the pollution potential improved to 'very low to low' for N and to 'low to medium' for P. The expert system corroborates the decision made by the court. It should be noted that the overall rating could also be lowered by harvesting more crops and also by reducing the number of swine.

The second case study is for a research site, where groundwater quality was monitored during 1998 to 2000. In order to keep confidentiality, the location and name of the site are not disclosed here. For identification in this study, the research site is named as RS1. The RS1 is a small animal husbandry, which is categorized as 'non-LMFO' (Licensed Managed Feeding Operation) by the Oklahoma Department of Agriculture (ODA). According to the ODA, the farm was raising 1,520 swine over 55 pounds (i.e., hogs on breeding or, finishers) and 960 swine under 55 pounds (i.e., hogs on feed) in 1998. The farm was growing winter wheat on about 80 acres of grazing land. Locations of the monitoring wells (MW) and potentiometric surface map for the unconfined aquifer

are shown in Figure 1.7. Manure was applied in the region where MW1 and MW6 are located. Note that the area for manure application extends about 500 feet North of MW6. There is no grazing land to the East of MW4 and MW5, or around MW9. Since MW9 is located outside the grazing area and the groundwater is flowing from MW4 towards MW9, the latter is considered to be the downgradient water well. The distance between the two wells is about 1,070 feet. The thickness of the unconfined aquifer could not be approximated from bore logs of the monitoring wells at the site, as the boreholes are shallow. An approximate value for aquifer thickness is obtained from bore logs of the nearest two sites (one is about 4 miles upgradient and the other is about 3 miles downgradient). The bore logs are obtained from the Oklahoma Water Resources Board (OWRB). The hydraulic gradient during the dry season in 1998 (August, 1998) is about 0.0063, and 0.005 during the wet season (February, 1998). An average gradient of 0.0056 was used in the expert system.

Table 1.8. Pollution potential from the Expert System for the two case studies.

Case Study	Selected Condition	WAR		Pollution Potential	
		N	P	N	P
Swine CAFO	Original	3.3	3.4	Medium to High	Medium to High
	Permit Requirements	1.3	2.5	Very Low to Low	Low to Medium
RS1	--	3.1	2.9	Medium to High	Low to Medium

Slug tests were conducted to obtain hydraulic conductivity of the saturated zone. The average hydraulic conductivity of the saturated zone is about 8.5 ft/day. Porosity was estimated from the moisture content, bulk density and specific gravity of the soil samples from the saturated zone. Three years of operation are considered, since the water quality was analyzed for three consecutive years. The soil type at the vadose zone in the grazing area between MW1 and MW4 is clay. Total annual and seasonal (maximum) rainfall in

1998 was 36 and 12 inches, respectively. The depth of water table varies from 4.5 to 7.1 feet between the wet and dry seasons, respectively. An average water table depth is used for input. The average nitrate concentration in the groundwater, pH, and AEC (Anion Exchange Capacity) used to estimate the RF value for nitrate are 6.6, 15.2 mg/L, and 1.1 cmol/kg, respectively. The RF value obtained from the pH and nitrate concentration is 1.0, while the RF value becomes unusually high (4.14) for only the AEC input. A RF value of 1.0 is used for nitrate, since both pH and nitrate concentration gives the same value. The RF value for phosphate is obtained from the average phosphate concentration, which is 0.6 mg/L (see Table 1.7).

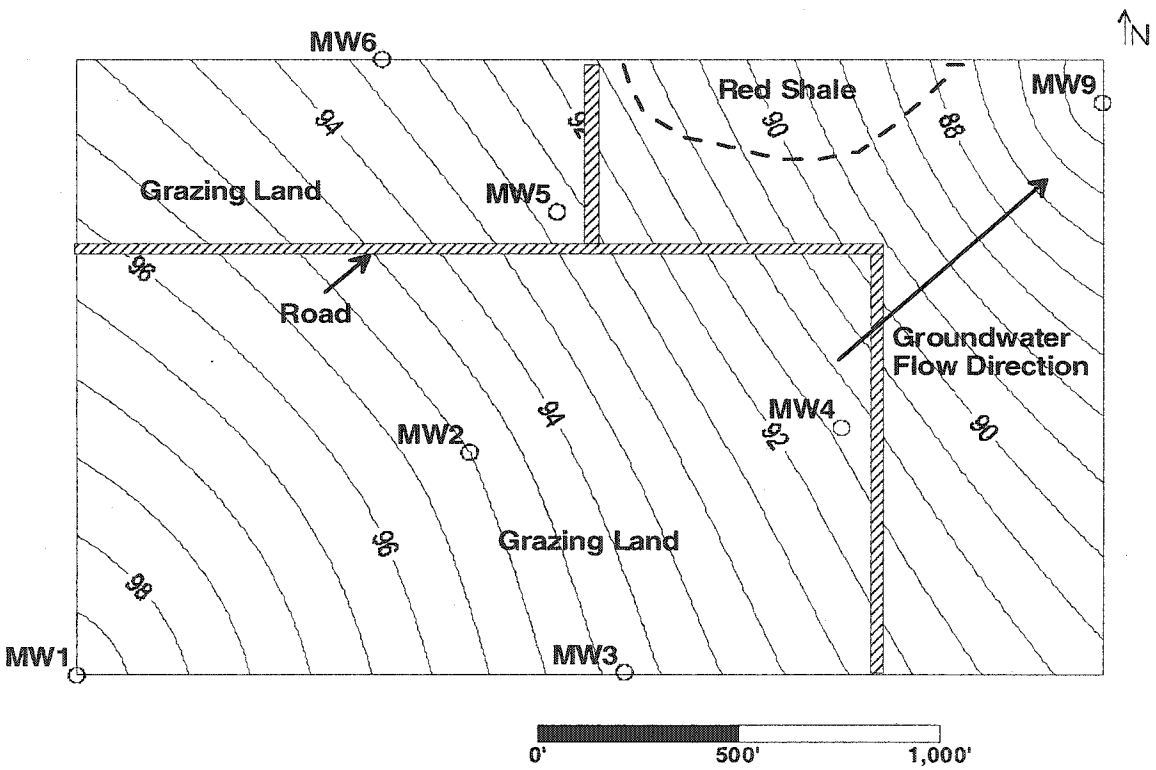


Figure 1.7. Potentiometric surface map for RS1 on July 1998.

The expert system shows 'medium to high' pollution potential for nitrate (see Table 1.8), which means the site has high risk for water quality. Figure 1.8 shows the nitrate concentration at MW4 and MW9 during the years 1999 and 2000. It is found that the maximum measured nitrate concentration at MW9 in the year 2000 was 17 mg/L, while the average in the same year was 15 mg/L. Since the well is not used as a drinking water source and the average nitrate concentration is on the brink of the drinking water standard (10 mg/L), the site could be characterized as a 'high risk' site rather than a 'severe risk' site, which is comparable to the expert system evaluation. The WAR value for nitrate is 3.1, and the individual rating values for the surface loading, vadose zone and saturated zone transport modules are 3.5, 5.0, and 1.0, respectively. Extremely high nitrate concentrations in MW2 and MW5 (320 and 680 mg/L, respectively in August 1998), which are located in the middle of the grazing land, justifies the high ratings for the surface loading and vadose zone transport modules. Also, low hydraulic conductivity in the saturated zone justifies the very low rating for the corresponding module. In 2000, the RS1 reduced the number of animals to 200 finishers. As a result, the nitrate concentrations at MW2 and MW5 decreased to 12 and 35 mg/L, respectively in the year 2000. The expert system shows that the overall GWPP for 200 finishers decreases to 'very low to low' from 'medium to high', as the rating for the surface loading module drops from 3.1 to 1.0. As the nitrate concentration in the source area decreased, the concentration in the downgradient well (MW9) should consequently decrease in the following years. However, the response could not be verified due to unavailability of water quality data after the year 2000.

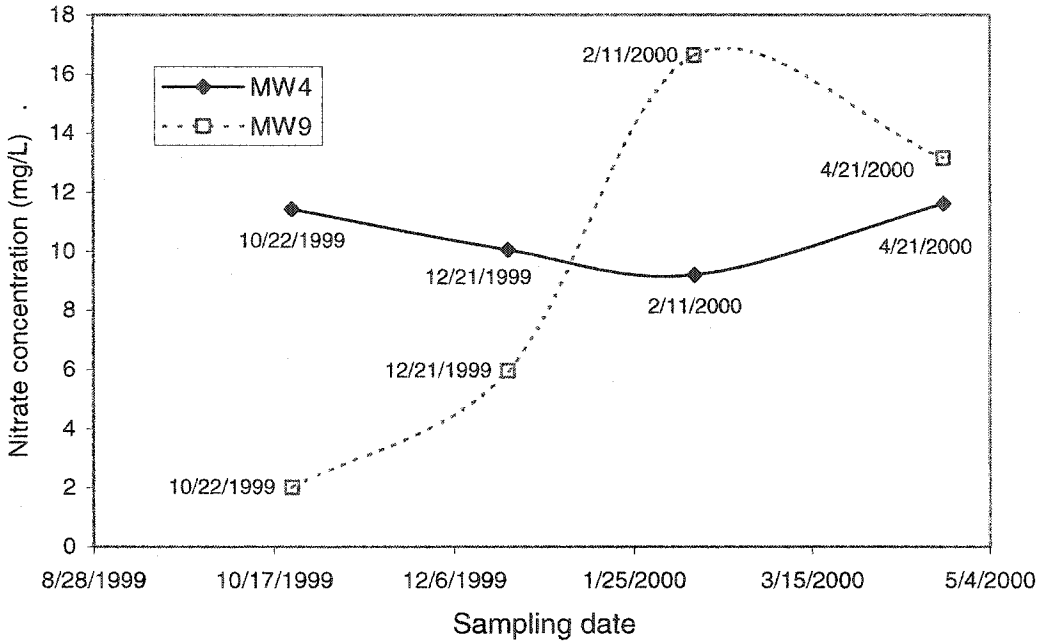


Figure 1.8. Nitrate concentration at MW4 and MW9 of RS1.

Pollution potential from phosphate is 'low to medium', i.e., moderate risk for water quality (see Table 1.6). The evaluation for phosphate could not be verified due to unavailability of data at MW9 after the year 1998. However, low phosphate concentration (0.6 mg/L) at the source area in the year 1998 supports the expert system evaluation. During the wet season of the year 1998, the phosphate was not detected in the groundwater, while in the dry season (August, 1998) it was as high as 5.22 mg/L, which is slightly above the drinking water standard (5 mg/L). Traces of phosphate in the dry season could be due to cracked soil surface in the dry season. The presence of higher phosphate concentration during certain periods of the year means that the groundwater is somewhat vulnerable. This justifies one level higher GWPP than the lowest level (which is 'very low to low'). The WAR value for phosphate is 2.9, and the rating values for the individual modules are 4.5, 1.8, and 1.0 for the surface loading, vadose zone and

saturated zone transport modules, respectively. It is indicative from the rating values that reduction of manure load at the source would further reduce the overall GWPP. For 200 finishers in 2000, the rating for the surface loading module drops to the minimum value (i.e., 1.0), which causes the overall GWPP to decrease by one level, i.e., to 'very low to low'.

1.9. Sensitivity Analyses

The sensitivity analyses of the simple expert system are conducted in two steps. In the first step, the change in the final number rating (WAR) with respect to the change in the rating of each module is studied. In the second step, the sensitivity of each individual module is studied. From the relative weights of the modules, it is found that a one-point change in the rating of the surface loading, vadose zone or saturated zone modules changes the final number rating by 0.5, 0.2 or 0.3, respectively. The sensitivity of the final qualitative rating with respect to the change in the number rating of each module follows the conditions discussed in the previous section (Table 1.5).

In the surface loading module, the number of animals, number of crops, crop type, and land area can change the rating for the module from 1 to 5, while it is only sensitive to aquifer thickness when the rating is between 3 and 5. This is because aquifer thickness is a function of the critical concentration, which becomes effective when the available nutrient is greater than the maximum crop uptake (i.e., rating > 3). It should be noted that the land area, aquifer thickness, and number of crops are inversely proportional to the rating, while the number of animals is directly proportional to the rating.

In the sorption module, the retardation factor (RF) for nitrate varies between 1 and 3.86 for a given input of pH and nitrate concentration, while the RF value varies between

1 and 3.8 for AEC between 0.14 and 1 cmol/kg. The RF value for phosphate is inversely proportional to square of the phosphate concentration (Equation 1.9). The RF value for phosphate varies between 1.06 and 20 for phosphate concentrations between 100 and 5 mg/L, respectively.

The sensitivity of the vadose zone transport module is studied by comparing the ratings for clay loam (low hydraulic conductivity) and sand (high hydraulic conductivity) for different input values of the water table depth and rainfall. The RF value is assumed to be 1 in the sensitivity analysis. The ranges of annual and seasonal rainfalls used in the analyses are 15 to 60 and 5 to 17 inches, respectively. The water table depth is varied from 20 to 100 feet. Figure 1.9 shows the change in the rating value with water table depth and rainfall amount. It is observed that sand has much higher rating than clay loam, which is obvious. Also, the ratings for sand at the lowest rainfall are higher than the ratings for clay loam at the highest rainfall. Furthermore, the difference in the rating between sand and clay loam under the same rainfall condition decreases with an increase in water table depth. For example, under the lowest rainfall condition in Figure 1.9, the difference in the rating is 2.41 when the water table depth is 20 feet, while it is 0.72 when the water table depth is increased to 100 feet.

The sensitivity of the saturated zone transport module is studied by comparing the ratings for different input values of well distance, RF value, and years of operation (Figure 1.8). Since the saturated zone module depends on the surface loading module, the 'original condition' of the site used in the first case study is considered for the sensitivity analysis. It is observed from Figure 1.10 that the rating value changes sharply with the well distance for higher values of RF. This is because the RF value not only delays the

transport but also reduces the concentration of the plume. As explained in the Section 1.6, the saturated zone transport module gives a rating of 1 if the rating for the surface loading module is less than 3, i.e., when the nutrient applied is less than the maximum crop uptake rate.

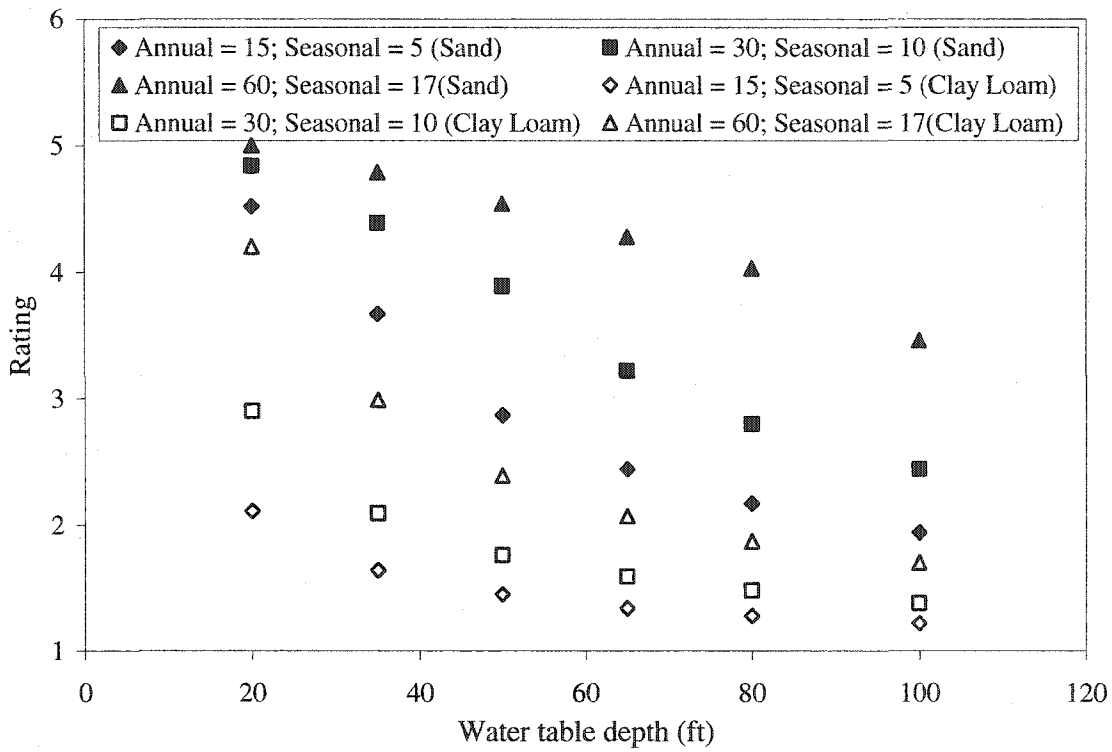


Figure 1.9. Sensitivity of the vadose zone transport module rating for different water table depths, rainfall amounts, and soil types.

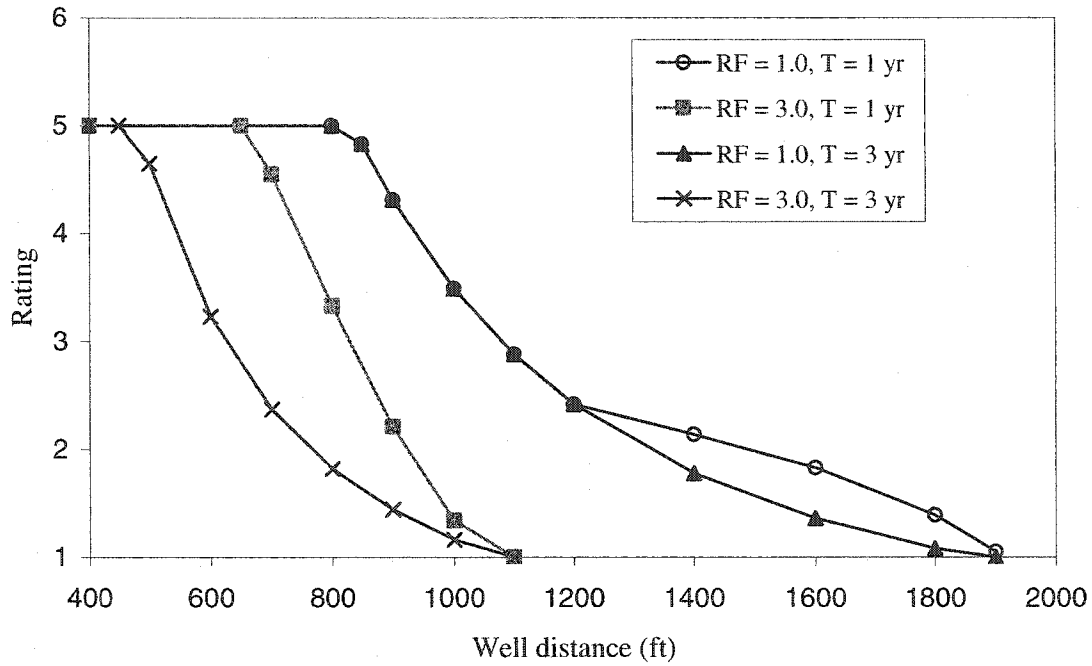


Figure 1.10. Sensitivity of the saturated zone transport module ratings for the swine CAFO (original conditions).

1.10. Advantages and Limitations of the Simple Expert System

The simple expert system developed herein has the following advantages:

- It is simple to use and requires few inputs;
- The evaluation can be done quickly;
- It is useful for comparing different operational conditions, e.g., number of animals and type, number of crops and type, and land area for manure application.
- It can be used to find suitable locations for new animal husbandries, and to screen existing facilities with high pollution potential.
- The expert system provides individual rating values for the surface loading, vadose zone and saturated zone modules, which could be used to identify the most critical components of the pollution pathway.

Limitations of the simple expert system are outlined in the following:

- It should be used for preliminary or screening level evaluation;
- As it uses simplified scientific methodology, accuracy in the evaluation may not be high; Therefore, professional judgment should be exercised while using this tool to optimize operational conditions;
- It is applicable for evaluating the pollution potential from either nitrate or phosphate, but it does not evaluate pollution potential from other chemicals or biological contaminants;
- It evaluates the pollution potential at a single downgradient well, so for multiple wells, the simulation needs to be repeated for each well;
- It is not applicable for multiple wells pumping at the same time (only single well);
- It assumes that the entire manure produced in a year is applied to the land, that is, off-site disposal is not considered.
- The total manure produced annually cannot be distributed to different periods of that year (it is applied uniformly).

1.11. Conclusions and Recommendations

The primary objective of this study was to develop an easy-to-use tool to conduct preliminary level assessment for pollution potential at a downgradient well from land application of manure. The expert system presented in this study is simple to use and requires less monetary investment in collecting the input data. A simplified scientific approach was used to develop the expert system. Emphasis was given on source control by putting the highest weight on the module representing the source and by linking the

saturated zone module with the source. The expert system is recommended to farmers for improving their management practices. For example, farmers can use the expert system to find whether or not the source and/or the transport media are the major contributor(s) to the ensuing pollution potential. If the source is responsible for high pollution, farmers can mitigate adverse effects by taking appropriate actions, such as, reducing the number of animals, increasing the number of crops, selecting different crop types, or increasing the land area for manure application. As demonstrated in the two case studies, pollution potential for the swine CAFO was reduced by increasing the land area, and the RS1 showed a lower pollution potential for a reduced number of animals. The farmers can take a similar approach to find optimum animal inventory, crop type, and land area for manure application.

The expert system can be used by the regulatory agencies for preliminary site assessment and site screening of both new and existing animal husbandries. For example, the regulatory agencies can use the expert system to find suitable locations for building new facilities, which could be decided based on the rating values for the transport modules. Existing facilities with a high pollution potential could be screened by the expert system and recommendation for an advanced assessment could be made accordingly. In addition, the expert system does not warrant high skill to conduct site assessment.

Reference

Arora, P. A., and W. F. McTernan. 1994. An expert system to determine the probability of pesticide leaching. *Agricultural Water management.* 25:57-70.

Barker, J. C. 1996. Lagoon design and management for livestock waste treatment and storage. North Carolina Cooperative Extension Service, EBAE 103-83, Raleigh, NC.

Bellini G., M.E. Sumner, D. E. Radcliffe, and N. P. Qafoku, 1996. Anion transport through columns of highly weathered acid soils: Adsorption and retardation. *Soil Sci. Soc. Am. J.* 60:132-137.

Bitton, G., G. E. Gifford, and C. P. Oscar. 1976. *Removal of Viruses from Water by Magnetic Filtration.* Water Resources Research Center, University of Florida, Gainesville, FL.

Borggaard, O. K. 1983. Influence of iron oxides on phosphate adsorption by soil. *Journal of Soil Science.* 34:333-341.

Borggaard, O. K., S. S. Jorgensen, J.P. Moberg, and B. Raben-Lange. 1990. Influence of organic matter on phosphate adsorption by aluminum and iron oxides in sandy soils. *Journal of Soil Science.* 41:443-449.

Bottani, E. J., L.E. Cascarini de torre, E. A. Fertitta, S. Lopez, and N. O. Barbaro. 1993. Adsorption of gases and phosphate ions on some Argentinean soil samples. *Soil Science.* 155(1):190-196.

Carsel, R. F., and R. S. Parrish.1988. Developing joint probability distributions of soil water retention characteristics. *Water Resources Research.* 24:755-769.

Christenson, S.C., R. B. Morton, and B. A. Mesander. 1992. Hydrogeologic maps of the Central Oklahoma Aquifer. Hydrogeologic atlas HA-724. U. S. Geologic Survey, Oklahoma City, OK.

Crowe, A. S., and J. P. Mutch. 1992. EXPRESS: An expert systems for assessing the fate of pesticides in the subsurface. *Environmental Monitoring and Assessment.* 23:19-43.

Crowe, A. S., and J. P. Mutch. 1994. An expert systems approach for assessing the potential for pesticide contamination of groundwater. *Ground Water.* 32(3):487-498.

Cussler, E.L. 1997. Diffusion Mass Transfer in Fluid Systems. 2nd Edition. Cambridge University Press, UK.

Fetter, C. W. 1999. Contaminant Hydrogeology. 2nd edn. Prentice-Hall, NJ.

Freeze, R. A., and J. A. Bennett. 1979. *Groundwater.* Prentice-Hall Inc., NJ.

Gelhar, L. W. 1986. Stochastic subsurface hydrology from theory to applications. *Water Resources Research.* 22(9):135-145.

Kellogg, R. L., and C. H. Lander. 1999. Trends in the potential for nutrient loading from confined livestock operations. Poster Presentation for *"The State of North America's Private Land,"*, Chicago, Illinois. USDA-NRCS. Retrieved, January 12, 2000. <http://www.nhq.nrcs.usda.gov/land/pubs/ntrend.html>

Lander C. H., D. Moffitt, and K. Alt. 1998. Nutrients available from livestock manure relative to growth requirements. Resource Assessment and Strategic Planning. Working Paper 98-1. USDA-NRCS. Retrieved, January 22, 2000. <http://www.nhq.nrcs.usda.gov/land/pubs/nlweb.html>

Lander, C. H., and D. Moffitt. 1996. Nutrient use in cropland agriculture (commercial fertilizer and manure): nitrogen and phosphorus. Working paper no. 14. USDA-NRCS. Retrieved, January 20, 2000. <http://www.nhq.nrcs.usda.gov/RCA_PAPERS/WP14/wp14text.html>

Mesonet, 2004. General Overview. Retrieved, January 22, 2004. <http://www.mesonet.ou.edu/overview/>

Morton, R.B., and R. L. Goemaat. 1973. Reconnaissance of water resources of Beaver County, Oklahoma. *Hydrogeologic Atlas HA-450.* U. S. Geologic Survey, Oklahoma City, OK.

Naidu, R., J. K. Syers, R. W.Tillman, and J. H. Kirkman. 1990. Effect of liming on phosphate sorption by acid soils. *Journal of Soil Science.* 41:165-175.

Nultsch, W. 1971. *General Botany.* Academic Press, NY.

Parfitt, R. L. 1978. Anion adsorption by soils and soil materials. *Advances in Agronomy.* 30:1-50.

Qafoku , N. P., M. E. Sumner, and D.E. Radcliffe. 2000a. Anion transport in columns of variable charge subsoils: Nitrate and Chloride. *Journal of Environmental Qual*ity 29:484-493.

Qafoku , N. P., M. E. Sumner, and L.T. West. 2000b. Mineralogy and chemistry of some variable charge subsoils. *Communications in Soil Science and Plant Analysis.* 31(7&8):1051-1070.

Simunek, J., K. Huang, and M. Th. Van Genuchten. 1998. The HYDRUS code for simulating the one-dimensional movement of water, heat, and multiple solutes in variably-saturated media. Version 6. Research Report No. 144. U.S. Salinity Laboratory, Riverside, CA.

Sun, N. Z. 1996. *Mathematical Modeling of Groundwater Pollution*, Springer, NY.

Tesoriero, A. J., H. Liebscher, and S.E. Cox. 2000. Mechanism and rate of denitrification in an agricultural watershed: electron and mass balance along groundwater flow paths. *Water Resources Research.* 36(6):1545-1559.

Theis, C.V. 1935. The relation between the lowering of the piezometric surface and the rate and the duration of discharge of a well using groundwater storage. *Transaction American Geophysical Union.* 16:519-524.

USDA. 1998. *An act relating to agriculture*. Passed by Oklahoma legislature. U. S. Department of Agriculture, Oklahoma City, OK.

USDA-NASS. 2000. Crop acreage, yield and production graphics. Retrieved, February, 14, 2000. <http://www.usda.gov/nass/aggraphs/crops.htm>

USEPA.1997. Cumulative Risk Index Analysis (CRIA): Swine concentrated animal feeding operations. Version 6.0. U.S. Environmental Protection Agency, Region 6, Dallas, TX.

USEPA. 1999. National recommended water quality criterion. EPA 822-Z-99-001. U.S. Environmental Protection Agency, Washington, DC.

Van der Zee, S. E. A. T. M., and W. H. Van Riemsdijk. 1986. Sorption kinetics and transport of phosphate in sandy soil. *Geoderma.* 38:293-309.

Van Genuchten, M. Th. 1980. A closed-form equation for predicting the hydraulic conductivity of unsaturated soils. *Soil Science Society of America Journal.* 44:892-898.

WHI. 1999. Visual MODFLOW: The fully integrated, three-dimensional, graphical modeling environment for professional groundwater flow and contaminant transport modeling. *Waterloo Hydrogeologic Inc.* Ontario, Canada.

Chapter 2: Analytical Models for Instantaneous Point and Finite Sources

Abstract

This chapter presents a simple analytical solute transport model for instantaneous point sources in infinite, semi-infinite, and finite vertical domains. Effectiveness of the superposition technique in representing a transient non-point source is also evaluated. Source dimensions are required to apply superposition of point sources in space to represent non-point sources. In this regard, mathematical equations for the limiting source dimensions of a point source are derived. It is found that the limiting point source dimensions give less than 1 percent error in the point source model when compared with the finite source model. Finally, analytical models for point and finite sources in a finite aquifer are derived. It is found that the analytical models for finite vertical domain predicts a conservative peak concentration in comparison with the numerical model. The minor difference in output (4 to 8%) could be due to numerical dispersion and error in calibration of the numerical model.

2.1. Introduction

Evaluation of solute transport from transient non-point sources (NPS) is commonly conducted through numerical models. At present, several three-dimensional

analytical models for finite or patch sources are also available (Cleary and Ungs, 1978; Domenico, 1987; Domenico and Robbins, 1985; Leij et al., 1991; Martin-Hayden and Robbins, 1997; Neville, 1994; Park and Zhan, 2001; Sim and Chrysikopolous, 1998; Wexler, 1992; and Yeh, 1981). Analytical models are simple in comparison to numerical models. Also, analytical models are very useful for testing and benchmarking numerical models (Leij et al., 1991; Park and Zhan, 2001; Sim and Chrysikopolous, 1998; and Zheng and Bennett, 2002;). Leij et al. (1991) presented analytical solutions, commercially available as 3DADE (USSL, 1994), for different shapes of sources in a domain that is semi-infinite in the direction of groundwater flow and infinite in the transverse and vertical directions. This implies that the sources in the horizontal plane should be placed in the middle of the aquifer so that lateral and vertical spreading cannot reach the boundaries. This consideration restricts the use of 3DADE for NPS at the water table of unconfined aquifers. Models by Cleary and Ungs (1988), Domenico (1987), Domenico and Robbins (1985), Martin-Hayden and Robbins (1997), Neville (1994), and Wexler (1992) are limited to constant or continuous patch sources. Park and Zhan (2001), Sim and Chrysikopolous (1998), and Yeh (1981) considered a time-dependent finite concentration source in aquifers with finite and infinite thickness. However, these analytical models are mathematically intensive, as they require numerical integration of complex mathematical functions.

In this study, the superposition technique for evaluating solute transport through groundwater from a transient NPS is evaluated. Since the advection-dispersion equation is linear (Sun, 1996) for the intended application, superposition of the instantaneous point source in space and time can be applied to obtain downgradient concentration from a

transient NPS. To apply superposition in space, the dimensions for the point source need to be defined. Accordingly, mathematical expressions for the source dimensions of a point source are derived. In addition, an analytical model for instantaneous point source at the water table of a semi-infinite aquifer is derived. The existing analytical model by Baetsle (1969) is applicable for instantaneous point source in an infinite aquifer, which means that the source should be in the middle of the aquifer. As a result, the Baetsle (1969) model cannot be applied when contaminants are leaching from the soil surface to the groundwater table. Finally, an analytical model for instantaneous point source at the water table of a finite aquifer is derived.

To summarize, the following analytical models are presented in this chapter.

- One-dimensional instantaneous point source model in an infinite aquifer by Crank (1956),
- Three-dimensional instantaneous point source model in an infinite aquifer by Baetsle (1969),
- Three-dimensional instantaneous finite source models in an infinite aquifer by Hunt (1978), and Domenico and Robbins (1985),
- Three-dimensional constant and continuous finite source model in an infinite aquifer by Domenico and Robbins (1985),
- Three-dimensional constant and continuous point source model in an infinite aquifer by Hunt (1978),
- Three-dimensional instantaneous point source model in a semi-infinite aquifer (developed in this study),

- Three-dimensional instantaneous point and finite source models in a finite aquifer (developed in this study).

2.2. Advection-Dispersion Equation for Solute Transport

The advection-dispersion equation (ADE) for solute transport through a saturated soil is derived from conservation of mass in an elementary volume of the porous media. The ADE used herein is based on the assumptions that the porous media is homogeneous and isotropic, and that the flow condition follows Darcy's law. Also, it is assumed that the solute migrates at the same flow velocity of the fluid, and that the solute is miscible, non-degradable, and non-reactive. The general form of the three-dimensional ADE is given by

$$\frac{\partial C}{\partial t} = -\left(v_x \frac{\partial C}{\partial x} + v_y \frac{\partial C}{\partial y} + v_z \frac{\partial C}{\partial z} \right) + \left(D_x \frac{\partial^2 C}{\partial x^2} + D_y \frac{\partial^2 C}{\partial y^2} + D_z \frac{\partial^2 C}{\partial z^2} \right) \tag{2.1}$$

where, C is the solute concentration, v_x, v_y, v_z are the average fluid velocities in the x, y and z directions, respectively, and D_x, D_y, D_z are the hydrodynamic dispersion coefficients in the respective directions.

Equation 2.1 can be rewritten for a homogeneous medium with uniform groundwater velocity in the x direction as

$$\frac{\partial C}{\partial t} = -\left(v_x \frac{\partial C}{\partial x} \right) + \left(D_x \frac{\partial^2 C}{\partial x^2} + D_y \frac{\partial^2 C}{\partial y^2} + D_z \frac{\partial^2 C}{\partial z^2} \right) \tag{2.2}$$

Equation 2.2 can be modified for source, sink and first-order decay terms as

$$\frac{\partial C}{\partial t} = -\left(v_x \frac{\partial C}{\partial x} \right) + \left(D_x \frac{\partial^2 C}{\partial x^2} + D_y \frac{\partial^2 C}{\partial y^2} + D_z \frac{\partial^2 C}{\partial z^2} \right) + \frac{W}{n} C_0 - \frac{Q}{n} C - \lambda C \tag{2.3}$$

where, C_0 is concentration of the injected tracer, n is porosity of the medium, W and Q are volume of water injected and extracted per unit volume of aquifer per unit time, respectively, and λ is first order decay constant in the liquid phase.

With equilibrium sorption, the ADE in Equation 2.3 can be presented by

$$RF\frac{\partial C}{\partial t} = -\left(v_x \frac{\partial C}{\partial x}\right) + \left(D_x \frac{\partial^2 C}{\partial x^2} + D_y \frac{\partial^2 C}{\partial y^2} + D_z \frac{\partial^2 C}{\partial z^2}\right) + \frac{W}{n} C_0 - \frac{Q}{n} C - \lambda C \quad (2.4)$$

where, RF is the retardation factor for sorption. For linear sorption, RF is expressed as

$$RF = 1 + \frac{p_b}{n} K_p \quad (2.5)$$

where, p_b is soil bulk density and K_p is linear sorption coefficient.

2.3. Analytical Model for Instantaneous Point Source in an Infinite Domain

Crank (1956) used the generalized probability function to define concentration in one-dimensional, non-advective flow domain (i.e., $v_x = D_y = D_z = 0$ in Equation 2.2) as

$$C(x,t) = \frac{A}{\sqrt{t}} \exp\left(-\frac{x^2}{4D_x t}\right) \quad (2.6)$$

where, A is an arbitrary constant.

By assuming the total amount of mass (M) diffusing in a cylinder of infinite length with unit cross-section, one finds M is given by

$$M/n = \int_{-\infty}^{\infty} C dx \quad (2.7)$$

Solving Equations 2.7 and 2.8, Crank (1956) derived the following solution

$$C(x,t) = \frac{M/n}{2\sqrt{\pi D_x t}} \exp\left(-\frac{x^2}{4D_x t}\right) \quad (2.8)$$

Baetsle (1969) extended Equation 2.8 to a three-dimensional dispersive field in a moving coordinate system, moving at velocity v_x in the direction of flow. Equation 2.9 is Baetsle's solution of the ADE (Equation 2.2) for instantaneous injection of solute as a point source in an infinite domain.

$$C(x,y,z,t) = \frac{M/n}{8(\pi t)^{3/2}\sqrt{D_x D_y D_z}} \exp\left\{-\frac{(x - v_x t)^2}{4D_x t} - \frac{y^2}{4D_y t} - \frac{z^2}{4D_z t}\right\} \qquad (2.9)$$

where, M is the mass of solute injected instantaneously at the origin at t = 0

Hunt (1978) and Sun (1996) solved Equation 2.2 analytically and obtained the same solution as Baestle (1969). Hunt (1978) used an analogous solution from heat conduction, derived by Turner (1972), to derive Equation 2.9. Sun (1996) used a completely analytical concept to solve the ADE. He assumed an infinitesimal spherical point mass, as explained by Equation 2.10, to solve the ADE in a spherical coordinate system (see Equation 2.11), which was then converted to a Cartesian coordinate system to derive Equation 2.9.

$$M = 4\pi\theta \int_0^\infty C r^2 dr \qquad (2.10)$$

$$C(r,t) = \frac{M/n}{8(\pi\ Dt)^{3/2}} \exp\left(-\frac{r^2}{4Dt}\right) \qquad (2.11)$$

2.4. Analytical Model for Instantaneous Finite Source in an Infinite Domain

Hunt (1978) integrated the point source model in Equation 2.9 over the area of the finite source dimensions and applied Fourier transformation to derive the solution for instantaneous cubic source of solute mass, with dimension equal to 'L_S'. Equation 2.12 is

the analytical model derived by Hunt (1978), which provides the concentration at any downgradient point (x,y,z) from the center of the source (0, 0, 0) at any time 't'.

$$C(x,y,z,t) = \frac{M/n}{8L_S^3}\left[erf\left(\frac{x - v_x t + L_S/2}{2\sqrt{D_x t}}\right) - erf\left(\frac{x - v_x t - L_S/2}{2\sqrt{D_x t}}\right)\right]$$
$$\left[erf\left(\frac{y + L_S/2}{2\sqrt{D_y t}}\right) - erf\left(\frac{y - L_S/2}{2\sqrt{D_y t}}\right)\right]\left[erf\left(\frac{z + L_S/2}{2\sqrt{D_z t}}\right) - erf\left(\frac{z - L_S/2}{2\sqrt{D_z t}}\right)\right] \quad (2.12)$$

where, '*erf*' represents the error function.

Domenico and Robbins (1985) modified Hunt's (1978) equation to represent an instantaneous parallelepiped source (see Equation 2.13). Note that the equation presented by Domenico and Robbins (1985) for an instantaneous parallelepiped source has a typographical error. Equation 2.13 is in the correct form.

$$C(x,y,z,t) = \frac{C_0}{8}\left[erf\left(\frac{x - v_x t + X_S/2}{2\sqrt{D_x t}}\right) - erf\left(\frac{x - v_x t - X_S/2}{2\sqrt{D_x t}}\right)\right]$$
$$\left[erf\left(\frac{y + Y_S/2}{2\sqrt{D_y t}}\right) - erf\left(\frac{y - Y_S/2}{2\sqrt{D_y t}}\right)\right]\left[erf\left(\frac{z + Z_S/2}{2\sqrt{D_z t}}\right) - erf\left(\frac{z - Z_S/2}{2\sqrt{D_z t}}\right)\right] \quad (2.13)$$

where, X_S, Y_S, and Z_S represent source dimensions along the x, y, and z directions, respectively, and C_0 is the solute concentration at the source, which is equal to $M/(nX_SY_SZ_S)$.

2.5. Superposition of Point Sources to Represent Non-Point Sources

Since the ADE is linear, superposition of the point sources in space can be applied to represent a NPS of any shape. To apply superposition in space, the number of point sources required to form the NPS, and the dimension of each point source are needed. The dimension of a point source is critical, as larger dimension can result in an erroneous estimation of downgradient concentrations. The limiting source dimension for a point source model, with less than 1% error in estimation, is derived by Ahsanuzzaman et al. (2003) (see Equation 2.14). The derivation of Equation 2.14 is presented in Appendix D.

$$\left(\frac{X_S/2}{2\sqrt{D_x\frac{x}{v_x}}}\right) or, \left(\frac{Y_S/2}{2\sqrt{D_y\frac{x}{v_x}}}\right) or, \left(\frac{Z_S/2}{2\sqrt{D_z\frac{x}{v_x}}}\right) \leq 0.10 \qquad (2.14)$$

Superposition of the point sources to represent a NPS can be obtained by continuous integral over the volume of source. However, discrete summation, as shown in Equation 2.15, can also be used as an alternative. Equation 2.15 is useful, as it can be easily converted into a computer code.

$$C(x, y, z, t) = \sum_{i=0}^{nx}\sum_{j=0}^{ny}\sum_{k=0}^{nz} C_{i,j,k}(t) \qquad (2.15)$$

where, C(x,y,z,t) is the concentration at any location downgradient to the source at any given time 't' after applying the load; $C_{i,j,k}(t)$ is the concentration at (x,y,z) due to the point source, (i,j,k) with dimensions Δx, Δy, and Δz in the x, y, and z directions, respectively at time 't'; and nx, ny, and nz are the number of point sources in the respective directions. That means, X_S, Y_S, and Z_S are equal to ($nx \times \Delta x$), ($ny \times \Delta y$), and ($nz \times \Delta z$), respectively.

To verify the effectiveness of the superposition technique, outputs from the analytical finite source model for a single parallelepiped source (Equation 2.13) and from superposition of a number of smaller point sources that constitute the same parallelepiped source are compared. The source dimensions used for the parallelepiped source are 700 ft long, 10 ft wide, and 3 ft thick (i.e., X_S = 700 ft, Y_S = 10 ft, and Z_S = 3 ft). The source dimension for the point source is 20 ft long, 2 ft wide, and 1 ft thick (i.e., Δx = 20 ft, Δy = 2 ft, and Δz = 1 ft), which means nx, ny, and nz are 35, 5, and 3, respectively (from Equation 2.14). The groundwater seepage velocity is assumed to be 1.17 ft/day; longitudinal, lateral, and vertical dispersivities are set to 15, 1.5, and 0.15 ft, respectively; the distance of observation point (x) is assumed to be 1,000 ft from the center of the parallelepiped source. Figure 2.1 shows a comparison of the breakthrough curves (BTC) at an observation point 1,000 ft away from the center of the parallelepiped source. The legend 'FS', and 'Superposition of PS' represent model simulations for finite source, and superposition of point sources, respectively. It is evident from Figure 2.1 that superposition of the point sources perfectly matches the finite source model output.

2.6. Transient Concentration Sources

The instantaneous point source model can also be applied to evaluate stepwise (in time) variable concentration sources by applying superposition in time. The stepwise concentration source is most common for agricultural releases, where the nutrients are applied seasonally (i.e., at different times) and at variable flux rates. The superposition of the instantaneous point source model to represent transient concentration source can be given by Equation 2.16.

$$C(x,y,z,t) = \sum_{k=1}^{nt} C_k(x,y,z,t_k) \tag{2.16}$$

where, *nt* is the number of time steps, C_k is the concentration for the k^{th} time step from instantaneous point source model (Equation 2.9), and t_k is the simulation period for the k^{th} time step. Note that t_k is equal to $(t - \Delta t \times k)$, where Δt is the time interval for each time step and t is the total simulation period.

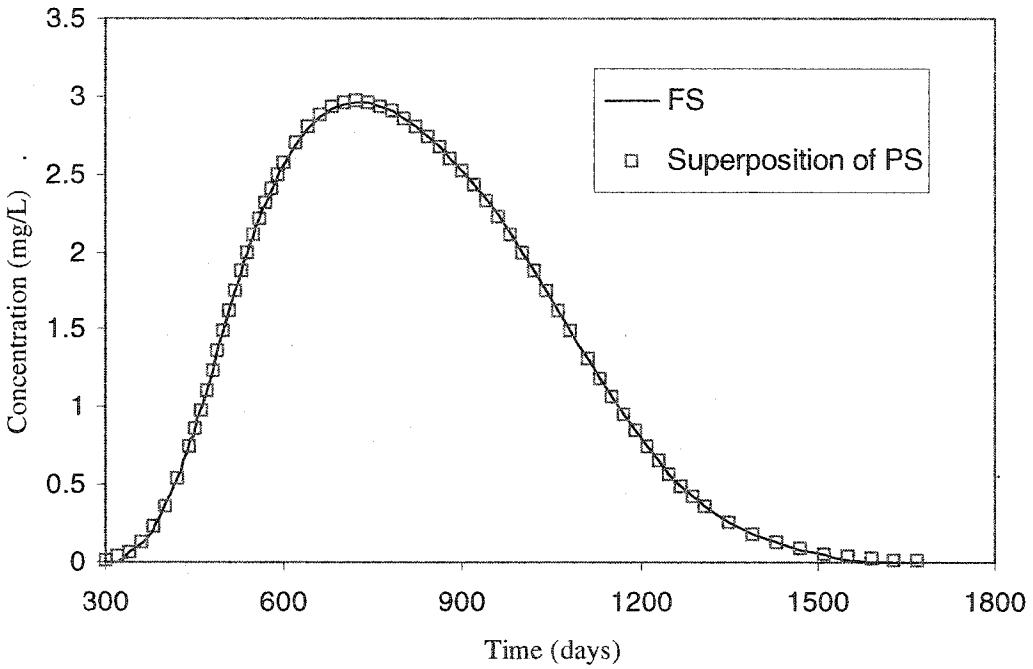


Figure 2.1. Comparison between the instantaneous finite source (FS) model and superposition of a point source (PS) model.

Since analytical solutions for transient concentration sources are not available, the superposition in time can only be verified against the analytical model for constant continuous sources. The analytical model for a constant continuous finite source, developed by Domenico and Robbins (1985), is presented in Equation 2.17.

$$C(x,y,z,t) = \frac{C_0}{8}\left[erfc\left(\frac{x - v_x t}{2\sqrt{D_x t}}\right)\right]$$
$$\left[erf\left(\frac{y + Y_S/2}{2\sqrt{D_y t}}\right) - erf\left(\frac{y - Y_S/2}{2\sqrt{D_y t}}\right)\right]\left[erf\left(\frac{z + Z_S/2}{2\sqrt{D_z t}}\right) - erf\left(\frac{z - Z_S/2}{2\sqrt{D_z t}}\right)\right] \quad (2.17)$$

where, *erfc* represent the complementary error function, and C_0 is the constant concentration at the source.

Equation 2.18 is the analytical model, derived by Hunt (1978), for constant continuous point sources.

$$C(x,y,z,t) = \frac{\left(\frac{M_c}{n}\right)exp\left(\frac{xv_x}{2D_x}\right)}{8\pi R\sqrt{D_y D_z}}\left[exp\left(\frac{-Rv_x}{2D_x}\right)erfc\left(\frac{R - v_x t}{2\sqrt{D_x t}}\right) + exp\left(\frac{Rv_x}{2D_x}\right)erfc\left(\frac{R + v_x t}{2\sqrt{D_x t}}\right)\right] \quad (2.18)$$

where, $R = [x^2 + y^2 D_x/D_y + z^2 D_x/D_z]^{1/2}$, and M_c is the constant mass flowing through a section vertical to the groundwater flow at the source.

Both the Hunt (1978) and Domenico and Robbins (1985) models are compared with the superposition of an instantaneous point source (IPS) in time (Equation 2.16). A constant concentration for the Domenico and Robbins model (i.e., C_0) is assumed to be 4000 mg/L. The corresponding mass at the source for the Hunt model (i.e., M_c) is equal to 1.19 Kg/day. The groundwater velocity (v_x) and dispersivities (D_x, D_y, D_z) are same as those used in §2.5. The source dimensions for the point source in the previous section are used in the finite source model (Equation 2.17) so that the resulting output becomes comparable to the point source models (Equations 2.16 and 2.18). Figure 2.2 shows the breakthrough curves at 400 ft away from the source for the superposition of IPS, and the constant continuous finite and point source models. It is evident from Figure 2.2 that

breakthrough curves for all three models match very well, although the superposition of IPS breaks through about 10 days earlier than the others. This discrepancy could be due to computational error form using the series distribution of the error function in Equations 2.17 and 2.18. A similar error was evidenced by Ahsanuzzaman et al. (2003).

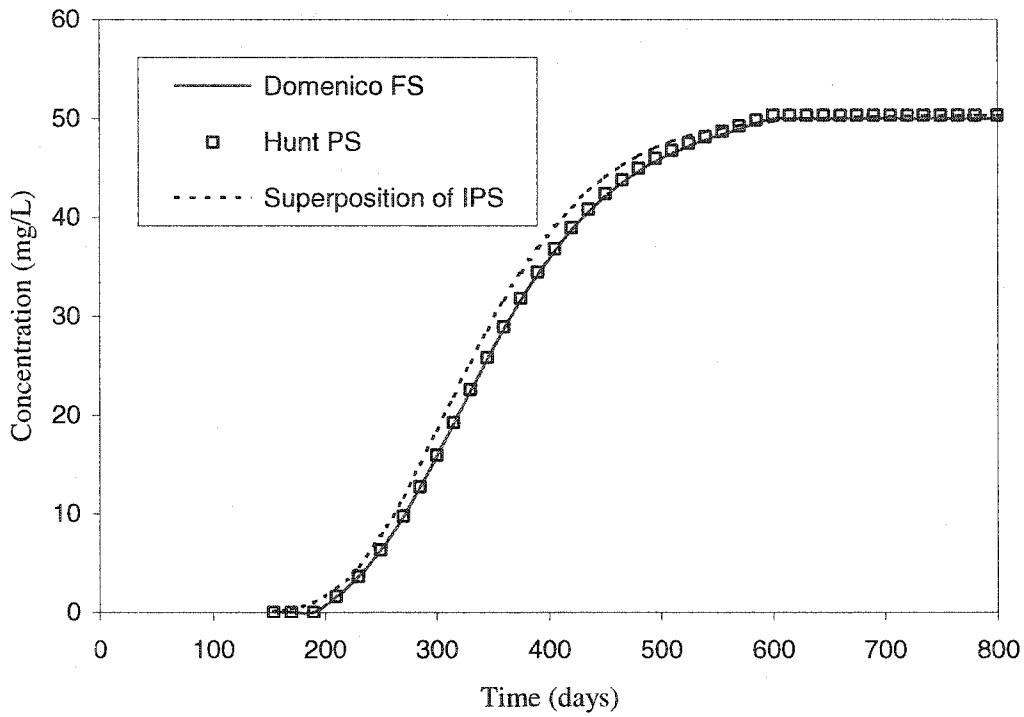


Figure 2.2. Comparison between the continuous source models and superposition in time of an instantaneous point source model.

2.7. Analytical Model for Instantaneous Point Source in a Semi-Infinite Domain

To derive the solution of the ADE for sources at the water table (i.e., in a semi-infinite domain), one can either consider that the mass (M) is spreading in a semi-infinite cylinder as opposed to an infinite cylinder in Crank's (1956) solution or that the point mass source is a hemisphere instead of a sphere in Sun's (1996) solution. Both of these

considerations mean that the mass (M) is spreading in half of the volume available for an infinite domain, which means the concentration should be two times of that for the infinite vertical domain. Therefore, the analytical solution for an instantaneous point source at the top of the water table can be given by Equation 2.19.

$$C(x,y,z,t) = \frac{M/n}{4(\pi t)^{3/2}\sqrt{D_x D_y D_z}} \exp\left\{-\frac{(x - v_x t)^2}{4D_x t} - \frac{y^2}{4D_y t} - \frac{z^2}{4D_z t}\right\} \tag{2.19}$$

According to Domenico and Robbins (1985), the finite source model for a source at the top of the aquifer can be obtained by replacing the $Z_S/2$ term with Z_S in Equation 2.13. Therefore, the instantaneous finite source model for a source at the water table is,

$$C(x,y,z,t) = \frac{M/n}{8X_S Y_S Z_S}\left[erf\left(\frac{x - v_x t + X_S/2}{2\sqrt{D_x t}}\right) - erf\left(\frac{x - v_x t - X_S/2}{2\sqrt{D_x t}}\right)\right]$$
$$\left[erf\left(\frac{y + Y_S/2}{2\sqrt{D_y t}}\right) - erf\left(\frac{y - Y_S/2}{2\sqrt{D_y t}}\right)\right]\left[erf\left(\frac{z + Z_S}{2\sqrt{D_z t}}\right) - erf\left(\frac{z - Z_S}{2\sqrt{D_z t}}\right)\right] \tag{2.20}$$

To verify the instantaneous point source model for a source at the water table (Equation 2.19), it is compared with the Domenico and Robbins (1985) model (Equation 2.20). Figure 2.3 shows the breakthrough curves at an observation point 400 ft away from the source for both models. The source dimensions (Xs = 30.98 ft, Ys = 9.8 ft, and Zs = 1.55 ft) used in the simulation are obtained from Equation 2.14 with the exception that the $Z_S/2$ term is replaced by Z_S. The velocity and mass input are considered to be 1.17 ft/day and 100 Kg, respectively. It is evident from Figure 2.3 that breakthrough curve for the instantaneous point source model for source at the water table matches perfectly with

that of the finite source model. Therefore, the equation derived for instantaneous point source is acceptable (Equation 2.19).

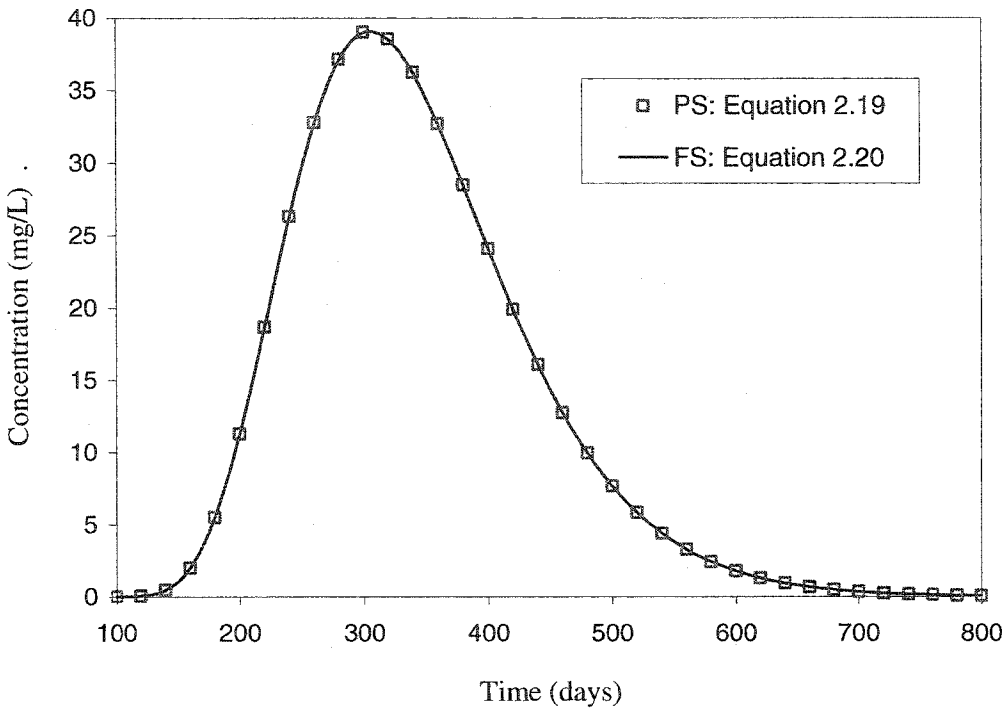


Figure 2.3. Comparison between the instantaneous point source (PS) and finite source (FS) models for a semi-infinite domain.

2.8. Instantaneous Point and Finite Source Models for Finite Aquifer Thickness

One major limitation of the aforementioned analytical models is that the depth or thickness of the aquifer is assumed infinite. However, in reality aquifers are finite with variable thicknesses. The analytical models for an infinite vertical domain would underestimate the downgradient concentrations if the solute reaches the bottom of the aquifer during migration. Crank (1956) used the method of images to develop a one-dimensional dispersion model for a finite system. Similarly, by applying the method of

images to the function representing the vertical dimension of Equation 2.20, the following equation is derived herein for an instantaneous finite source in a three-dimensional finite aquifer.

$$C(x,y,z,t)=\frac{M/n}{8X_S Y_S Z_S}\left[erf\left(\frac{x-v_x t+X_S/2}{2\sqrt{D_x t}}\right)-erf\left(\frac{x-v_x t-X_S/2}{2\sqrt{D_x t}}\right)\right]\times$$
$$\left[erf\left(\frac{y+Y_S/2}{2\sqrt{D_y t}}\right)-erf\left(\frac{y-Y_S/2}{2\sqrt{D_y t}}\right)\right]\times \qquad (2.21)$$
$$\left[erf\left(\frac{z+Z_S}{2\sqrt{D_z t}}\right)-erf\left(\frac{z-Z_S}{2\sqrt{D_z t}}\right)+\sum_{h=-\infty}^{\infty}\left\{erf\left(\frac{z+Z_S-2hH}{2\sqrt{D_z t}}\right)-erf\left(\frac{z-Z_S-2hH}{2\sqrt{D_z t}}\right)\right\}\right]$$

where, H is the aquifer thickness, and h is the number of series (images) to include.

Similarly, three-dimensional instantaneous point source model for finite aquifers is derived by applying the method of images in the z-direction of Equation 2.19 (see Equation 2.22).

$$C(x,y,z,t)=\frac{M/n}{4(\pi t)^{3/2}\sqrt{D_x D_y D_z}}\exp\left\{-\frac{(x-v_x t)^2}{4D_x t}-\frac{y^2}{4D_y t}\right\}\times$$
$$\left[\exp\left(-\frac{z^2}{4D_z t}\right)+\sum_{h=-\infty}^{\infty}\left\{\exp\left(-\frac{(z-2hH)^2}{4D_z t}\right)\right\}\right] \qquad (2.22)$$

The analytical models for finite aquifer thickness are verified against a numerical model, Visual MODFLOW (WHI, 1999). This provides a Windows-based pre- and post-processing interface for MODFLOW (McDonald and Harbaugh, 1988) and MT3D (Zheng, 1990). The following subsections present the setup and simulation of the numerical model.

2.8.1 Numerical Model Setup

First, the numerical model is calibrated against the existing point source model for a semi-infinite vertical domain (Equation 2.19). The semi-infinite vertical domain is ensured by assigning a large enough model domain in the vertical direction so that the plume does not reach the bottom layer of the model. Then, the model domain in the vertical direction is reduced to a size where the boundary effect is considerable. Breakthrough curves (BTC) generated from the numerical model with the smaller aquifer thickness is then compared to that from the analytical model.

The input parameters needed for the numerical model are hydraulic conductivity, porosity, hydraulic gradient, and dispersitivity in longitudinal, lateral, and vertical directions. Hydraulic conductivity and porosity are assumed to be 70 ft/day and 0.3, respectively, which are common values for fine sand (Morris and Johnson, 1967). The hydraulic gradient is assumed to be 0.005; longitudinal, lateral, and vertical dispersitivities are assumed to be 15, 1.5, and 0.15 ft, respectively; molecular diffusion is negligible.

The width and depth of the domain are selected to ensure that the plume does not reach the boundary, as the analytical models assume an infinite domain. According to Baetsle (1969), 99.7% of the mass is conserved within $3\sqrt{(2Dt)}$ from the center of the plume in all three directions, where D is the coefficient of dispersion in the respective directions and t is the simulation time. The time for the groundwater to travel 2,000 ft, along with the lateral and vertical dispersion coefficients, are applied to the expression given by Baetsle (1969) to estimate the maximum possible plume width and thickness. To ensure infinite lateral and vertical domain, the width and depth of the model domain

are set greater than the respective maximum values. Thus, the model domain is selected to be 2,000 ft long, 600 ft wide, and 120 ft deep.

A constant head at the upgradient and downgradient boundaries, no-flow boundaries at the bottom, and linearly varying constant head boundary at the lateral sides of the model domain are selected for the flow model. The groundwater heads at the upgradient and downgradient boundaries are selected to be 120 and 110 ft, respectively, which gives a uniform gradient of 0.005. For the transport model (MT3D), an initial concentration of 10,000 mg/L is assigned to one cell at the top of the aquifer.

Several solution methods are available in MT3D. These are MOC (Method Of Characteristics), MMOC (Modified Method Of Characteristics), HMOC (Hybrid Method Of Characteristics), UFD (Upstream Finite Difference), and CFD (Central Finite Difference). The MOC uses a conventional particle tracking technique based on a mixed Eularian-Lagrangian method for solving the advection term. Processing speed and memory requirement of the MOC is improved in MMOC. The HMOC technique combines the strengths of the MOC and MMOC techniques by using an automatic adaptive scheme that uses the MOC technique at sharp concentration fronts and the MMOC technique away from the front (Visual MODFLOW, 1999). The advantage of all of the method-of-characteristic techniques is that they are virtually free from numerical dispersion. However, these techniques are known to have problem in conservation of mass (Visual MODFLOW, 1999). Conversely, the finite difference methods (UFD and CFD) show better agreement in conservation of mass, but these methods can give numerical dispersion for sharp concentration fronts. The UFD method is more susceptible

to numerical dispersion than the CFD (Visual MODFLOW, 1999; Zheng and Bennett, 2002). Therefore, the CFD is selected for simulation of MT3D.

Selection of a grid size for numerical models is important to minimize numerical dispersion as well as to avoid numerical errors associated with artificial oscillations (Zheng and Bennett, 2002). Numerical oscillations are more likely when a sharp concentration front is present. To minimize this effect, the grids are designed to maintain a grid Peclet Number (PN), which is the ratio of grid spacing to dispersitivity, less than or equal to 2 (Huyakorn and Pinder, 1983). Since longitudinal dispersion is assumed to be 15 ft for the simulation, the maximum longitudinal grid spacing from the PN limit is 30 ft. Another source of numerical error lies in the approximation of the time-step size, which can be controlled by restricting the Courant Number (CN), which is defined to be $v_x\Delta t/\Delta x$. To obtain a stable and sufficiently accurate solution, it is often required that the CN be less than or equal to one (Zheng and Bennett, 2002). Therefore, the CN for the model simulation is selected to be 0.75.

2.8.2 Adjustment of grid spacing in the Numerical Model

The grid spacing is adjusted to match the BTC generated from the numerical model with the same from the analytical model (Equation 2.19). Four uniform grid configurations were selected for comparison with the analytical model. Figure 2.4 shows the concentration BTC at an observation point, 300 ft away from the source, for all grid configurations. It is observed from Figure 2.4 that of all grid configurations attempted, the BTC for the 10×10×5 ft (length×width×depth) grid produces the closest match with the BTC from the analytical model. To verify the calibration at additional locations, ten observation points along the direction of flow are selected. Since transport is

predominantly in the longitudinal direction, the observation points are selected along that direction. The concentration ratio (CR), defined as the ratio of maximum concentration of the BTC for the numerical and analytical models, are determined at each observation point. Figure 2.5 shows the variation of CR with the longitudinal distance for all grid configurations examined. It is observed that the CR values are not consistent with the longitudinal distance. Although the 10×10×5 ft grid configuration matches better with the analytical model at 300 ft from the source, the match is not good away from the source. The most inconsistent conditions are observed for the observation points closer than 300 ft from the source. This is because the source is relatively close to the observation point and the source size relative to the distance is too large to be defined as a point. To avoid this, any observation points closer than 300 ft are not considered.

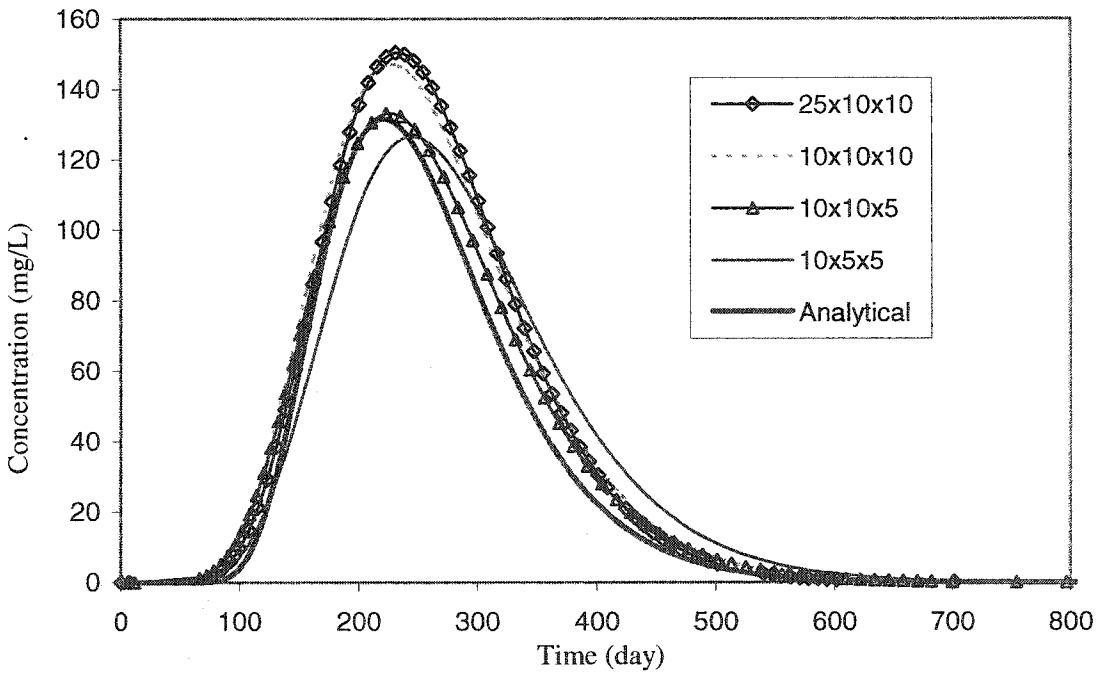


Figure 2.4. Comparison between the numerical and analytical models for uniform grid spacing.

To further adjust the numerical model, five non-uniform grid configurations were selected (Table 2.1). A finer grid spacing was selected at or near the source to minimize the numerical dispersion. Away from the source, a 25-ft grid spacing was selected in the longitudinal direction, since it was found that this spacing shows better calibration away from the source (see Figure 2.5). It also helps to reduce the simulation time. Twenty-eight observation wells, fourteen in the longitudinal and fourteen in the lateral direction were selected for calibration. The wells in the longitudinal direction are spaced at 100 ft intervals, starting at 305 ft away from source. The observation wells in the lateral direction are placed within 120 ft from the center of plume. Each well has five observation points at 0, 2.5, 5, 7.5, 11.25, and 16.25 ft depths from the source, giving a total of one-hundred-forty observation points for model calibration. The CR values for each observation point are calculated from the numerical and analytical model outputs. One-sample t-test is conducted with SPSS, a statistical software package, to determine the grid configuration that most closely matches the analytical model. Table 2.2 presents the statistical evaluation of the CR values for all grid configurations. It is observed that the mean CR for GC4 is closest to one, which is the perfect condition. Although the mean CR for GC1 is 2.5% greater than the perfect condition, it has the lowest value of standard deviation, standard error, and 95% confidence interval, hence, was selected. Figure 2.6 shows the concentration BTCs generated from the numerical (GC1) and analytical models at two observation points. It is observed that the BTCs from the numerical and analytical models match very well.

Table 2.1. Non-uniform grid configurations.

Name	Source size (ft)	Rows	Columns	Layers
GC1	5×5×2.5	[Ψ]6×2.5′; 5×5′; rest 10′	1×5′; 4×10′; 1×20′; rest 25′	3×2.5′; 2×5′; rest 10′
GC2	5×5×2.5	6×2.5′; 5×5′; rest 10′	3×5′; 5×10′; rest 25′	3×2.5′; 2×5′; rest 10′
GC3	5×5×2.5	6×2.5′; 5×5′; rest 10′	5×5′; 4×10′; rest 25′	3×2.5′; 2×5′; rest 10′
GC4	5×5×2.5	6×2.5′; 5×5′; rest 10′	7×5′; 3×10′; rest 25′	3×2.5′; 2×5′; rest 10′
GC5	5×5×2.5	6×2.5′; 5×5′; rest 10′	1×5′; 6×10′; rest 25′	3×2.5′; 2×5′; rest 10′

[Ψ] From the edge of the source, 6 rows @ 2.5 ft intervals, and rest are @ 10 ft intervals

Table 2.2. Statistical evaluations of the concentration ratio.

Name	Mean	Standard Deviation	Standard Error	95% Confidence Interval		
				Lower	Upper	Difference
GC1	1.025	0.095	0.0084	1.0092	1.0425	0.0333
GC2	1.051	0.134	0.0114	1.0281	1.0730	0.0449
GC3	0.969	0.144	0.0122	0.9449	0.9932	0.0483
GC4	0.996	0.125	0.0106	0.9756	1.0174	0.0418
GC5	1.081	0.219	0.0186	1.0448	1.1180	0.0732

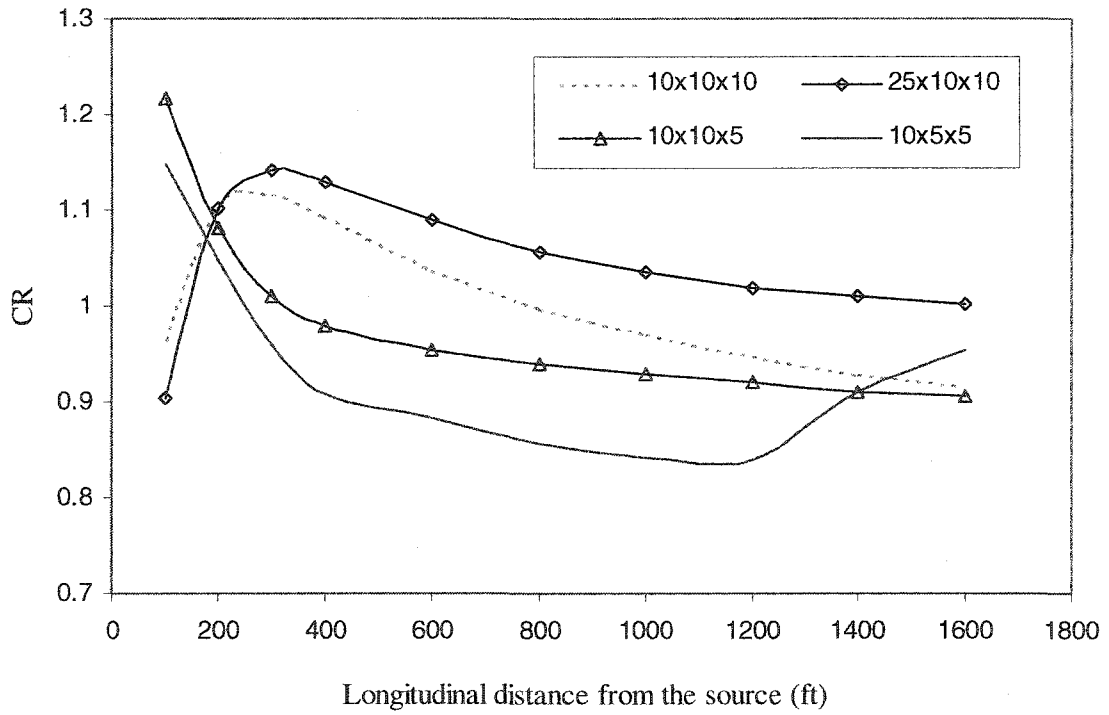


Figure 2.5. Maximum concentration ratio (CR) along the direction of flow.

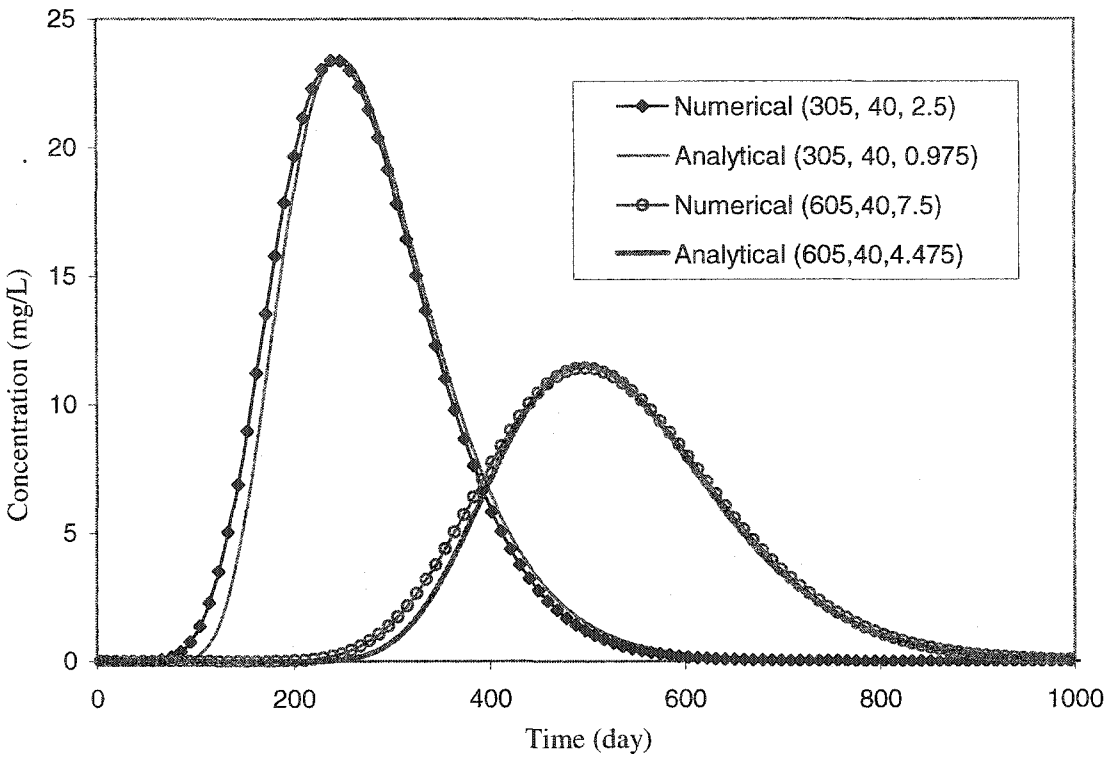


Figure 2.6. Comparison between the selected numerical (GC1) and analytical models.

2.8.3 Verification of Analytical Models for Finite Aquifer

It is evident from Equation 2.21 that the effect of aquifer thickness would be larger for smaller values of the dimensionless term $H/\sqrt{(D_z t)}$ or, $H/\sqrt{(D_z x/v_x)}$ at the peak concentration. In order to verify the analytical model for finite aquifer thickness, the numerical model is run for a smaller aquifer thickness (H) than that used for calibration. The aquifer thickness (H) and the vertical dispersivity (α_z) values selected for the simulation are 15 ft and 0.15 ft, respectively. The breakthrough curves from both analytical and numerical models are generated for two arbitrarily chosen observation points at 705 and 1,005 ft from the source. Figure 2.7 shows a comparison between the two models. It is observed that the smaller aquifer thickness caused an increase in the

concentration for both observation points. At 705 ft away from the source, the peak concentrations predicted by the analytical and numerical models are 1.24 and 1.19 times higher than that for the semi-infinite model (Equation 2.19), respectively. The corresponding peak concentrations at 1,005 ft away from the source are 1.52 and 1.40 times higher than that for the semi-infinite model. It is also observed that the breakthrough curves for the analytical and numerical models do not match perfectly and the difference increases with the distance from the source. The peak concentrations at 705 and 1,005 ft from the numerical model are 4 and 8% smaller than the analytical model, respectively. This inconsistency might be attributed to numerical dispersion, since the breakthrough curves from the numerical model are wider than those from the analytical model. It could also be due to not finding a grid configuration that shows perfect match during grid adjustment, i.e., a CR value of 1 (see Section 2.8.2). However, this discrepancy in estimating the peak concentration can be considered minor, as prediction from the analytical model is conservative than the numerical model.

Besides comparing the peak concentration, it is also important to compare the total solute flux flowing through the observation cells. The difference in the flux can be assessed by comparing the area under the BTCs. It is evident from Figure 2.7 that the areas under the BTCs for the analytical and numerical models for finite aquifer are comparable. This shows that the analytical model for a finite aquifer produces comparable result. Also, the area under the BTC for the semi-infinite analytical model is smaller than the same for the analytical and numerical models for finite aquifers. Such a smaller flux rate at the top of the aquifer for the semi-infinite model is obvious, as the plume spreads deeper than the finite aquifer thickness used in the other models.

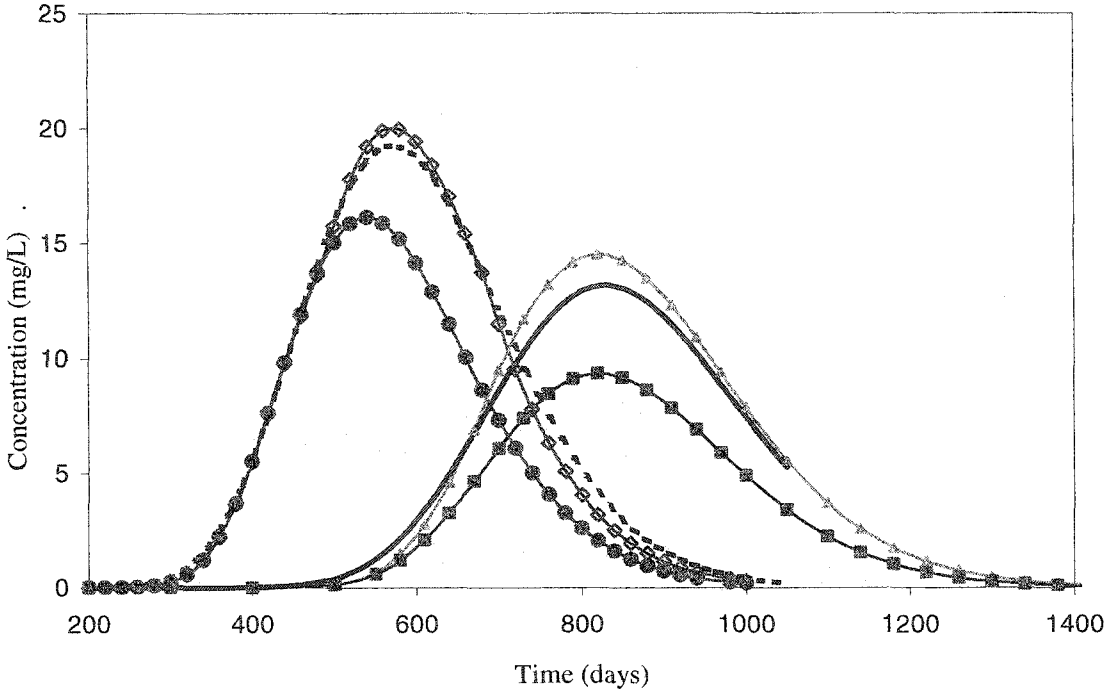


Figure 2.7. Verification of analytical model for finite aquifer thickness.

2.9. Conclusions

It was verified that superposition of instantaneous point sources in space and time is an effective technique for representing transient non-point sources. The equations derived for the limiting source dimension of a point source are necessary for applying superposition in space. Also, the equations for the limiting source dimension would justify the application of the analytical point source model for a given site. It was found that the limiting source dimension gives less than 1% error when compared with the finite source model. Analytical models for semi-infinite and finite aquifers were also derived in this study. The models for semi-infinite and finite aquifers could be applied in conditions where the contaminants are leaching from the soil surface to the water table. The

analytical model for a finite aquifer showed a better match with the numerical model near the source. However, the peak concentration estimated by the analytical model is slightly higher than that for the numerical model away from the source.

References

Ahsanuzzaman, A. N. M., M. Zaman, and R. L. Kolar. 2003. Limiting Source Dimensions of Three-Dimensional Analytical Point Source Model for Solute Transport. Proceedings of the 23rd annual AGU hydrology days. Colorado State University, Fort Collins, CO.

Baetsle, L. H. 1969. Migration of Radionuclides in Porous Media, Progress in Nuclear Energy, Series XII, Health Physics, ed. A. M. F. Duhamel Pergamon Press, Elmsford, NY. Pp. 707-730.

Cleary, R. W., and M. J. Ungs. 1978. Analytical Methods for Ground Water Pollution and Hydrology. Water Resources Program Report: 78-WR-15. Princeton University, Princeton, NJ.

Crank, J. 1956. *The Mathematics of Diffusion*. Oxford University Press Inc., New York, NY.

Domenico, P. A. 1987. An Analytical Model for Multidimensional Transport of a Decaying Contaminant Species. *Journal of Hydrogeology*. 91:49-58.

Domenico, P. A., and G. A. Robbins. 1985. A New Method of Contaminant Plume Analysis. *Ground Water*. 23(4): 51-59.

Fetter, C. W. 1999. *Contaminant Hydrogeology*. 2nd Edition. Prentice-Hall, NJ.

Hunt, B. 1978. Dispersive Sources in Uniform Ground-Water Flow, Journal of the Hydraulics Division, Proceeding of American Society of Civil Engineering. 104:75-85.

Huyakorn, P.S., and G. F. Pinder. 1983. *Computational Methods in Subsurface Flow*. Academic Press, San Diego, CA.

Leij, F. J., T. H. Skaggs, and M. T vanGenuchten. 1991. Analytical Solutions for Solute Transport in Three-Dimensional Semi-Infinite Porous Media. *Water Resources Research*. 27(10): 2719-2733.

Martin-Hayden, J. M., and G. A. Robbins. 1997. Plume Distortion and Apparent Attenuation Due to Concentration Averaging in Monitoring Wells. *Ground Water*. 35(2): 339-346.

McDonald, M. G., and A. W. Harbaugh. 1988. MODFLOW: A Modular Three-Dimensional Finite-Difference Groundwater Flow Model. U. S. Geological Survey, Reston, VA.

Morris D. A., and A. I. Johnson. 1967. Summary of Hydrologic and Physical Properties of Rock and Soil Materials as Analyzed by the Hydrogeologic Laboratory of the U. S. Geological Survey. Water Supply Paper 1839-D. U.S. Geological Survey.

Neville, C. J. 1994. Compilation of Analytical Solutions for Solute Transport in Uniform Flow. S. S. Papadopulos & Associates, Bethesda, MD.

Park. E., and H. Zhan. 2001. Analytical Solutions of Contaminant Transport from Finite One-, Two-, Three-Dimensional Sources in a Finite-Thickness. *Journal of Contaminant Hydrology*. 53: 41-61.

Sim, Y., and C. V. Chrysikopoulos. 1999. Analytical Solutions for Solute Transport in Saturated Porous Media with Semi-Infinite or Finite Thickness. *Advances in Water Resources*. 22(5): 507-519.

Sun, N. Z. 1996. *Mathematical Modeling of Groundwater Pollution*. Springer, NY.

Turner, G. A. 1972. *Heat and Concentration Waves*. Academic Press, New York, NY.

USSL 1994. 3DADE: A Computer Program for Evaluating Three-Dimensional Equilibrium Solute Transport in Porous Media, Research Report No. 134, U. S. Salinity Laboratory, Riverside, CA.

WHI 1999. *Visual MODFLOW User's Manual*, Waterloo Hydrogeologic Inc., Ontario, Canada.

Wexler, E. J. 1992. Analytical Solutions for Chemical Transport in Ground-Water Systems with Uniform Flow. Techniques of Water-Resources Investigations, Book 3. U. S. Geological Survey.

Yeh, G. T. 1981. AT123D: Analytical Transient One-, Two-, and Three-Dimensional Simulation of Waste Transport in an Aquifer System. Report ORNL-5602. Oak Ridge National Laboratory, Oak Ridge, TN.

Zheng, C. 1990. MT3D: A Modular Three-Dimensional Transport Model for Simulation of Advection, Dispersion and Chemical Reactions of Contaminants in Groundwater Systems. Robert S. Kerr Environmental Research Center, U.S. EPA, Ada, OK.

Zheng, C., and G. D. Bennett. 2002. *Applied Contaminant Transport Modeling*, 2nd ed., John Wiley & Sons Inc., NY.

Chapter 3: Regression Model for Estimating Flow Through the Vadose Zone

Abstract

Regression models are developed in this study to characterize the breakthrough curve for drainage to the water table from application of water at the soil surface. The variables required to characterize the breakthrough curve are time for initial breakthrough (T_1), time to reach the maximum flow rate (T_2), and times for recession to reach 30 ($T_{4\text{-}30}$) and 10 ($T_{4\text{-}10}$) percent of the surface application rate following cessation of the surface load. The data generated for developing the regression models was obtained from numerical model simulations. A parameter, called breakthrough time, is defined to develop correlations for T_1 and T_2. Breakthrough time is defined as a function of the hydraulic properties of unsaturated soil, initial moisture within the soil, and the depth of water table. Two other parameters, named recession time for soils with high and low hydraulic conductivity, are similarly defined to develop a correlation for the recession times ($T_{4\text{-}30}$ and $T_{4\text{-}10}$). Power-type (log-log) regression models showed the best correlation for all variables. The R-squared values and the standard errors of estimations at 95 percent level of significance showed a strong correlation for the regression models of T_1 and T_2 during model generation. Strong correlations were also obtained for $T_{4\text{-}30}$ and $T_{4\text{-}10}$ for soils with high hydraulic conductivity, while the correlations for the same models for soils with low hydraulic conductivity were not as satisfactory. Model

validation showed strong correlations for T_1 and T_2 for all soils, and $T_{4\text{-}30}$ and $T_{4\text{-}10}$ for soils with a high hydraulic conductivity also.

3.1. Introduction

Flow of water through unsaturated soil generally occurs in three stages: infiltration, redistribution, and drainage or deep percolation (Ravi and Williams, 1988). Infiltration is defined as the initial process of water flowing through the soil due to application of water at the soil surface. This stage is also called surface infiltration. During this stage, capillary forces or matric potential are dominant. Redistribution occurs after cessation of water application at the soil surface. During redistribution, the gravitational forces (water head), as well as matric potential, are dominant forces. Redistribution is also called the drying phase. Finally, drainage or deep percolation occurs when the wetting front reaches the water table. Collectively these three stages of water movement are usually called infiltration (Ravi and Williams, 1988).

Analysis of water flow through the vadose zone is complicated due to the presence of air in the pore spaces of unsaturated soils. With the presence of air in the pore spaces, the hydraulic properties of unsaturated soils vary from that of saturated soils. Green and Ampt (1911) and Richards (1928) proposed physics-based equations for analyzing flow through the vadose zone. Green and Ampt (1911) first derived a physics-based equation for infiltration of water into soil. They assumed a piston-like water content profile with a well-defined wetting front. For the piston-like profile, the soil is saturated from the surface to the wetting front. At the wetting front, the water content drops abruptly to the initial water content of that location. Because of its simplicity and

the need for few hydraulic parameters, the Green-Ampt equation is widely-used for infiltration estimation in many hydrologic models (Ravi and Williams, 1998). Richards' equation was developed by combining the Darcy's law and the equation of continuity. Unlike the Green-Ampt equation, water content at the wetting front gradually decreases from saturation to initial water content in Richards' equation. Therefore, Richards' equation is scientifically more acceptable than the Green-Ampt model for estimating flow through the vadose zone. A comparison between Richards' equation and the Green-Ampt model in estimating the distance traveled by the wetting front is presented in Appendix E.

Williams et al. (1998) presented a set of infiltration models applicable to a variety of hydrogeologic and climatic conditions. Williams et al. (1998) categorized all the available models into six types based on their application, simplicity, and on the ability to handle various types of boundary conditions. The six categories, as listed, are: semi-empirical, homogeneous, non-homogeneous, ponding, non-ponding, and wetting-and-drying models. All models, except the semi-empirical models, are based on either the Green-Ampt or Richards' equations. A common limitation of these models is that they are only useful for estimating the surface infiltration rate, not the drainage to the water table. None of the models presented by Ravi and Williams (1988) and by Williams et al. (1988) considered finite column length as the boundary condition required for drainage (i.e., at the water table the matric potential should be zero, or the moisture content should be the saturated moisture content). Therefore, these models are not useful for estimating the lag time between the surface application and the initial breakthrough at the groundwater table. Additional limitations of these infiltration models include the following: (1) they assume a constant and uniform initial soil water content profile, while

in reality water content is not constant with depth; and (2) almost all of the models assume constant and near saturation water content at the soil surface, while in reality water content at the soil surface could be much drier than saturation. Also, there are few analytical models available for estimating drainage and redistribution of soil moisture in a finite soil column (e.g., Warrick et al., 1990; Sisson et al., 1980); however, none of those give an analytical solution for the flux rate at the bottom of the soil column (i.e., to the water table).

It is evident from the literature that estimating the lag time between the surface application and the initial breakthrough at the groundwater table and the recession of the bottom flux rate following cessation of the surface application (i.e., the breakthrough curve for drainage) have not received much attention in the past. Numerical models are the best available tools for estimating the breakthrough curve for drainage. However, numerical modeling warrants skillful personnel and requires more model input and simulation time. Therefore, a tool for a simple and quick estimation of the drainage flux rate to the water table is warranted. This study presents a series of regression models to estimate the flux rate through the vadose zone to groundwater. Numerical model simulations for a variety of model inputs were used to generate the data required to develop these regression models.

3.2. Materials and Methods

3.2.1 Flow through Unsaturated Soil

Richards' (1931) equation for one-dimensional flow of water through unsaturated soil is developed by combining the Darcy's law and the equation of continuity. The general form of Richards' equation is given by

$$\frac{\partial \theta}{\partial t} = \frac{\partial}{\partial z}\left(K_{us} \frac{\partial h_{us}}{\partial z} \right) - \frac{\partial (K_{us})}{\partial z} \tag{3.1}$$

where, θ is volumetric water content and K_{us} and h_{us} are unsaturated hydraulic conductivity and soil suction potential, respectively.

In unsaturated soils, a negative pressure, called matric or suction potential (h_{us}), exists due to the presence of capillary forces in the air-water interfaces. The matric potential is a function of volumetric water content of soil (θ). The lower the water content, the higher the absolute value of the matric potential. The relationship between water content and matric potential of a soil is called the soil-water characteristic curve. If the soil-moisture curve is constructed based on data obtained from an initially saturated soil subjected to drying, the curve is called a drying curve. If the soil sample is rewetted to saturation, the soil-moisture curve is called a wetting curve. Typically, the wetting and drying curves do not follow the same path. This phenomenon is called hysteresis.

The presence of air in the pore spaces also changes the behavior of the hydraulic conductivity of soil. Because of the inability to transmit water by pore spaces occupied by air, soil at an unsaturated state has a lower hydraulic conductivity than that at saturation. Hydraulic conductivity of an unsaturated soil (K_{us}) is a function of the volumetric water content or the matric potential. The lower the volumetric water content, the lower is the unsaturated hydraulic conductivity. Several empirical models describe the hydraulic properties of unsaturated soil (e.g., volumetric water content and unsaturated hydraulic conductivity). Of those, Brooks and Corey (1966), and Van Genuchten (1980) are the most widely used (Williams et al., 1998).

The Brooks and Corey (1966) model for soil hydraulic properties is given by

$$S_e = \begin{cases} |\alpha h|^{-n}, & h < -1/\alpha \\ 1, & h \geq -1/\alpha \end{cases} \tag{3.2}$$

$$K_{us} = K_s S_e^{2/n+l+2} \tag{3.3}$$

where, α is the inverse of the air-entry value (or bubbling pressure), n is the pore size distribution index, h is the initial soil suction potential, l is the pore connectivity parameter, K_s and K_{us} are the hydraulic conductivities of the saturated and unsaturated soil, respectively, and finally, S_e is the effective water content, which is given by

$$S_e = \frac{\theta - \theta_r}{\theta_s - \theta_r} \tag{3.4}$$

where, θ, θ_r, and θ_s are the initial, residual, and saturated volumetric moisture content of the soil, respectively.

The Van Genuchten (1980) model for soil hydraulic properties is given by

$$\theta = \theta_r + \frac{\theta_s - \theta_r}{[1+|\alpha h|^n]^m}, \qquad h \leq 0 \tag{3.5}$$

$$K_{us} = K_s S_e^{\ l}[1-(1-S_e^{\ 1/m})^m]^2 \tag{3.6}$$

where,

$$m = 1 - 1/n\,, \qquad n > 1 \tag{3.7}$$

The Van Genuchten model contains five independent parameters: α, n, K_s, θ_r, and θ_s. These parameters define the hydraulic properties of unsaturated soils. Carsel and Parrish (1988) presented input values of these parameters for each USDA soil class (see Table 3.1). Finally, the pore connectivity parameter (l) in the hydraulic conductivity function is generally assumed to be 2.0 in the Brooks and Corey (1964) model, and 0.5 in the van Genuchten (1980) model for all soil types (Simunek et al., 1998).

Table 3.1. Unsaturated soil hydraulic properties for different USDA soil classes.

USDA soil types	θ_r	θ_s	n	α (cm^{-1})	K_s cm/day
Sand	0.045	0.43	2.68	0.145	713
Loamy Sand	0.057	0.41	2.28	0.124	350
Sandy Loam	0.065	0.41	1.89	0.075	106
Sandy Clay Loam	0.10	0.39	1.48	0.059	31.4
Loam	0.078	0.43	1.56	0.036	25.0
Silt Loam	0.067	0.45	1.41	0.02	10.8
Clay Loam	0.095	0.41	1.31	0.019	6.24
Silt	0.034	0.46	1.37	0.016	6.0
Clay	0.068	0.38	1.09	0.008	4.8
Sandy Clay	0.10	0.38	1.23	0.027	2.88
Silty Clay Loam	0.089	0.43	1.23	0.01	1.68
Silty Clay	0.07	0.36	1.09	0.005	0.48

Source: Carsel and Parrish (1988)

3.2.2 Numerical Model

There are many numerical models available for estimating drainage rates due to application of water at the soil surface. HYDRUS (Simunek et al., 1998) is a robust and widely accepted model. HYDRUS was developed by the U.S. Salinity Laboratory for simulating water, heat, and solute transport in one-dimensional, variably-saturated media. HYDRUS solves Richards' equation for variably saturated flow and the advection-dispersion equations for heat and solute transport. The governing equations are solved numerically using a Galerkin linear finite element scheme. The flow equation incorporates a sink term to account for water uptake by plant roots. The solute transport equation considers advective-dispersive transport in the liquid phase and diffusion in the gaseous phase. The solute transport equations also include provisions for nonlinear and nonequilibrium reactions between solid and liquid phases (sorption), linear equilibrium reactions for liquid and gaseous phases, zero order production, and first order degradation. The water flow part of the model can handle any head or flux boundary condition, as well as boundaries controlled by atmospheric conditions and free drainage.

3.2.3 *Conceptual Model for Flow through the Vadose Zone*

HYDRUS was used to generate the data required for developing the regression model. The conceptual model used for simulations is shown in Figure 3.1. A constant continuous flux rate (Q_{in}) is assumed at the soil surface, which represents a net flux of rainfall minus run off and evapotranspiration. A zero initial matric potential is assumed at the bottom of the soil profile to represent the initial location of the groundwater table. The initial condition within the soil profile is defined by assigning variable matric potential values with depth. It is assumed that the soil is initially dry at the surface and saturated at the bottom. The breakthrough curve (BTC) for bottom drainage is divided into four phases (Figure 3.1): Phase-1 is the time required for the wetting front to reach the water table; Phase-2 is the time for the flow at the bottom (Q_{drain}) to reach its peak value, which is equal to the flow rate at the surface (Q_{in}); Phase-3 is the time when the flow stays at the peak rate; and Phase-4 is the recession of the bottom flow following cessation of the top flux.

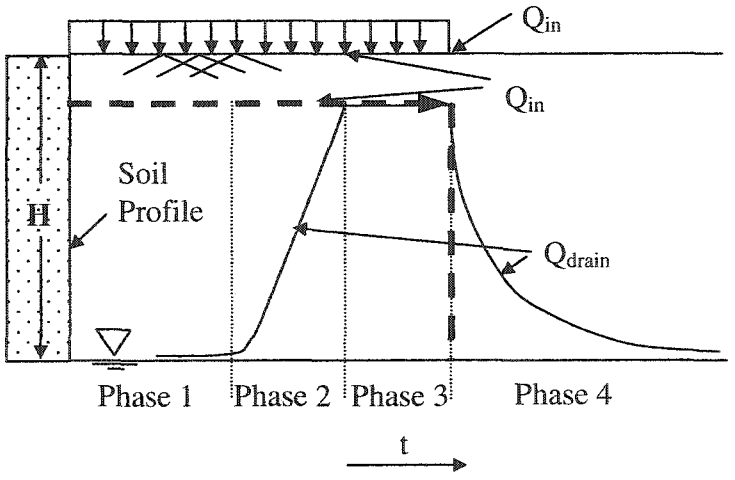


Figure 3.1. Conceptual model for flow through the vadose zone.

It should be noted that hysteresis of the soil-moisture characteristics curve is not considered in compiling HYDRUS. Since the boundary condition at the soil surface is continuous until the drainage rate reaches the surface inflow rate, the soil would experience only the wetting phase during the first three phases. However, the final phase (Phase-4) starts after cessation of the surface inflow rate, which means that the soil would experience drying during Phase-4. Therefore, it would be ideal to consider hysteresis for Phase-4. Since hysteresis is more pronounced for soils with low hydraulic conductivity, the limitation is only applicable to the regression model (Phase-4) for those soils.

3.2.4 Model Simulation

HYDRUS was run for different input values of surface flux (Q_{in}), water table depths (H), and initial conditions (soil matric potential versus depth from surface). For each set of input values (Q_{in}, H, and initial conditions), the model was run for all USDA soil classes. The Van Genuchten (1980) model for hydraulic properties of unsaturated soil (Equations 3.5 to 3.7) was used in the model simulations. The input values of the hydraulic properties for each USDA soil type were obtained from Carsel and Parrish (1988) (see Table 3.1). Six sets of simulations (a total of eighty-six simulations) were conducted with different input values of Q_{in}, H, and initial conditions (see Table 3.2). The input values for surface flux rates were assigned as a fraction of the saturated hydraulic conductivity by dividing that with an integer number (F). Three values of F (20, 50, and 100) were chosen for the simulations. The depth to the water table (H) was limited to shallow depths between 150 and 600 cm, which is within the range found at two irrigation facilities in Oklahoma. Initial conditions in the model were defined by assigning matric/suction potential values to each node in the soil profile. Two initial

conditions, named dry and wet conditions, were considered for each soil type. The dry condition assumed a linear variation in matric potential from the top (maximum at the soil surface) to the bottom, while the wet condition follows Equation 3.8.

$$h(y) = h_{top} \times \exp(-0.025 \times y) \quad (3.8)$$

where, h(y) is the matric potential at any distance y from the soil surface, and h_{top} is the matric potential at the soil surface. Figure 3.2 shows the initial conditions used in the simulations.

Table 3.2. Datasets used in simulating HYDRUS for developing the regression model.

Parameters	Unit	Dataset 1	Dataset 2	Dataset 3	Dataset 4	Dataset 5	Dataset 6
F^{ζ}	None	100	20	20	50	50	50
H	cm	150	300	600	600	300	150
h_{top}	cm	- 400	- 4000	- 4000	- 4000	- 4000	- 2000
Number of simulations	-	24	14	14	12	12	10

$^{\zeta} Q_{in} = K_s/F$

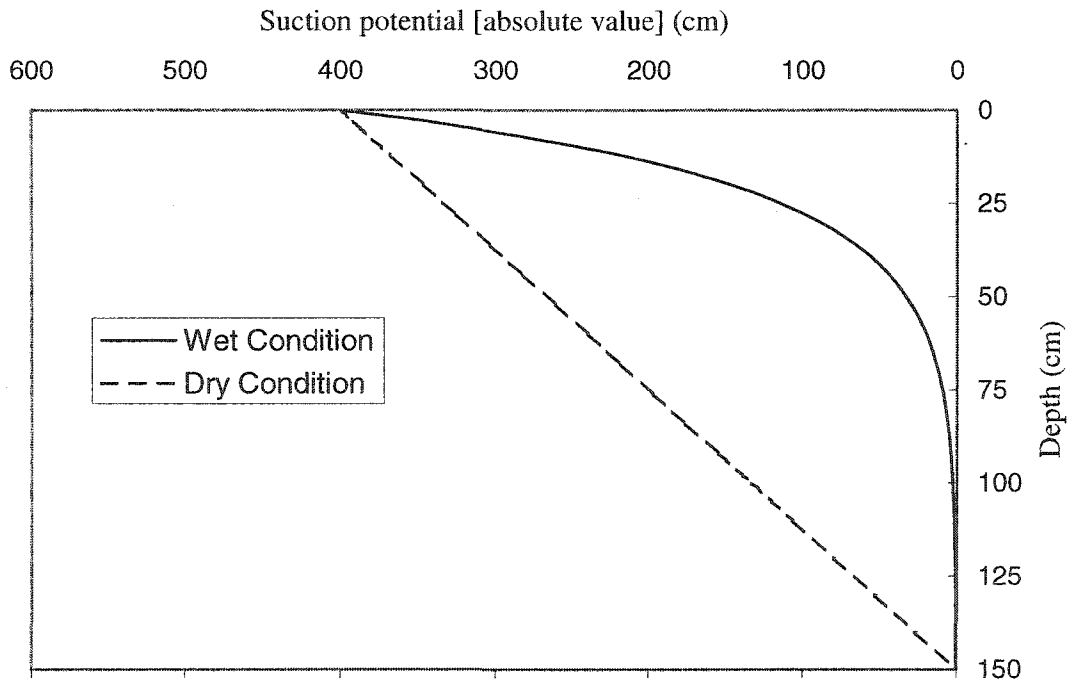


Figure 3.2. Initial conditions used in dataset-1

It should be noted that the regression model is not limited to the initial soil moisture profile, since the initial soil-moisture profile has been characterized in the regression model by a single term (A_i), which represents the volume of water present within the soil from the surface to the water table per unit soil area. The term 'A_i' is computed as the area under the soil moisture content versus depth profile, which is generated by applying Equation 3.5 to the initial conditions (soil matric potential versus depth profile). The first dataset was run for all twelve USDA soil classes with both dry and wet initial conditions (i.e., a total of 24 simulations), while the soil types are selected randomly for the rest of the datasets. From each compilation, the bottom drainage flux at each time step was obtained from the model output.

3.3. Results and Discussion

3.3.1 Development of the Regression Equations

As noted previously, the parameters required in defining the breakthrough curve for the drainage flow rate at the water table (Q_{drain}) are: time for initial breakthrough in Phase-1 (T_1); time to reach the surface flow rate (Q_{in}) in Phase-2 (T_2); and the parameters required to define the recession curve in Phase-4. In order to develop a regression model for estimating T_1, a single parameter called the breakthrough time (T_b) is defined. Equation 3.9 shows the expression for T_b.

$$T_b = \frac{H}{K_s/F}\frac{(\theta_s H - A_i)}{(\theta_s - \theta_r)H} \tag{3.9}$$

The first term in Equation 3.9, '$H/(K_s/F)$', has the unit of time. It represents the ratio of the travel distance (the depth of the water table, H) to the inflow rate (K_s/F), which is equivalent to the time required for a water particle to travel from the surface to

the water table when the soil is saturated. Since the soil is not fully saturated, a second unitless term, representing the soil moisture capacity, is multiplied by the first term. In the second term, $\theta_s H$ is the maximum amount of water that the soil profile can hold, and A_i is the amount of water present as initial moisture per square unit of the soil. Therefore, the numerator of the second term represents the amount of water required to saturate the entire soil profile. The denominator of the second term represents the maximum amount of water that can be drained out of the soil profile per unit square of the soil. Therefore, the second term represents the fraction of water required to infiltrate into the soil before the wetting front can reach the water table. It should be noted that the parameters α and n are not considered in defining T_b. These parameters represent the shape of the soil-moisture characteristic curve (Simunek et al., 1998; Piggott and Cawlfield, 1996). It is assumed that α and n would have insignificant effect on the breakthrough time within the respective range of values used for model development (see Table 3.1).

Figure 3.3 shows a scatter plot of T_l versus T_b and the linear regression model between the two parameters. Figure 3.4 shows the logarithmic plot of T_l versus T_b and the power-type ($T_l = cT_b^d$; where c and d are regression coefficients) or log-log regression model between the two parameters. The R-squared values (also called as the coefficient of determination) for the linear and the power-type models are 0.89 and 0.958, respectively. The R-squared value indicates the fraction of the variation in the dependent variable (T_l) that can be explained by the independent variable (T_b) (Irish et al., 1998). Therefore, the power-type model is more acceptable than the linear model, as it can explain 95.8 percent of the variation in T_l (Equation 3.10). The estimated regression coefficients, standard error of estimation, and the confidence limits (upper and lower) at

95 percent level of significance for the power-type regression model are presented in Table 3.3. The confidence limits (which is ± 2 times the standard error of estimation) show that there is a 95 percent probability that the true value of the regression coefficient is within the lower and upper limiting values (Irish et al., 1998). The standard errors of estimation are 12 and 2.25 percent of the estimated values of coefficients c and d, respectively (see Table 3.3). Figure 3.4 shows the lines for the upper and lower confidence limits (also called the confidence band) as well as the trend line for the power-type regression model for Phase-1. It is observed that all data points except one fall within the confidence band for 95 percent level of significance.

$$T_l = 0.225\ T_b^{0.927} \tag{3.10}$$

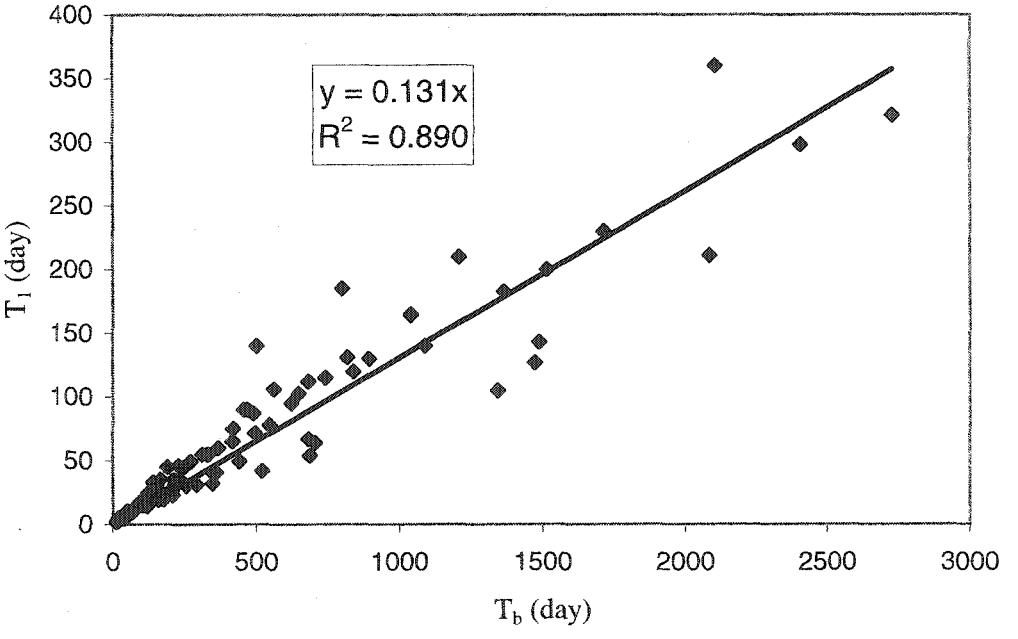


Figure 3.3. Scatter plot and linear regression model for Phase-1.

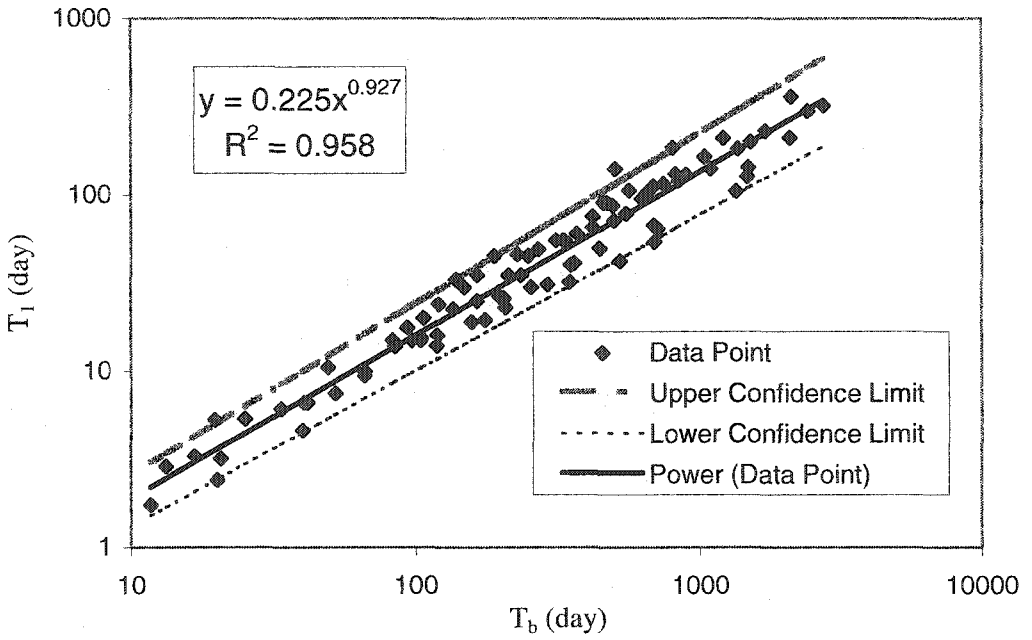


Figure 3.4. Logarithmic plot and regression model for Phase-1.

Table 3.3. Regression model for Phase-1

Coefficient	Estimate	Standard error	Upper limit$^{\zeta}$	Lower limit$^{\zeta}$
c	0.225	0.027	0.279	0.171
d	0.927	0.021	0.969	0.885

$^{\zeta}$ Confidence limits at 95% level of significance; $T_1 = cT_b^d$

Power-type and linear regression models are also used to estimate the time to reach the surface flow rate (Q_{in}) in Phase-2 (i.e., T_2). The breakthrough time, T_b in Equation 3.9, is againused as independent parameter in the regression model. It is evident from the R-squared values that the power-type model is better than the linear model for Phase-2 as well. Figure 3.5 shows a log-log plot for T_2 versus T_b, the trend line for the power-type regression model, and the confidence band at 95% level of significance. The R-squared value for the model is 0.944, which means that the model can explain 94.4%

of the variation of T_2. The estimated regression coefficients, standard error of estimation, and the confidence limits (upper and lower) at 95% level of significance for the power-type model are presented in Table 3.4. The standard error of estimation is 14.5 and 2.5% of the estimated values of coefficients e and f, respectively (see Table 3.4). Similar to Phase-1, only one data point falls outside the confidence band (see Figure 3.5).

$$T_2 = 0.268\ T_b^{0.97} \tag{3.11}$$

Table 3.4. Regression model for Phase-2

Coefficient	Estimate	Standard error	Upper limit$^{\zeta}$	Lower limit$^{\zeta}$
e	0.268	0.039	0.346	0.190
f	0.97	0.025	1.020	0.920

$^{\zeta}$ Confidence limits at 95% level of significance; $T_2 = eT_b^f$

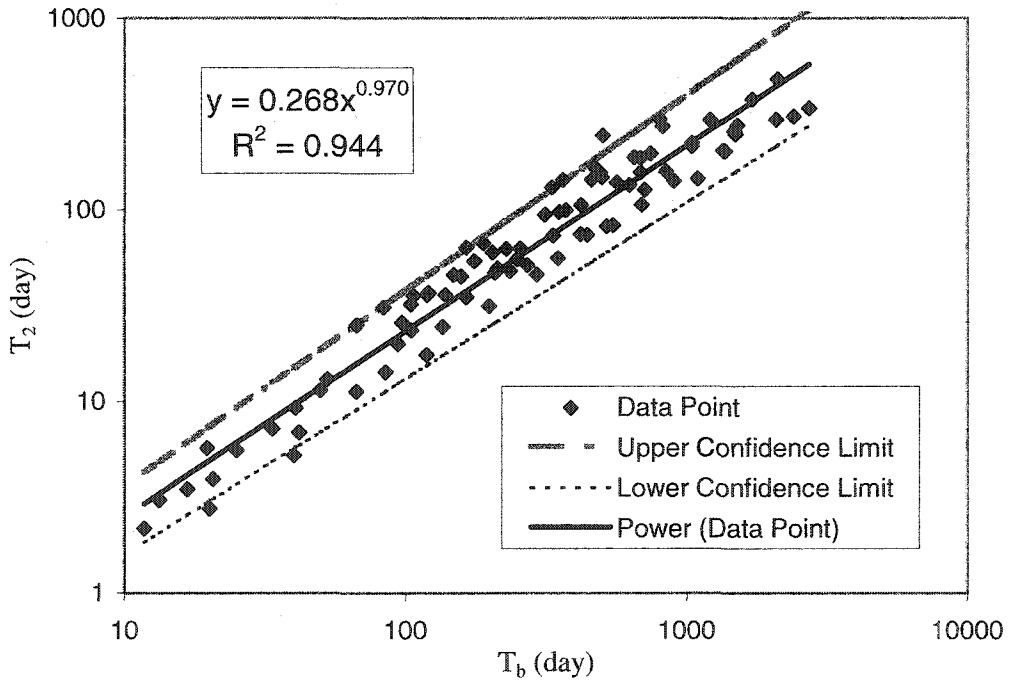


Figure 3.5. Logarithmic plot and regression model for Phase-2.

The recession curve for Phase-4 can be represented by an exponentially decaying curve. Figures 3.6 and 3.7 show the recession curve of the bottom flux for sandy-clay soil, simulated under the condition of Dataset 6 (see Table 3.1). The R-squared value of the exponential decay model for Q_{10} (i.e., 10% of inflow rate Q_{in}) is 0.965, while the same for Q_{30} (i.e., 30% of inflow rate Q_{in}) is 0.994. Similarly, for all the other datasets used for developing the regression model, the exponential decay curves show better matches for Q_{30} than Q_{10}. The R-squared values of the exponential decay curves for Q_{30} remain above 0.98 for all datasets, while the R-squared values for Q_{10} drop to about 0.90 for some observations. This happens because the recession curves for some observations start to become flatter and asymptotic (with the zero flow line) after dropping to flow rates smaller than Q_{30}, which causes the regression model to show inferior fit. Since the exponentially decaying model for Q_{30} shows a better match than Q_{10}, regression equations for estimating both times to reach 10 ($T_{4\text{-}10}$), and 30 ($T_{4\text{-}30}$) percent of the surface inflow rate were developed. If $T_{4\text{-}10}$ and/or $T_{4\text{-}30}$ could be estimated from the regression model, the decay rate (λ) of the recession curve could be obtained mathematically from the following equations:

$$\lambda_{10} = -(1/T_{4\text{-}10}) \times \text{Ln}\,(Q_{10}/Q_{in}) \text{ or,}$$

$$\lambda_{30} = -(1/T_{4\text{-}30}) \times \text{Ln}\,(Q_{30}/Q_{in}) \qquad (3.12)$$

where, λ_{10} and λ_{30} are the decay rates for reaching 10 and 30 percent of inflow rate, respectively. It should be noted that λ_{30} should be greater than or equal to λ_{10}, as the recession initially occurs at a faster rate, and then becomes slower with time (see Figures 3.6 and 3.7).

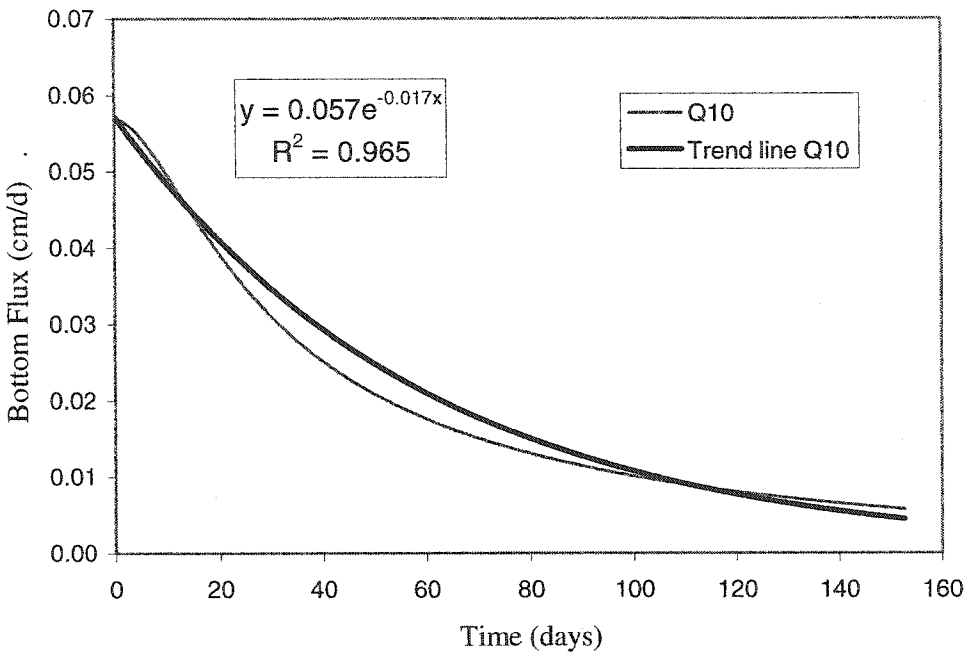


Figure 3.6. Recession curve for Phase-4 and trend line for Q_{10}.

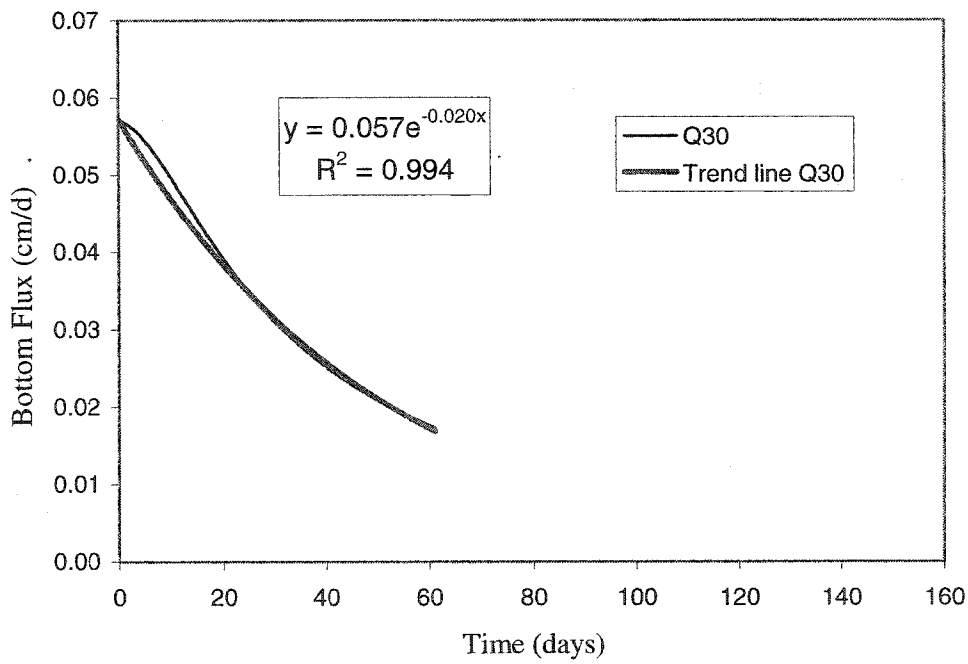


Figure 3.7. Recession curve for Phase-4 and trend line for Q_{30}.

To develop a regression model for estimating $T_{4\text{-}10}$ or $T_{4\text{-}30}$, a single parameter with the unit of time, called recession time (T_r), is defined (see Equation 3.13).

$$T_r = \frac{(\theta_s - \theta_r)H}{K_s/F} \tag{3.13}$$

The numerator in Equation 3.13 represents the maximum volume of water that can be drained from the soil profile per unit area, and the denominator represents the inflow rate at the soil surface. Figure 3.8 shows the scatter plot for all the data points and the corresponding power-type regression equations for $T_{4\text{-}10}$ and $T_{4\text{-}30}$. It is found that the R-squared values for $T_{4\text{-}10}$ and $T_{4\text{-}30}$ models are 0.659 and 0.725, respectively. These values are not as good as those of the models for Phase-1 or Phase-2. A relatively poor correlation resulted due to the numerator of Equation 3.13, where the second term reflects complete drainage. Usually, soils with a low conductivity retain more water than the residual water content (θ_r) following recession. Therefore, the regression model with the recession time (T_r) should be better for soils with higher K_s values. Figure 3.9 shows the regression model for $T_{4\text{-}10}$ and $T_{4\text{-}30}$ based on T_r for soils with high K_s ($\geq$ 25 cm/d), i.e., loam type soil or the others with higher K_s values. It is found that the R-squared values of $T_{4\text{-}10}$ and $T_{4\text{-}30}$ models (Equations 3.14 and 3.15) for soils with high K_s values improve to 0.936 and 0.946, respectively. The R-squared values of the same models for the soils with low K_s values (< 10.8 cm/d), i.e., silt loam type soil or the others with lower K_s values, are 0.067 and 0.136, respectively. Therefore, a better regression model needs to be developed for the soils with low K_s values.

$$T_{4\text{-}10} = 0.692\ T_r^{0.95} \tag{3.14}$$

$$T_{4\text{-}30} = 0.283\ T_r^{0.93} \tag{3.15}$$

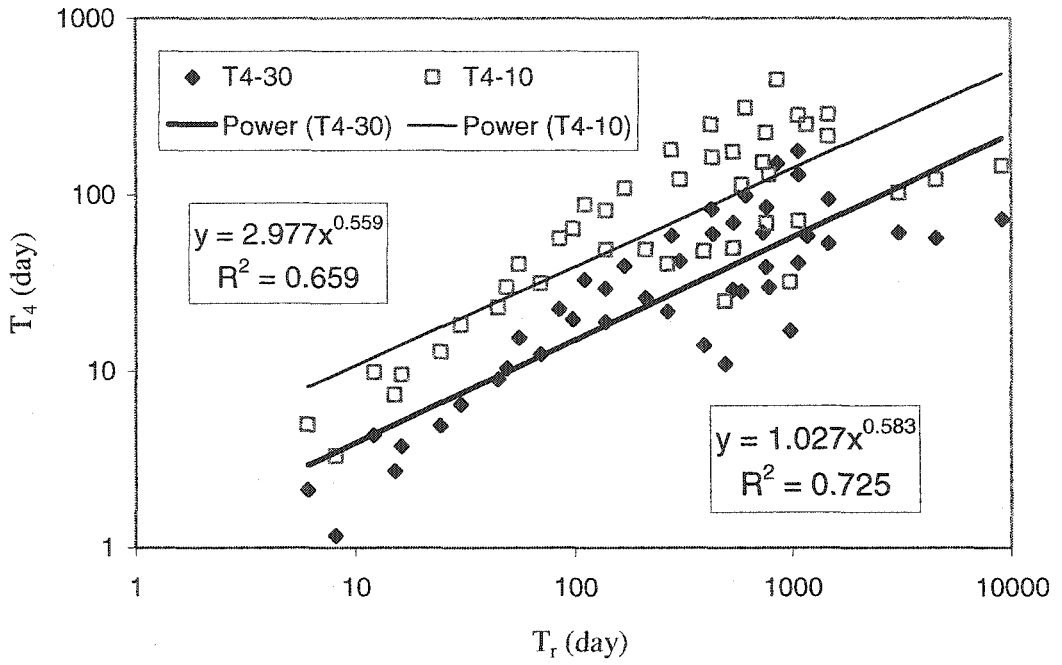


Figure 3.8. Regression model with all data for Phase-4.

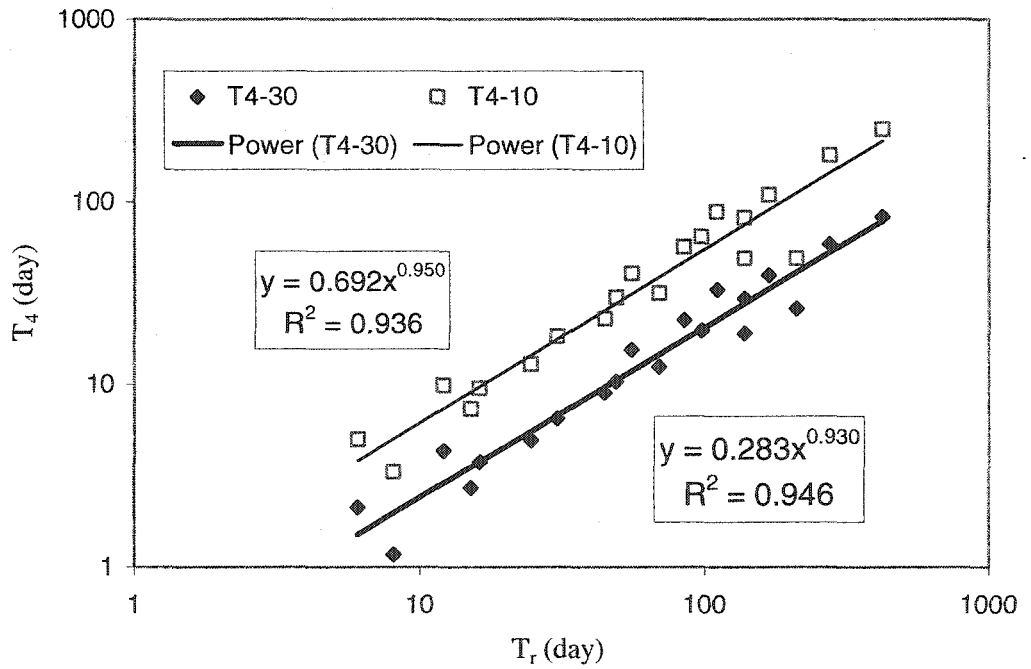


Figure 3.9. Regression model for soil with high Ks (Phase-4).

In order to develop a better regression model for soils with low K_s values, the recession time from Equation 3.13 needs to be redefined so that it can include the effect of water retained in the soil profile following recession. The recession time for soils with low K_s (T_{rl}) is redefined as Equation 3.16.

$$T_{rl} = \frac{(\theta_s - \theta_{rl})H}{K_s/F} \tag{3.16}$$

Equation 3.16 is obtained by replacing the residual moisture content (θ_r) in Equation 3.13 with a higher moisture content (θ_{rl}) following recession. Ideally, θ_{rl} should be the actual moisture content following recession. However, the θ_{rl} value varies with depth and with the time elapsed following cessation of surface inflow; hence, it is not possible to make a prior estimate of the θ_{rl} value. Regression models for estimating $T_{4\text{-}10}$ or $T_{4\text{-}30}$ from T_{rl} were attempted by assuming that the θ_{rl} value corresponds to a fraction of the maximum initial suction potential within the soil profile (h_m). A series of regression analyses was conducted with different suction potential values as a fraction of the h_m value. It was found that the θ_{rl} value corresponding to $h_m/6$ (using Equation 3.5) gives the best R-squared values (0.775) for $T_{4\text{-}30}$, and the θ_{rl} value corresponding to $h_m/5$ gives the best R-squared values (0.783) for $T_{4\text{-}10}$ (see Figure 3.10). The corresponding models for $T_{4\text{-}10}$ and $T_{4\text{-}30}$ are given by Equations 3.17 and 3.18, respectively.

$$T_{4\text{-}10} = 1.045\ T_{rl}^{0.872} \tag{3.17}$$

$$T_{4\text{-}30} = 0.684\ T_{rl}^{0.793} \tag{3.18}$$

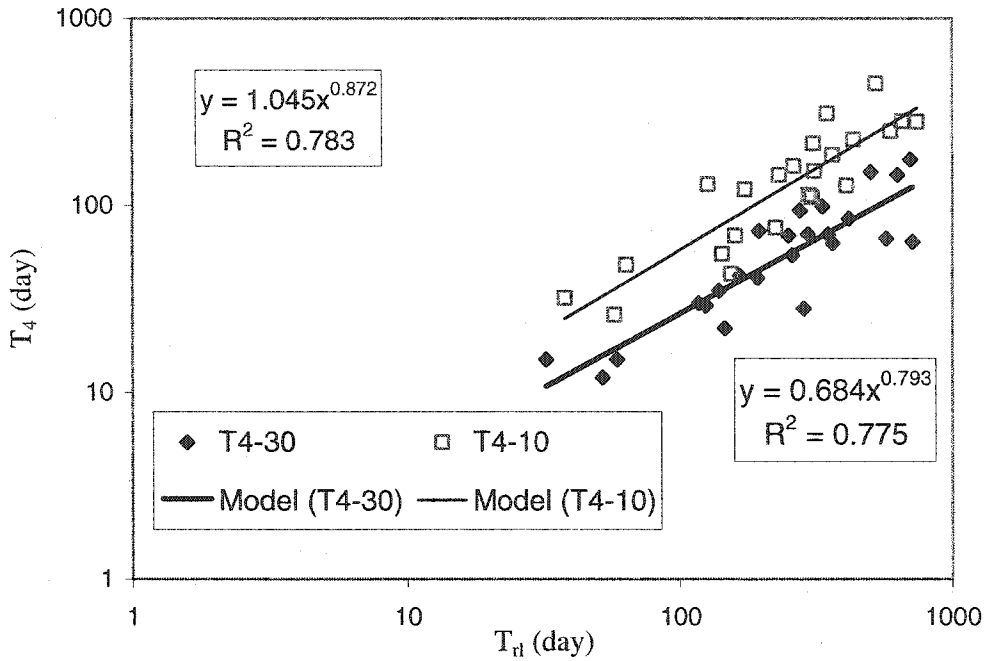


Figure 3.10. Regression model for soil with low Ks (Phase-4)

3.3.2 Validation of the Regression Models

A validation of the regression models was conducted by compiling HYDRUS for three more datasets as shown in Table 3.5. Combinations of the parameters (F, H and h_{top}) are selected in a way that they differ from the datasets used for the development of the regression model (Table 3.2). All of these datasets are arranged in a way that the regression model does not exceed the range of values for each parameter used in model development. Forty-two simulations were conducted for Phases 1 and 2. Figures 3.11 and 3.12 show the predicted versus the actual (computed from HYDRUS) values and the validation statistics for Phases 1 and 2, respectively. For perfect regression, the predicted result would be equal to the actual result (y = x line in the figures). It is found from the figures that 80% of the data points fall within the confidence band at 95% level of significance. Also, the mean residuals for Phases 1 and 2 are nominal compared to the

range of observed values (see Figures 3.11 and 12). Phase-1 shows a mean error of 8.48 days for an observation range of 324 days. If the mean error is normalized by the observation range, the normalized mean error becomes 2.62%. Similarly, the normalized mean error for Phase-2 is about 2 percent. The R-squared values for the perfect match line (y = x line) are 0.934 and 0.875 for phases 1 and 2, respectively. The correlation coefficient, which indicates the extent to which a series of numbers for any two variables lie on a straight line, also shows a very strong correlation (1.0 being the perfect match) for both Phases 1 and 2 (see Figures 3.11 and 12).

Table 3.5. Datasets used in simulating HYDRUS for validating the regression model

Parameters	Unit	Dataset 7	Dataset 8	Dataset 9
F^{ζ}	None	100	50	25
H	cm	300	450	300
h_{top}	cm	- 4000	- 4000	- 4000
Number of simulations	-	14	10	18

$^{\zeta}$ $Q_{in} = K_s/F$

Statistics for validation of the regression model for Phase-4 are presented in Table 3.6. Mean error (residual), standard deviation, root mean square of errors (RMSE), normalized RMSE (normalized by the range of observation), normalized mean error, and the correlation coefficients for the regression models (for $T_{4\text{-}10}$ and $T_{4\text{-}30}$) of high and low K_s soils are presented in Table 3.6. It is found that the normalized mean errors are relatively smaller for the soils with high K_s values than the soils with low K_s values. Also, the correlation coefficients for soils with high K_s values show excellent fit for both $T_{4\text{-}10}$ and $T_{4\text{-}30}$, while the same coefficients for soils with low K_s values are not as good. An inferior validation for the soils with low K_s values is not unexpected, as the regression models for the soils with low K_s values are not as good as those for the soils with high K_s values.

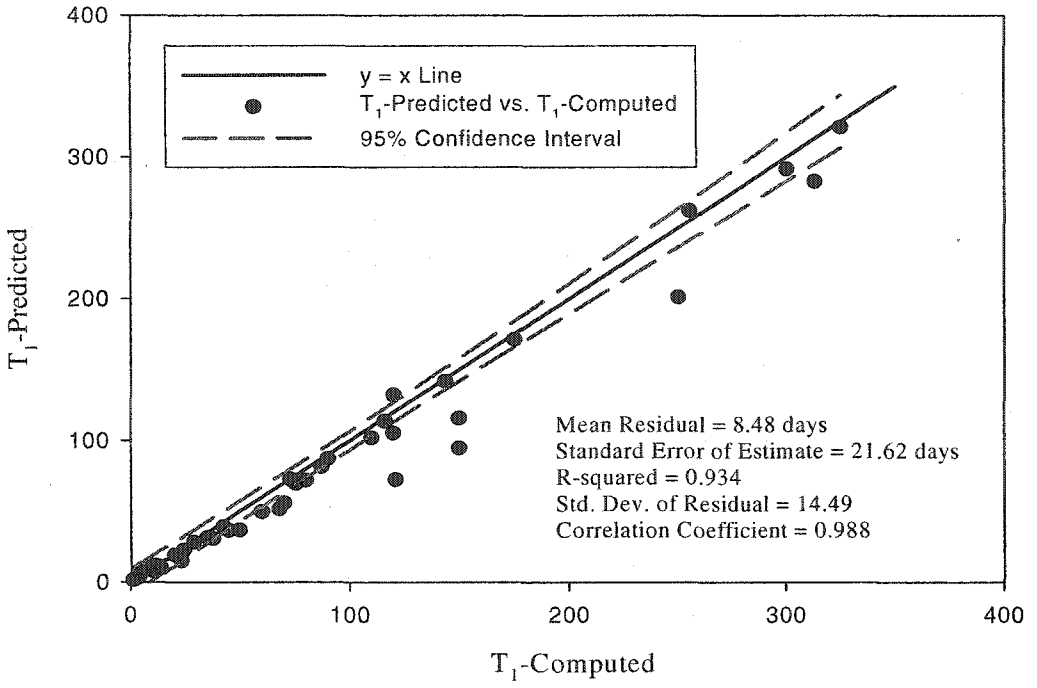


Figure 3.11. Validation of the regression model for Phase-1.

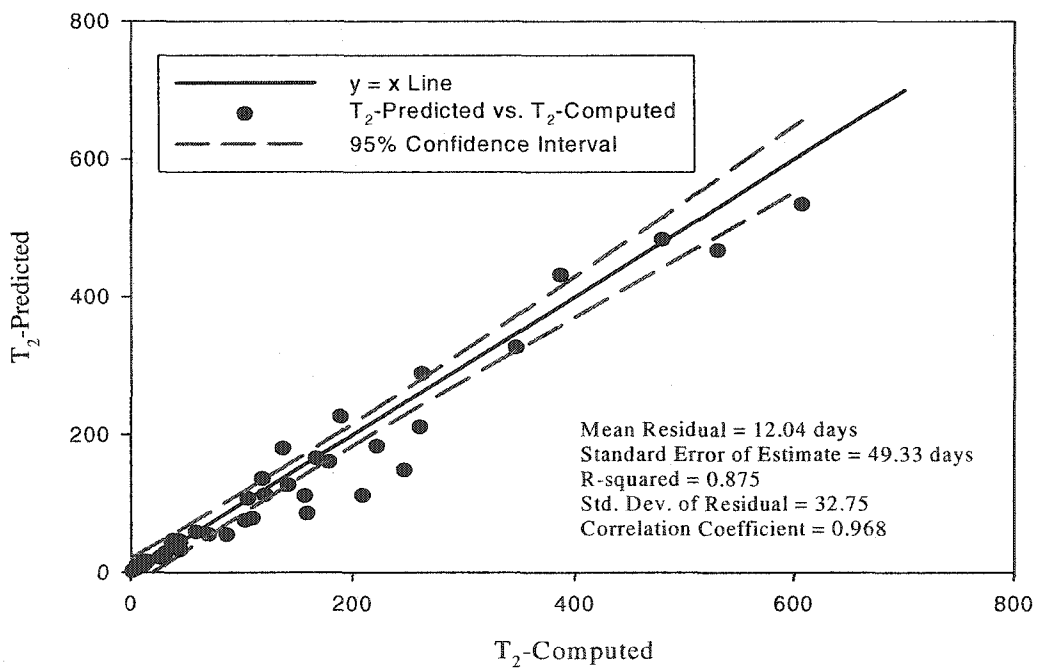


Figure 3.12. Validation of the regression model for Phase-2.

Table 3.6. Statistics for validation of the regression model for Phase-4

	High K_s soils		Low K_s soils	
Parameters	$T_{4\text{-}30}$	$T_{4\text{-}10}$	$T_{4\text{-}30}$	$T_{4\text{-}10}$
Mean error (days)	2.69	2.51	24.3	52.4
Standard deviation (days)	3.08	12.92	46.0	85.2
RMSE[ζ]	3.99	12.62	49.9	96.3
Range of observations (days)	76.38	184.3	237	513
Normalized RMSE (%)	5.22	6.85	21.1	18.7
Normalized mean error (%)	3.53	1.36	10.3	10.2
Correlation coefficient	0.992	0.982	0.82	0.90
Number of simulations	12	12	10	10

[ζ]Root Mean Square of Errors

An additional validation was conducted for two soils with hydraulic parameters different from that used for model development. Unsaturated hydraulic properties of the two soils selected for further model validation are listed in Table 3.7. HYDRUS was run for both Soil1 and Soil2 with identical boundary and initial conditions. The depth of water table (H) for both simulations was assumed to be 300 cm. The initial condition was assumed to be wet with h_{top} value equal to −1000 cm. Surface application rates (Q_{in}) were assumed to be $K_s/50$ and $K_s/100$ for Soil1 and Soil2, respectively. Output from HYDRUS and the regression models are listed in Table 3.8. It is found that the soil with high hydraulic conductivity (Soil2) shows a better prediction than the soil with a low conductivity (Soil1). The regression models give less than 2 days error (HYDRUS minus regression model output) in estimating T_1, T_2, and $T_{4\text{-}30}$ for Soil2, while the same for Soil1 is less than 12.2 days. The most error occurs in estimating $T_{4\text{-}10}$ for Soil1. This could be attributed to the weak correlation obtained for soils with low K_s value (see Table 3.8).

Table 3.7. Hydraulic properties of the soils used for further validation.

Soil Names	θ_r	θ_s	n	α (cm^{-1})	K_s cm/day
Soil1 (0-083[Ψ])	0.046	0.349	1.646	0.0069	10.4
Soil2 (0-107[Ψ])	0.014	0.35	1.552	0.2034	205

[Ψ] Soil sample number used by Khaleel et al. (1995)

Table 3.8. Comparison between the regression models and HYDRUS outputs

Parameters	Soil1			Soil2		
	Regression Model	HYDRUS	Error	Regression Model	HYDRUS	Error
A_i (cm)	92.0	--	--	35.5	--	--
T_1 (day)	30.2	18	-12.2	16.2	16.8	0.6
T_2 (day)	46.1	43.0	-3.1	23.5	21.7	-1.8
$T_{4\text{-}30}$ (day)	30.1	21.2	-8.9	10.6	12.6	2.0
$T_{4\text{-}10}$ (day)	78.3	39.6	-38.7	28.0	33.5	5.5

3.3.3 Assumptions and Limitations of the Regression Model

The basic assumptions for the regression models discussed in the preceding sections can be outlined in the following:

- The regression models consider a homogeneous soil.
- The surface application rate is less than the saturated hydraulic conductivity of the soil; hence, no ponding of water at the soil surface is assumed.
- The surface application rate is constant and continuous until the bottom drainage becomes equal to the surface inflow rate (see Figure 3.1).
- The regression models are applicable for shallow aquifers (preferably, between 150 and 600 cm deep).
- The initial soil moisture versus the depth profile is represented by a variable, named A_i; hence, the model can handle variable initial condition.
- The Van Genuchten (1980) model is used to define the hydraulic properties of the soil.

The regression models developed herein have the following limitations:

- The models are not applicable to heterogeneous soils.

- A ponding condition cannot be considered. However, the user can make approximation by spreading out the application rate above the K_s value (condition for ponding to occur) to successive days.
- The models are limited to shallow aquifer depths (between 150 and 600 cm).
- The models are not applicable to cracked or expansive soils.
- The models cannot handle root uptake.
- The application rate is limited to a constant continuous condition, while it is variable and discontinuous in reality. However, the user can run the model for variable application rates by making reasonable assumptions (see the following section).
- The models do not consider hysteresis, which could affect the output for the soils with low K_s values in Phase-4 (the drying phase).
- The regression model for the soils with low K_s values in Phase-4 is not as dependable as the other regression models.

3.4. Application of the Regression Model to Variable Surface Inflow Rates

An example scenario was created to demonstrate the application of the proposed regression models for a variable and discontinuous surface application rate. Figure 3.13 shows the assumed variable surface application rate. The soil type selected for the example is clay, and the initial condition is assumed to be dry (i.e., linearly varying from the soil surface to the water table) with the absolute h_{top} value equal to 1000 cm. The water table is assumed to be a 150 cm from the surface (i.e., H = 150 cm). The computation for determining the breakthrough curve using the regression models is presented in the following steps.

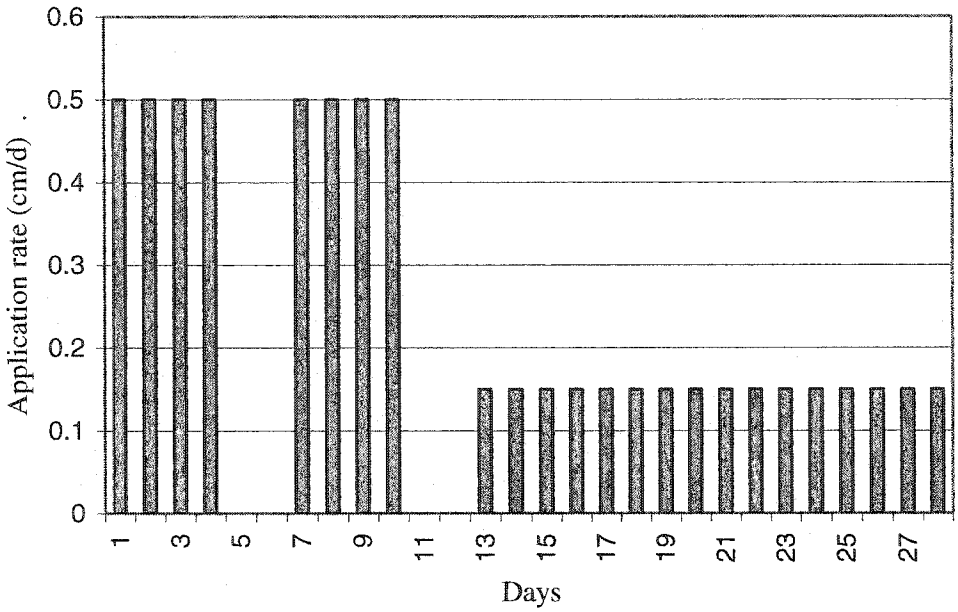


Figure 3.13. Variable surface application rate used to demonstrate the application of the regression models.

Step 1:

Calculate T_b (Equation 3.9) for the initial application rate (Q_{in}), which is 0.5 cm/d (see Figure 3.13) for 4 days. The parameter, 'A_i' for the assumed initial condition is 50 cm. K_s, θ_r, and θ_s for clay are 4.8 cm/d, 0.068, and 0.38, respectively (see Table 3.1). The calculated value of T_b is 44.8 days, and the corresponding value of T_1 is 7.65 days (Equation 3.10), which is longer than the duration of the initial constant continuous application rate (i.e., 4 days from Figure 3.13). This means that the initial breakthrough would not occur within the first 4 days.

Step 2:

Since no breakthrough occurs in step 1, there is no drainage of water during the first 4 days. During days 5 and 6, the surface application rate is zero. Therefore, it is assumed that the recession does not occur during days 5 and 6. The next condition starts

at day 7 with an application rate (Q_{in}) of 0.5 cm/d for 4 days. Since no breakthrough occurred during the first four days and 2 cm (= 0.5 cm/d × 4 d) of water infiltrated into the soil during that period, the initial condition for the next application condition would increase by 2 cm. That is, A_i is equal to 52 cm for this condition. With all other inputs the same, T_b and the corresponding T_1 are 32 and 5.6 days, respectively. Since T_1 is greater than 4 days (duration of the 0.5 cm/d application rate from day 7 to day 10), a breakthrough would not occur by the end of day 10.

Step 3:

The next condition starts at day 13 with an application rate (Q_{in}) of 0.15 cm/d for 15 days. The adjusted value of 'A_i' is 54 cm (= 52 + 4 × 0.5). Now, T_b and the corresponding T_1 values are 64.1 and 10.6 days, respectively. Since T_1 is smaller than 15 days, breakthrough would occur at 22.6 days (= 12 + 10.6).

Step 4:

The T_2 value for Phase-2 (i.e., time for the bottom flux to become equal to the surface application rate) is calculated from the regression model using the T_b value obtained in the previous step (64.1 days). From the regression model, the T_2 value is 15.2 days (= $0.268 \times 64.1^{0.97}$, from Equation 3.11). The total T_2 value from the beginning is 27.2 days (= 12 + 15.2).

Step 5:

Recession (Phase-4) starts at the end of day 28, when the application rate is discontinued. Since the K_s value for the soil is smaller than 10.8 cm/d, Equations 3.17 and 3.18 are used to determine the $T_{4\text{-}10}$ and $T_{4\text{-}30}$ values, respectively. To apply Equations 3.17 and 3.18, T_{rl} needs to be calculated from Equation 3.16, which requires an

input value for θ_{rl}. θ_{rl} values corresponding to $T_{4\text{-}10}$ and $T_{4\text{-}30}$ are obtained from Equation 3.5 for suction potentials equal to $h_m/5$ and $h_m/6$, respectively, where h_m for this example is equal to -1000 cm. θ_{rl} values obtained from Equation 3.5 are 0.343 and 0.347 for Equations 3.17 and 3.18, respectively. The corresponding $T_{4\text{-}10}$ and $T_{4\text{-}30}$ values from the regression models are 24.3 and 10.9 days, respectively.

For comparison, HYDRUS was run with identical boundary conditions, initial conditions, and hydraulic parameters used in the example. Output from the HYDRUS and the regression models are presented in Table 3.9. The regression model shows a delay of 6.4 days in the initial breakthrough time (T_1) than that from HYDRUS. The T_2 value obtained from the regression model is only 0.6 days higher than that from HYDRUS. Finally, the $T_{4\text{-}30}$ and $T_{4\text{-}10}$ values from the regression model are 10.9 and 24.3 days, respectively, while the corresponding HYDRUS output are 8.2 and 19.8 days. These values are smaller than those from the regression models. Although the regression model for Phase-4 with low K_s soils is not as dependable as the other phases (see Section 3.3), the predicted values for this example condition are quite comparable.

Table 3.9. Application of the regression models.

Parameters	HYDRUS	Regression Model	Error
T_1 (day)	16.2	22.6	-6.4
T_2 (day)	26.6	27.2	-0.6
$T_{4\text{-}30}$ (day)	8.2	10.9	-2.7
$T_{4\text{-}10}$ (day)	19.8	24.3	-4.5

3.5. Conclusions

Currently, there is a need for a simple tool to estimate the drainage/recharge rate to the groundwater from application of water at the soil surface. Existing infiltration models, except numerical models, are typically used to estimate the infiltration rate at the

soil surface; hence, those are not useful for estimating the lag time between surface application and initial breakthrough to the groundwater table. Regression models were developed herein to characterize the breakthrough curve for drainage to the groundwater from a constant, continuous application of water at the soil surface. Power-type (log-log) regression models were developed to estimate the parameters required for characterizing the breakthrough curve. The advantage of the regression models developed in this study is that the input parameters required for the model are readily available. Also, the regression models for Phases 1 and 2 are not limited to constant initial moisture content within the soil profile, which is a common limiting condition for many flow models for vadose zone. Since the initial moisture is represented by the initial volume of water within the soil profile (A_i), any initial soil moisture distribution could be assumed.

Statistics from model development and model validation shows that the regression models for Phases 1 and 2 are reasonably accurate for all soil types. The same conclusion is also applicable to the regression model of the recession phase for soils with high K_s values. However, the regression model of the recession phase for soils with low K_s values is not as accurate as the other phases. The assumption of no hysteresis during the recession phase would further limit the application of the regression model for soils with low K_s values, since hysteresis is more pronounced for such soils. However, as evidenced in the model application section, the regression model for the recession phase of soils with low K_s values is expected to give a reasonable initial estimate.

References

Brooks, R. H., and A. T. Corey. 1966. Properties of porous media affecting fluid flow. *Journal of Irrigation Drainage Division*, ASCE Proc. 72(IR2):61-88.

Carsel, R. F., and R. S. Parrish. 1988. Developing joint probability distributions of soil water retention characteristics. *Water Resources Research.* 24(5):755-769.

Green, W. H., and C. A. Ampt. 1911. Studies on Physics I. The flow of air and water through soils. *Journal of Agricultural Science.* IV (Part I):1-24.

Irish, L. B., Jr., M. E. Barrett, J. F. Malina, Jr., and R. J. Charbeneau. 1998. Use of regression models for analyzing highway storm-water loads. *Journal of Environmental Engineering.* 124(10):987-993.

Khaleel, R, J. F. Relyea, and J. L. Conca. 1995. Evaluation of van Genuchten-Mualem relationship to estimate unsaturated hydraulic conductivity at low water contents. *Water Resources Research.* 31(11):2659-2668.

Piggott, J. H., and J. D. Cawlfield. 1996. Probabilistic sensitivity analysis for one-dimensional contaminant transport in the vadose zone. *Journal of Contaminant Hydrology.* 24:97-115.

Ravi, V., and J. R. Williams. 1998. Estimation of infiltration rate in the vadose zone: compilation of simple mathematical models. Volume I. EPA/600/R-97/128a. U.S. Environmental Protection Agency, Ada, OK.

Richards, L. A. 1931. Capillary Conduction of Liquids in Porous Mediums. *Physics.* 1: 318-333.

Simunek, J., K. Huang, and M. Th. Van Genuchten, 1998, The HYDRUS code for simulating the one-dimensional movement of water, heat, and multiple solutes in variably-saturated media. Version 6. Research Report No. 144. U.S. Salinity Laboratory, Riverside, CA.

Sisson, J. B., A. H. Ferguson, and M. Th. Van Genuchten. 1980. Simple method for predicting drainage from field plots. *Soil Science Society of America Journal.* 44:1147-1152.

Van Genuchten, M. Th. 1980. A closed-form equation for predicting the hydraulic conductivity of unsaturated soils. *Soil Science Society of America Journal.* 44:892-898.

Warrick, A. W., D. O. Lomen, and A. Islas. 1990. An analytical solution to Richards' equation for a draining soil profile. *Water Resources Research.* 26(2):253-258.

Williams, J. R., Y. Ouyang, J. Chen, and V. Ravi. 1998. Estimation of infiltration rate in the vadose zone: application of selected mathematical models. Volume II. EPA/600/R-97/128b. U.S. Environmental Protection Agency, Ada, OK.

Chapter 4: Advanced Expert System

Abstract

An advanced expert system is developed for evaluating the groundwater pollution potential from land application of manure. The limitations of the simple expert system, presented in Chapter 1, in evaluating each module as an isolated condition is overcome in the advanced expert system by sequentially interconnecting all the modules from the source to the receptor. The pollution potential in the advanced expert system is evaluated at the final stage based on the predicted nutrient concentration at the receptor well and the possible health risk from that contamination. Additional advanced features include a vadose zone transport model, a non-point source transport model for the saturated zone, and a module for assessing the health effects from exposure. A numerical solute transport model is used to estimate the nutrient flux through the vadose zone. Finally, a case study is presented to demonstrate the performance of the advanced expert system.

4.1. Introduction

An expert system for evaluating groundwater pollution potential at a downgradient well from land application of manure is presented in Chapter 1. The expert system is named 'simple' to emphasize that it is simple to use, requires easily-available

inputs, and does not warrant highly skilled personnel to conduct the simulation. The overall objective in developing the simple expert system was to aid farmers and regulators in developing best management practices for land application of manure, and in selecting sites suitable for building new CAFO without the need for complex mathematical models. Reasonable simplification was done to avoid the direct use of numerical models. The groundwater pollution potential of each nutrient (nitrate and phosphate) was obtained from the weighted average rating based on the assigned relative weight and the calculated individual rating of each module (surface loading, vadose zone transport and saturated zone transport). One of the limitations of the methodology used in the simple expert system is that the modules were individually rated, while in reality the modules are interconnected. Specifically, the surface loading module contributes nutrient mass to the vadose zone module, and the latter inputs mass to the saturated zone module. These associations were neglected in the simple expert system. The objective of the advanced expert system is to conduct the simulation as an integrated problem and to use more advanced models in the vadose and saturated zone transport modules than those in the simple expert system. Also, the potential health risk from consumption of water from the receptor well is incorporated into the evaluation of the overall pollution potential in the advanced expert system. The process involved in the advanced expert system requires more input parameters, simulation time, and skill than the simple expert system.

4.2. Structure of the Advanced Expert System

The advanced expert system has two more modules than the simple expert system. These are the general information module and the health effect module. The

general information module is developed to input information required in more than one modules. The health effect module is developed to assess the health risks from exposure to nutrients at any down gradient well. The structure of the advanced expert system is shown in Figure 4.1. Modules in the advanced expert system are interconnected in a manner similar to the transport path of nutrients from the source (soil surface) to the sink (receptor well). Each module, except the general information and the sorption modules, reads the output of the previous module and uses that output as input for the evaluation. The sorption module evaluates the partitioning of nutrients in subsurface and passes that to the transport modules. The surface loading module estimates the nutrient mass leaching through the root zone and passes that to the vadose zone transport module. The latter then estimates the nutrient flux leaching to the water table. The saturated zone transport module uses the nutrient flux at the water table as input and estimates the maximum nutrient at any downgradient well. The health effect module uses the maximum concentration at the well to evaluate the potential health risk from consumption. Finally, the decision module evaluates the pollution potential from the output of the health effect and the saturated zone transport modules.

4.3. General Information Module

The general information (GI) module receives inputs pertaining to the site location, the land area used for cultivation, and the nutrient of concern (nitrate or phosphate). The normal rainfall and evaporation data for all counties of Oklahoma are incorporated into the expert system as default inputs. Depending on the site location, this module reads the default values of daily rainfall and daily evaporation data from the

database and passes that information to the vadose zone transport module. The user can also import the daily rainfall and evaporation data from a text file. This makes the expert system applicable to locations outside of Oklahoma. Finally, the general information module inputs the land area to the surface loading and the saturated zone transport modules.

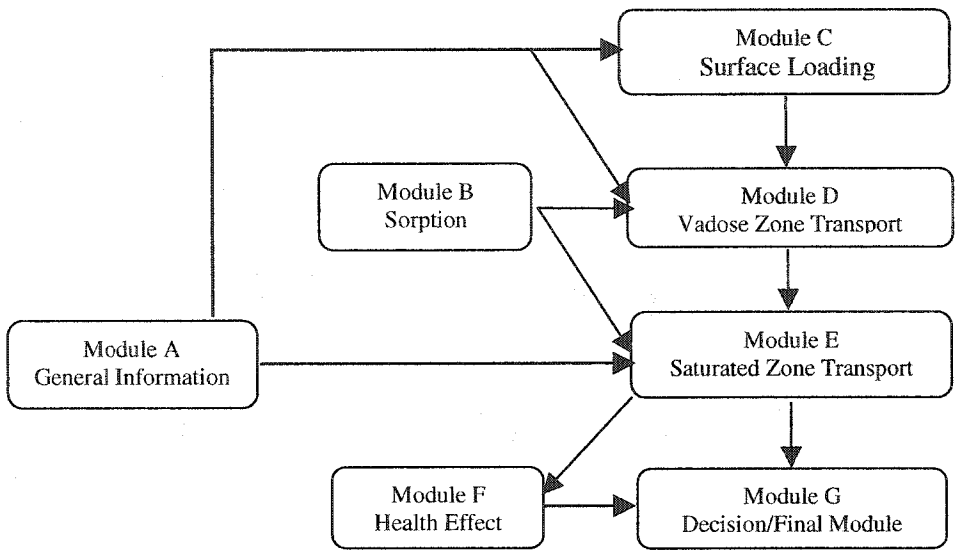


Figure 4.1. Structure of the advanced expert system

4.4. Sorption

The sorption module estimates the retardation factor (RF) and the corresponding soil-water partitioning coefficient (K_p) for the nutrient of interest (i.e., nitrate or phosphate) and passes those values to the vadose zone and saturated zone transport modules. The expert system rules used for estimating the RF values in the simple expert system are followed herein (see Chapter 1). It should be noted that the RF values

approximated by the expert system is the default value for evaluation. The user has the option to change the default RF value, if necessary.

4.5. Surface Loading

The surface loading module calculates the net nutrient flux for the days when nutrients are applied on the land. The net nutrient flux is the difference between the nutrient load from sources and uptake by sinks. The nutrient sources are manure, fertilizer, and the background concentration in the topsoil, while the sinks are the cultivated crops. This module has the option to input data for a maximum of ten years. For each year, the user needs to input the animal inventory data, select the type and number of crops, input nitrogen or phosphorus content in the fertilizer, input background concentrations of nitrogen or phosphorus in the soil, and select the days on which manure was applied on the land. From the animal inventory data, the expert system estimates the total waste (manure) generated annually, and the nitrogen and phosphorous concentrations in the manure (see Appendix A). The average nitrogen and phosphorous uptake by the crops is obtained from Tables B.1 and B.2 (see Appendix B). The users need to input the date of manure application and the volume applied on respective dates. Finally, the surface loading module passes the volume of manure applied per acre land and the net nutrient concentrations in the manure to the vadose zone transport module.

4.6. Vadose Zone Transport

The vadose zone transport module evaluates nutrient transport through the vadose zone to the groundwater table. Analysis of transport through the vadose zone becomes

complicated due to the presence of air in the pore spaces of unsaturated soil. As the hydraulic characteristic of unsaturated soil is complex, simplified assumptions, such as constant moisture content profile throughout the modeling period, are required to develop analytical models for soil moisture flow and solute transport through the vadose zone. On the contrary, numerical models are more comprehensive in solving the flow and transport equations for the vadose zone. The advanced expert system incorporates a numerical model to simulate nutrient transport through the vadose zone. Since numerical modeling is complicated and warrants skilled personnel, it would be difficult for the common users of the expert system (e.g., farmers and regulators) to conduct numerical modeling. To minimize the level of effort, a user-friendly pre- and post-processor for the numerical model is included in the expert system.

HYDRUS (Simunek et al., 1998), a well-known numerical model for flow and solute transport, is used in the advanced expert system. Boundary conditions of the numerical model are set to satisfy the conceptual model for the expert system. An atmospheric boundary is used at the soil surface, which represents the net maximum infiltration or exfiltration at the surface layer. Infiltration is possible when the net water application at the soil surface (rainfall plus irrigation water) is greater than the evaporation on a given day. Otherwise, exfiltration or loss of water due to evaporation is possible at the soil surface. It should be noted that HYDRUS does not allow the evaporation to exceed the maximum allowable suction potential value for the soil. The daily rainfall and evaporation data are obtained from the general information module.

A specified-head boundary is used at the bottom of the soil profile. A head value of zero is assigned to represent saturated soil at the water table. The initial condition is

assumed to be exponentially varying with the maximum suction potential at the soil surface and zero potential at the bottom (see Equation 4.1).

$$h(y) = h_{top} \times \exp(-0.025 \times y);\ y < D_{wt}$$

$$h(D_{wt}) = 0 \qquad (4.1)$$

where, h(y) is the suction potential at any distance y from the soil surface, h_{top} is the suction potential at the soil surface, and D_{wt} is the depth of water table.

The maximum suction potential for each USDA soil type is assumed to be the h_0 value in Table 1.4 (see Chapter 1), which is the average suction potential from the Oklahoma Mesonet stations. The zero suction potential at the bottom is important as it indicates saturation and thus, represents the initial location of the water table.

Van Genuchten's unsaturated soil hydraulic properties determined by Carsel and Parrish (1988) are used as default input for HYDRUS. The equilibrium partitioning coefficient (K_p) is input from the sorption module. The user has the option to select up to three different soil types and up to five different soil layers to incorporate heterogeneity in the soil profile. A maximum of twenty years time period is allowed for running HYDRUS. It should be noted that the expert system provides an option for the users to change any of the default inputs. By setting the boundary conditions and default input values, the level of difficulty to use HYDRUS is reduced considerably. The user needs to input the soil type(s), depth to the water table, and simulation time in this module.

4.7. Saturated Zone Transport

The saturated zone transport module estimates the maximum solute concentration in a downgradient well (C_w) at any distance (x,y,z) from the center of the source, and the

time required for the center of the plume to reach the well (T_w). Solute mass from the vadose zone is input in this module. The instantaneous finite source model for aquifers with finite thickness is used to estimate C_w (Equation 4.2).

$$C(x,y,z,t)=\frac{M/n}{8X_SY_SZ_S}\left[erf\left(\frac{x-V_et+X_S/2}{2\sqrt{D_xt}}\right)-erf\left(\frac{x-v_xt-X_S/2}{2\sqrt{D_xt}}\right)\right]\times$$
$$\left[erf\left(\frac{y+Y_S/2}{2\sqrt{D_yt}}\right)-erf\left(\frac{y-Y_S/2}{2\sqrt{D_yt}}\right)\right]\times \qquad (4.2)$$
$$\left[erf\left(\frac{z+Z_S}{2\sqrt{D_zt}}\right)-erf\left(\frac{z-Z_S}{2\sqrt{D_zt}}\right)+\sum_{h=-\infty}^{\infty}\left\{erf\left(\frac{z+Z_S-2hH}{2\sqrt{D_zt}}\right)-erf\left(\frac{z-Z_S-2hH}{2\sqrt{D_zt}}\right)\right\}\right]$$

where, C(x,y,z,t) is the solute concentration at any point (x,y,z) at time t, V_e is the effective velocity in the x directions, D_x, D_y, D_z are the hydrodynamic dispersion coefficients in the x, y and z directions, respectively, Xs, Ys, Zs are the dimensions of the source in the respective directions, M is the mass of solute injected instantaneously at the source, and H is the aquifer thickness.

The effective velocity (V_e) is obtained by dividing the seepage velocity by the retardation factor. The sorption module estimates the retardation factor for each nutrient and passes that to the saturated zone transport module. The time required for the center of the plume to reach the well (T_w) is calculated by dividing the distance to the well by V_e. In order to get the maximum concentration at the well, the total transport time (t) in Equation 4.2 is assumed to be the sum of T_w and the time when the input solute flux is maximum. The latter is found from the vadose zone transport module. The longitudinal dispersivity is assumed to be 10% of the well distance. Transverse and vertical

dispersivities are assumed to be 10% and 1% of longitudinal dispersivity, respectively (Fetter, 1999). Hydrodynamic dispersion coefficients (D_x, D_y, D_z) are calculated by adding molecular diffusion with advective dispersion (which is the product of dispersivity and the seepage velocity). The effect of sorption on dispersion is incorporated by using effective hydrodynamic dispersions.

The land area is assumed to be square in shape, i.e., the source dimensions in the longitudinal and transverse directions are assumed equal. Source dimension in the vertical direction is assumed to be one foot, which represents the initial mixing zone for the solute flux from the vadose zone. It should be noted that the vertical dispersion coefficient in Equation 4.2 controls the vertical mixing with time. The solute mass (M) in Equation 4.2 is obtained from the vadose zone transport module. The advanced expert system has the option to include pumping at the well. It calculates the average velocity due to pumping similar to the simple expert system, and uses that velocity in Equation 4.2. The saturated zone transport module of the advanced expert system is different from that of the simple expert system, as the latter considers a single point source model and does not consider input from the vadose zone.

4.8. Health Effect

The health effect module calculates the hazard index (HI) for the maximum nutrient concentration at the well. The HI is equal to the intake rate (I) divided by the oral reference dose (RfD). EPA's integrated risk information system (IRIS) reported that the RfD for nitrate is 1.6 mg/kg/day. Since no RfD is reported for phosphate in IRIS, the health effects are ignored for this nutrient. The Intake rate (I) is the mass of chemical

ingested per day per unit body weight. The intake rate is calculated from Equation 4.3 (USEPA, 1989).

$$I = \frac{C \times CR \times EF \times ED}{BW \times AT} \tag{4.3}$$

where, C is the concentration at the well, CR is the contact rate, EF is the exposure frequency, ED is exposure duration, BW is the body weight, and AT is the averaging time.

The concentration at the well (C) is equal to the maximum nutrient concentration at the well (C_w), which is obtained from the saturated zone transport module. The contact rate (CR) is the volume of water ingested every day. Age specific values for CR are listed in USEPA (1989). Since nitrate is toxic to infants, the age group at the most significant risk is from 2 to 6. The CR for children from age 2 to 6 is 1 L/day. The exposure frequency (EF) is the number of days in a year a person is exposed to the contamination. Since manure is usually applied every year, the EF is assumed to be 365 days. The exposure duration (ED) is the number of years a person is exposed to the contamination. Since exposure to nitrate is toxic to younger children, the expert system assumes the ED to be 6 years. The body weight (BW) is the average weight of the group of people exposed to the contamination. For the target age group, the BW is assumed to be 16 kg, which is approximately the average body weight of a 4-year-old child (Healthcental, 2004). The averaging time (AT) is exposure duration in life. The expert system assumes AT to be 6 years, which is the highest age of the age group at risk.

4.9. Decision Module

The decision module reads the output from the saturated zone transport and the health effect modules and provides the pollution potential for the site. The input parameters from the saturated zone transport module are the maximum solute concentration at the well (C_w) and the time required to reach the well (T_w), while the input from the health effect module is the hazard index (HI). The expert system calculates the rating for each parameter in a scale of 1 to 5, 5 being the most critical scenario. The rating for concentration (C_r) is obtained from Equation 4.4.

$$C_r = \frac{C_w}{C_{th}} * 5 \leq 5 \tag{4.4}$$

where, C_{th} is the threshold concentration of the nutrient. The C_{th} values for the nutrients are assumed to be equal to the drinking water standards, which are 10 and 5 mg/L for nitrate and phosphate, respectively (USEPA, 1999).

The rating for time (T_r) is based on the assumption that nutrient is applied each year and the time to reach the well is less than a year (see Equation 4.5).

$$T_r = \frac{365}{T_w} * 5 \leq 5 \tag{4.5}$$

The rating for the health effect (H_r) is the product of the HI and maximum rating scale (see Equation 4.6).

$$H_r = HI * 5 \leq 5 \tag{4.6}$$

A total of five rules are defined to evaluate the pollution potential from the advanced expert system.

Rule #1: The groundwater pollution potential (GWPP) is 'High to Very High', if either C_r or H_r is maximum, i.e.,

If $C_r = 5$ or $H_r = 5$ Then GWPP = 'High to Very High'

If both C_r and H_r are smaller than the maximum rating, the pollution potential is estimated from the average rating (AR) value, which is the arithmetic mean of C_r, T_r, and H_r. The following four rules are defined to evaluate the pollution potential based on the AR values.

Rule #2: If AR ≥ 4 And AR < 5 Then GWPP = 'High to Very High'

Rule #3: If AR ≥ 3 And AR < 4 Then GWPP = 'Medium to High'

Rule #4: If AR ≥ 2 And AR < 3 Then GWPP = 'Low to Medium'

Rule #5: If AR ≥ 1 And AR < 2 Then GWPP = 'Very Low to Low'

4.10. Case Study

A case study is conducted to demonstrate the performance of the advanced expert system. The research site (RS1) used for the second case study in the simple expert system is considered herein. Groundwater quality was monitored in RS1 from 1998 to 2000. As noted in Chapter 1, the Oklahoma Department of Agriculture (ODA) categorizes RS1 as 'non-LMFO' (Licensed Managed Feeding Operation). Table 4.1 shows the input parameters to compile the advanced expert system for RS1. Remaining details of the site are presented in Chapter 1. Additional input parameters required for the advanced expert system are the average daily evaporation rate, average daily rainfall, and the volume of manure applied to the land. The daily evaporation and rainfall data are obtained from the Oklahoma Climatological Survey (OCS) for the station nearest to RS1. The volume of manure is estimated from the lagoon size. RS1 has two lagoons of about 300ft × 100ft × 9ft (length × width × depth). With the assumption that the lagoons contain

an average of 5 feet of liquid manure, the volume of manure in the two lagoons is about 2.2 million gallons, which is approximately equal to 1 inch of liquid manure over the 80 acres of grazing land in RS1. Since the exact dates of manure application at RS1 are not known, it is assumed that the entire manure was applied in one day. The first day in the HYDRUS simulation is assumed to be the day when the manure was applied. Therefore, 1 inch of water is added as rainfall in the atmospheric boundary at the soil surface.

Table 4.1. Input parameters for RS1 for compiling the advanced expert system.

Surface Loading Module	**RS1**
Animal types and numbers in year 1998	Hogs-breeding: 1,520; Hogs-feed: 960
Types and numbers of crops	wheat
Thickness of the aquifer (ft)	20
Land area for manure application (acres)	80
Irrigation water (in/acre)	1.0
Sorption Module: ***Nitrate Sorption:***	
pH	6.6
Nitrate in water (mg/L as N)	15.2
AEC (cmol/kg)	1.1
Retardation factor (RF)	1.0
Phosphate Sorption:	
Phosphate in water (mg/L as P)	0.6
Retardation factor (RF)	20.0
Vadose Zone Transport Module	
Depth of water table (ft)	6.3
Daily normal rainfall and evaporation (in)	obtained from the OCS
USDA soil class	clay
Saturated Zone Transport	
Distance to the well (ft),	1,070
Hydraulic gradient (ft/ft),	0.0056
Hydraulic conductivity (ft/d)	8.5
Effective porosity	0.20

[1] <http://climate.ocs.ou.edu/rainfall_update.html>

The advanced expert system shows 'high to very high' pollution potential from nitrate. That means the site has severe risk for water quality according to the recommendations made in Chapter 1 (see Table 1.6). The maximum nitrate concentration

at the well (C_w) is found to be 13.2 mg/L, which gives the maximum values for C_r and H_r (i.e., 5). However, the AR value for nitrate is 3.67, because the T_r value is 1.0 for the saturated zone. Therefore, if the C_w value were fractionally smaller than the drinking water standard (i.e., 10 mg/L), the pollution potential would be 'medium to high', which is comparable to the simple expert system evaluation for RS1. As the structure and computational methodologies vary between the simple and advanced expert systems, it is likely that evaluation from the expert systems would not match for certain case studies.

Pollution potential from phosphate is 'very low to low', i.e., no risk for water quality (see Table 1.6), while the pollution potential from the simple expert system is a level higher at 'low to medium' or moderate risk level. The C_r and T_r values, and the corresponding AR value are at the minimum level, i.e., equal to 1. The evaluation for phosphate could not be verified due to unavailability of data at MW9 after the year 1998. However, the pollution potential from phosphate at the downgradient well from the site (MW9) is expected to be low, as the groundwater velocity is very slow (about 0.24 ft/d) and the retardation factor is very high. On the other hand, the groundwater immediately underneath the grazing land is likely to have a higher pollution potential, as the aquifer is shallow. Elevated phosphate concentration (5.22 mg/L) was evidenced at the middle of the grazing land during the dry season in 1998. A cracked soil surface during the dry season could be the reason for the transport of phosphate to the water table. Therefore, depending on the location, the RS1 could be considered to have either no or moderate risk from phosphate.

4.11. Advantages and Limitations of the Advanced Expert System

The advanced expert system has the following advantages over the simple expert system:

- It has a better structure than the simple expert system, as it follows the nutrient transport pathway from the source to the receptor;
- The solute transport models used for the vadose and saturated zones are improved in the advanced expert system;
- The total manure produced annually can be distributed to different periods within the year.

Limitations of the advanced expert system are outlined in the following:

- It requires additional input parameters, skill, and simulation time as compared to the simple expert system;
- As in the case of the simple expert system, the advanced expert system considers no off-site disposal of manure and is applicable for evaluating the pollution potential from either nitrate or phosphate at a single downgradient pumping or non-pumping well.

4.12. Concluding Remarks

The advanced expert system presented in this chapter simulates the groundwater pollution potential at a receptor well from land application of manure. The primary objective of the advanced expert system is to evaluate nutrient transport as an integrated problem; that is, all the modules are linked following the path of the nutrient transport. The pollution potential is evaluated at the final stage based on the predicted nutrient concentration at the receptor well and on the possible health risk from that contamination.

In addition, the advanced expert system uses more advanced scientific concepts in the two transport modules than the simple expert system. A numerical model is used for simulating nutrient transport through the vadose zone. Nutrient transport from a non-point source is considered in the saturated zone module, while the same module for the simple expert system used a single point source. Furthermore, a health risk module evaluates the pollution potential from exposure to the nutrients. The advanced expert system can be used if more site specific hydrogeologic and water quality data are available.

References

Carsel, R. F., and R. S. Parrish. 1988. Developing joint probability distributions of soil water retention characteristics. *Water Resources Research.* 24(5):755-769.

Fetter, C. W. 1999. *Contaminant Hydrology.* Prentice-Hall, NJ.

Healthcentral. 2004. General Health Encyclopedia, Height and Weight Tables. Retrieved, March 04, 2004. <http://www.healthcentral.com/mhc/top/001938.cfm>.

Richards, L. A. 1928. The usefulness of capillary potential to soil-moisture and investigators. *Journal of Agricultural Research.* 37:719-742.

Simunek, J., K. Huang, and M. T. Van Genuchten. 1998. The HYDRUS code for simulating the one-dimensional movement of water, heat, multiple solutes in variably saturated media. Version 6.0. Research report no. 144. U. S. Salinity Laboratory. Riverside, CA.

USEPA. 1989. Risk assessment guidance for superfund, EPA/540/1-89/001. U.S. Environmental Protection Agency, Washington, DC.

USEPA.1999. National recommended water quality criterion. EPA 822-Z-99-001. U.S. Environmental Protection Agency, Washington, DC.

Van Genuchten, M. T. 1980. A closed-form equation for predicting the hydraulic conductivity of unsaturated soils. *Soil Science Society of America Journal.* 44:892-898.

APPENDICES

Appendix A: Manure Nutrient Content

Table A.1. Nitrogen and phosphorus content in manure for different animals.

Animal Types	Manure Production Factor (Tons/AU†)	Animals per AU	Manure Recovery Factor	Manure Nitrogen content after losses (lbs/Ton)	Manure Phosphorus content after losses (lbs/Ton)
Calves/Steers/Bulls (K807)	10.59	1.64	0.80	3.30	2.86
Beef Cows (K812)	11.50	1.00	0.80	4.39	2.86
Dairy Cows (K805)	15.24	0.74	0.65	4.30	1.65
Hogs (breeding) (K816)	6.11	2.67	0.75	3.32	3.62
Hogs on Feed (K817)	14.69	9.09	0.75	2.82	2.80
Layer Chicken (K892)	11.45	250.0	1.00	18.46	8.50
Broiler Chicken (K898)	14.97	455.0	1.00	16.10	6.61
Turkeys (breeding) (K902)	9.12	67.0	0.80	11.2	11.23
Heifers, & Heifer Calves (K806)	12.05	1.82	0.65	1.82	1.10

Source: Lander et al. (1998); † Animal Unit

Appendix B: Nutrient Application Rates for Crops, Hays and Forages

Table B.1 shows nutrient (nitrogen and phosphorus) application rates for thirty-six crops (Lander and Mofitt, 1996). The original source of the data is USDA National Agricultural Statistic Service (NASS). USDA Natural Resources Conservation Service (NRCS) has conducted the calculation to find the average values from thirty-four selected crops. For each crop, except Lima Bean and Durum Wheat, average, minimum and maximum nutrient application rates are reported by Lander and Moffitt (1996). For Lima Bean and Durum Wheat only the average nutrient application rates are reported. Minimum and maximum values for these crops are approximated by applying the mean differences with the average values for the crops of same group.

Table B.2 shows nutrient application rates for some hays and forages. The database is prepared from different sources. Nutrient contents in pounds per ton for each crop, except Bluestem and Tall Fescue, are obtained from NRCS's National Agronomy Manual. For Bluestem and Tall Fescue only nitrogen contents are reported in the NRCS manual. Phosphorus contents for those crops are calculated by dividing the respective nitrogen contents by 7.2, which is the stoichiometric mass ratio of nitrogen and phosphorus in plant biomass (Nultsch, 1971). Average, minimum and maximum yields in tons per acre are collected from different USDA extension services and USDA-NASS. For example, yield data for Alfalfa are collected from USDA-NASS online database for all states. Yield data for Bermudagrass are collected from Oklahoma Cooperative Extension Service fact sheet F-2584. Yield data for Bluestem are collected from Oklahoma Cooperative Extension Service fact sheet F-2568 and from Ohio State University Extension fact sheet AGF-022-95. To be conservative, lower values for

average, minimum and maximum are selected from the two sources. Yield data sources for the others hays and forages are listed as footnote of Table B.2. It should be noted that the fact sheets of Oklahoma Cooperative Extension Service start with the letter 'F'.

Table B.1. Nutrient application rates for common crops

Crops	N_{crop} (lb/acre)			P_{crop} (lb/acre)		
	Avg	Min	Max	Avg	Min	Max
Asparagus	124	63	215	66	37	139
Beans, lima (fresh)	98	64†	153†	52	29†	104†
Beans, snap (fresh)	82	43	120	87	62	111
Beans, snap (processed)	64	35	136	64	42	141
Broccoli	233	149	275	99	90	222
Cabage (fresh)	155	88	186	111	71	144
Cabage (processed)	103	36	114	83	79	92
Cantaloupe	105	66	138	102	92	125
Carrots	234	41	276	187	71	219
Cauliflower	260	80	283	125	38	240
Celery	157	97	371	230	129	237
Corn, grain or silage	129	78	160	57	37	77
Corn, sweet (fresh)	119	67	180	88	53	103
Corn, sweet (processed)	135	110	241	63	37	134
Cotton, upland	88	66	131	48	44	86
Cucumbers (fresh)	120	51	439	80	37	99
Cucumbers (processed)	86	69	185	66	45	175
Eggplant	191	189	198	124	121	133
Green peas (processed)	33	26	101	57	42	153
Lettuce, head	230	32	329	163	51	267
Lettuce, other	186	88	390	108	79	295
Melons, honeydew	80	57	156	61	49	141
Melons, water	126	65	270	86	54	116
Onions, dry	185	92	305	129	86	195
Peppers, bell	208	81	254	113	78	153
Potatoes, Irish	200	90	308	159	66	246
Rice	133	111	143	44	40	45
Soybean	31	12	44	47	31	74
Spinach (fresh)	119	79	152	80	75	95
Spinach (processed)	212	173	231	115	67	165
Strawberries	189	32	280	85	59	116
Tomatoes (fresh)	167	72	187	113	67	163
Tomatoes (processed)	155	66	157	93	75	125
Wheat, durum	51	21†	83†	26	12†	46†
Wheat, spring	57	28	86	29	24	34
Wheat, winter	66	35	101	38	16	73

Source: Lander and Moffitt (1996); †Approximated

Table B.2. Nitrogen and phosphorus application rates for common hays and forages

Hays and Forages	N_{crop}	P_{crop}	Yield (ton/acre)			N_{crop} (lb/acre)			P_{crop} (lb/acre)		
	(lb/ton)	(lb/ton)	Avg	Min	Max	Avg	Min	Max	Avg	Min	Max
Alfalfa	50.4 [a]	4.72 [a]	3.47 [h]	1.7 [h]	8.3 [h]	175	85.6	418	16.4	8.02	39.2
Bermudagrass, Hardie	25 [a]	3.46 [a]	6.3 [b]	3.7 [b]	9.3 [b]	158	92.5	233	21.8	12.8	32.2
Bermudagrass, Midland	25 [a]	3.46 [a]	6.0 [b]	3.2 [b]	8.0 [b]	150	80.0	200	20.8	11.1	27.7
Bermudagrass, Tifton	25 [a]	3.46 [a]	6.6 [b]	3.9 [b]	9.0 [b]	165	97.5	225	22.8	13.5	31.1
Bluestem	16 [a]	2.2 [g]	2.43 [f]	1.15 [f]	3.7 [c]	35.2	18.4	59.2	5.35	2.53	8.14
Clover, red	40.2 [a]	4.1 [a]	2.5 [e]	2.0 [e]	3.0 [e]	101	80.4	121	10.3	8.2	12.3
Clover, white	55.8 [a]	6.36 [a]	2.25 [e]	2.0 [e]	2.5 [e]	126	112	140	14.3	12.7	15.9
Orchard grass	30.6 [a]	4.52 [a]	3.0 [f]	1.64 [f]	5.69 [f]	91.2	50.2	174	13.6	7.41	25.7
Rye grass	25.7 [a]	5.07 [a]	2.3 [c]	1.5 [c]	3.0 [c]	59.1	38.6	77.1	11.7	7.61	15.2
Sorghum/Sudangrass	8.2 [a]	1.5 [a]	3.83 [d]	2.5 [d]	5.0 [d]	31.4	20.5	41.0	5.75	3.75	7.5
Tall Fescue	27.2 [a]	3.8 [g]	2.65 [c]	1.7 [c]	3.5 [c]	72.1	46.2	95.2	10.1	6.46	13.3
Vetch, hairy	61.5 [a]	6.15 [a]	1.25 [e]	1.0 [e]	1.5 [e]	76.9	61.5	92.3	7.69	6.15	9.23

[a] NRCS (National Agronomy Manual); [b] F-2583; [c] F-2568; [d] F-2559; [e] F-2584; [f] AGF-022-095; [g] Approximate; [h] USDA-NASS

Appendix C: Well Function

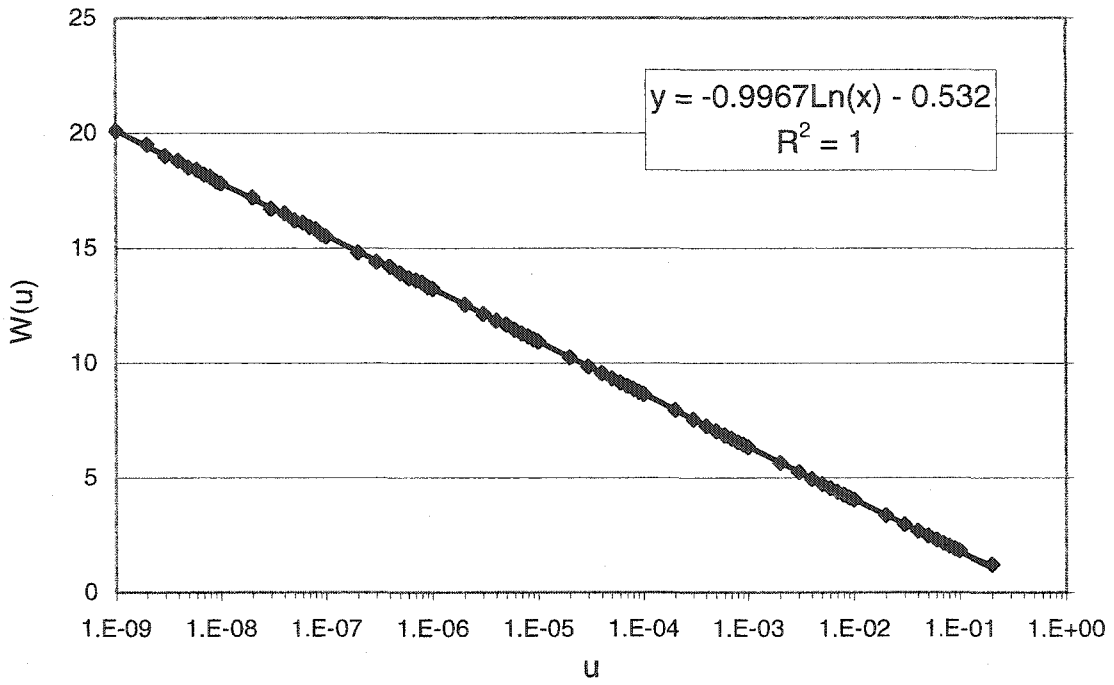


Figure C.1. Regression equation of Theis well function for 1e-8 < u ≤ 0.2

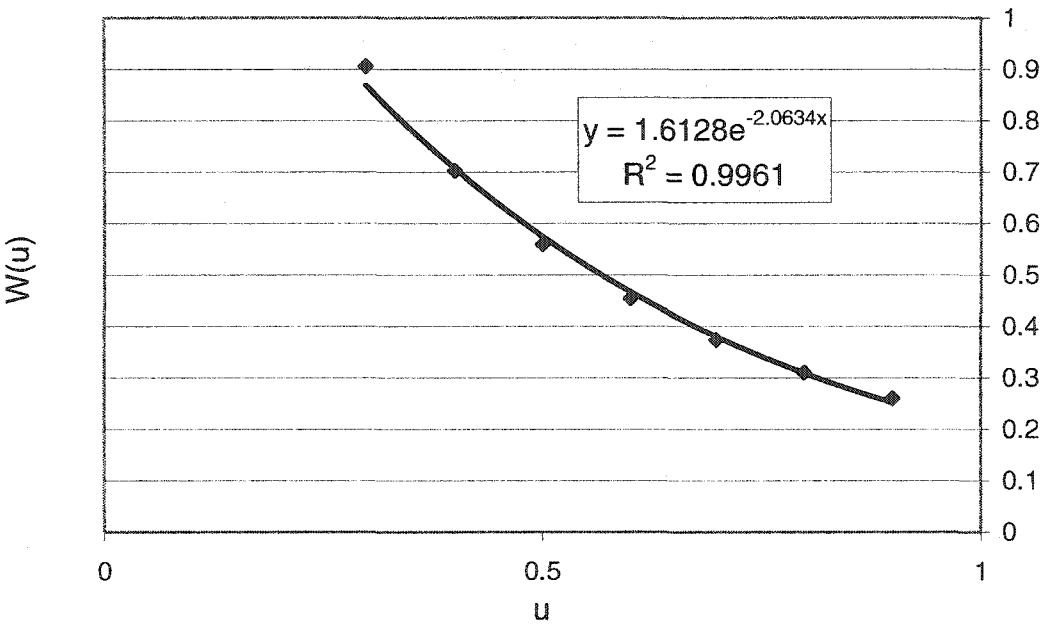


Figure C.2. Regression equation of Theis well function for 0.2 < u <1

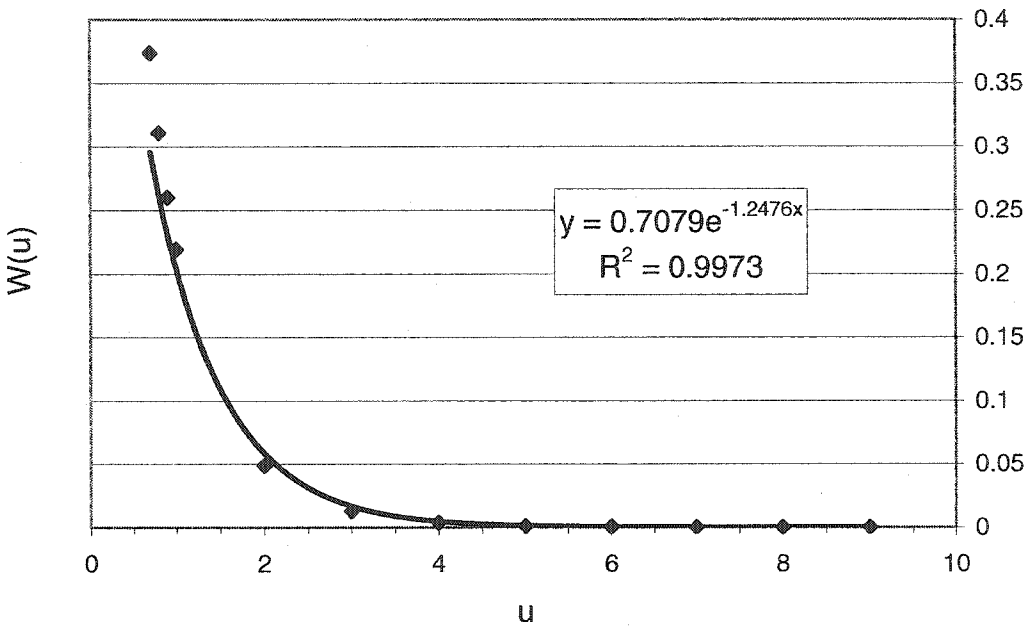


Figure C.3. Regression equation of Theis well function for $1 \leq u \leq 9$.

Appendix D: Limiting Source Dimensions for Analytical Point Source Model

The analytical solutions of the ADE for instantaneous point and finite sources at the center of the plume i.e., at ($v_x t$, 0,0) and at time equal to 't' can be written as Equations D.1 and D.2, respectively.

$$C(v_x t,0,0,t) = \frac{M/n}{8(\pi t)^{3/2}\sqrt{D_x D_y D_z}} \tag{D.1}$$

$$C(v_x t,0,0,t) = \frac{M/n}{X_S Y_S Z_S}\left[erf\left(\frac{X_S/2}{2\sqrt{D_x t}}\right)\right]\left[erf\left(\frac{Y_S/2}{2\sqrt{D_y t}}\right)\right]\left[erf\left(\frac{Z_S/2}{2\sqrt{D_z t}}\right)\right] \tag{D.2}$$

For the analytical point and finite source models to present equivalent concentration at the center of the plume, Equations D.1 and D.2 should be equal. Equation D.3 represents the condition when the point source and the finite source models are equivalent. Equation D.3 can be divided into three equations (Equations D.4, D.5, and D.6) representing probability density functions representing each dimension.

$$\begin{aligned}&\frac{1}{2\sqrt{\pi D_x t}}\times\frac{1}{2\sqrt{\pi D_y t}}\times\frac{1}{2\sqrt{\pi D_z t}}\\ &=\frac{1}{X_S}\left[erf\left(\frac{X_S/2}{2\sqrt{D_x t}}\right)\right]\times\frac{1}{Y_S}\left[erf\left(\frac{Y_S/2}{2\sqrt{D_y t}}\right)\right]\times\frac{1}{Z_S}\left[erf\left(\frac{Z_S/2}{2\sqrt{D_z t}}\right)\right]\end{aligned} \tag{D.3}$$

$$\frac{1}{2\sqrt{\pi D_x t}} = \frac{1}{X_S}\left[erf\left(\frac{X_S/2}{2\sqrt{D_x t}}\right)\right] \tag{D.4}$$

$$\frac{1}{2\sqrt{\pi D_y t}} = \frac{1}{Y_S}\left[erf\left(\frac{Y_S/2}{2\sqrt{D_y t}}\right)\right] \tag{D.5}$$

$$\frac{1}{2\sqrt{\pi D_z t}} = \frac{1}{Z_S}\left[erf\left(\frac{Z_S/2}{2\sqrt{D_z t}}\right)\right] \tag{D.6}$$

By replacing the error function with its series distribution, Equation D.4 can be rewritten as,

$$\frac{1}{2\sqrt{\pi D_x t}} = \frac{1}{X_S}\frac{2}{\sqrt{\pi}}\left[\left(\frac{X_S/2}{2\sqrt{D_x t}}\right) - \frac{1}{3\cdot 1!}\left(\frac{X_S/2}{2\sqrt{D_x t}}\right)^3 + \frac{1}{5\cdot 2!}\left(\frac{X_S/2}{2\sqrt{D_x t}}\right)^5 - \ldots\ldots\right] \tag{D.7}$$

It is evident from Equation D.7 that the left side of this equation is exactly equal to the first term in the right side. Therefore, it can be concluded that the analytical point source model is equivalent to the analytical finite source model when the error function in the finite source model is equal to the linear term of its series distribution.

$$\left[erf\left(\frac{X_S/2}{2\sqrt{D_x t}}\right)\right] = \frac{2}{\sqrt{\pi}}\left(\frac{X_S/2}{2\sqrt{D_x t}}\right) \tag{D.8}$$

Similarly,

$$\left[erf\left(\frac{Y_S/2}{2\sqrt{D_y t}}\right)\right] = \frac{2}{\sqrt{\pi}}\left(\frac{Y_S/2}{2\sqrt{D_y t}}\right) \tag{D.9}$$

$$\left[erf\left(\frac{Z_S/2}{2\sqrt{D_z t}}\right)\right] = \frac{2}{\sqrt{\pi}}\left(\frac{Z_S/2}{2\sqrt{D_z t}}\right) \tag{D.10}$$

A graphical representation of the error function (Figure D.1) shows that the error function is linearly proportional to the independent variable at very small values. Therefore, the point source and the finite source model will generate equivalent result as

long as the error function in the finite source model varies linearly with the independent variable (i.e., when erf(x) ≈ x). From trial and error, it is found that the erf(0.17) is less than 1% smaller than 0.17. Therefore, Equations D.8 to D.10 satisfy with less than 1 percent error, when

$$\left(\frac{X_S/2}{2\sqrt{D_x t}}\right) or, \left(\frac{Y_S/2}{2\sqrt{D_y t}}\right) or, \left(\frac{Z_S/2}{2\sqrt{D_z t}}\right) \le 0.17 \qquad \text{(D.11)}$$

Equation D.11 can be used to find the dimension of a source (X_S, Y_S, and Z_S) for the analytical point source model. Since the comparison is at the center of the plume, the variable 't' can be replaced by 'x/v_x' in Equation D.11. Since the error function is about 1% less than the independent variable when the latter is equal to 0.17, each source dimension obtained from Equation D.11 produces 1% error for the point source model. Therefore, the three-dimensional point source model with the source dimension obtained from Equation D.11 results about 3% [= $100\times(1.01^3 - 1)$%] higher concentration than the finite source model. In order to reduce the total error to 1 percent, error produced by each source dimension should be 0.33% [= $100\times(1.01^{1/3} - 1)$%]. For the error function to produce 0.33% smaller value than the independent variable, the latter should be equal to 0.10. Therefore, for less than 1% total error from the point source model, the source dimensions need to satisfy the following equation.

$$\left(\frac{X_S/2}{2\sqrt{D_x \frac{x}{v_x}}}\right) or, \left(\frac{Y_S/2}{2\sqrt{D_y \frac{x}{v_x}}}\right) or, \left(\frac{Z_S/2}{2\sqrt{D_z \frac{x}{v_x}}}\right) \le 0.10 \qquad \text{(D.12)}$$

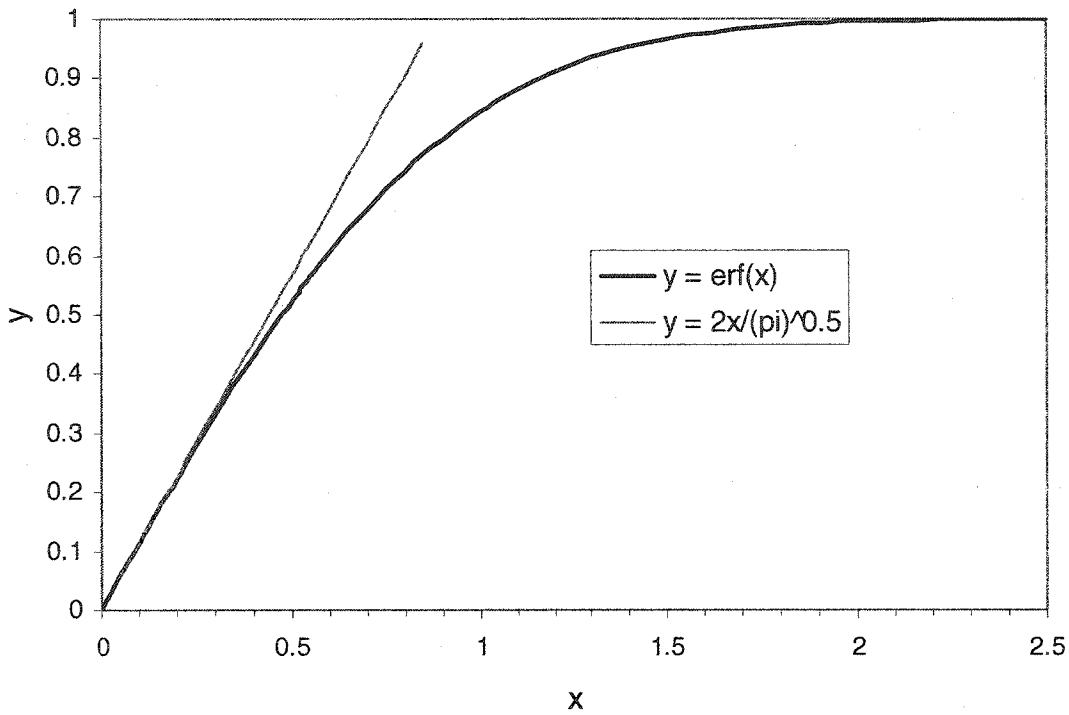


Figure D.1 Graphical representation of error function

Appendix E: Performance of the Green-Ampt Model in Estimating Flow through the Vadose Zone

Ahsanuzzaman, A. N. M., and Kolar, R. L.

Proceedings of the 22nd annual AGU hydrology days, Colorado State University, Fort Collins, CO. April 2002.

Abstract

Herein, the Green-Ampt model is compared with HYDRUS (a numerical model) to estimate the vertical distance traveled by a wetting-front through the vadose zone. Both the Green-Ampt (GA) model and HYDRUS are compiled for two soil types with largely different permeability (sand and clay loam) under identical sets of initial and boundary conditions. It is found that for sand the GA model predicts 4.6 to 9.8 times deeper penetration of the wetting-front than HYDRUS within 3 days, while for clay loam the GA model predicts 1.5 to 14.5 times higher values within 50 days. Performance of the GA model improves when the initial moisture content is closer to the saturation point.

E.1. Introduction

Green and Ampt (1911) derived the first physics-based equation for infiltration of water into soil (Ravi and Williams, 1998). Because of its simplicity and the requirement of fewer hydraulic parameters, the Green-Ampt (GA) model is widely used to estimate

infiltration in many hydrologic models (Freyberg et al., 1980). More sophisticated models for infiltration e.g., the models based on the nonlinear Richards (1931) equation, are available (Hogarth et al., 2001). However, it is sometimes impractical and inefficient to use the models based on the Richards equation in hydrological problems due to the requirement of more information on soil hydraulic parameters (Ravi and Williams 1998) and more computational time. Since the GA model is simple and requires minimal computational time, it would be useful for estimating flow through the vadose zone. However, the performance of the GA model should be studied before using the model in estimating flow through the vadose zone. Therefore, this study focuses on studying the difference between the GA model and a more advanced model based on the Richards equation, called HYDRUS (Simunek et. al.,1998).

E.2. Materials and Methods

The Green and Ampt (1911) model is compared with (Simunek et. al., 1998), a numerical model based on the Richards equation, to study the performance in estimating flow through the vadose zone. The flow parameter used for the comparison is the distance traveled by the wetting front through the vadose zone. Green and Ampt (1911) assume a piston-type water content profile with a well-defined wetting-front. For the piston-type profile, the soil is saturated (volumetric water content, θ_s) from the soil surface to the wetting-front. At the wetting-front, the water content drops abruptly to the initial water content (θ_0). Thus, the soil water potential at the wetting-front (h_f) is the matric potential for the initial water content. At the soil surface, the water potential is equal to the depth of the water accumulated on the soil surface (h_s) (see Figure E.1).

At any time t, if the depth of penetration by the wetting-front is 'H', the infiltration rate from applying Darcy's law is

$$Q = \frac{\partial I}{\partial t} = - K_s \left(\frac{h_f - (h_s + H)}{H} \right) \qquad \text{(E.1)}$$

where, Q = infiltration rate, I = cumulative infiltration at time t, K_s = saturated hydraulic conductivity, and H = distance traveled by the wetting-front.

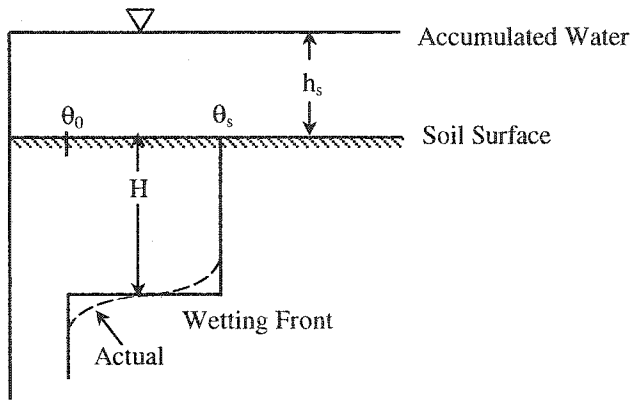


Figure E.1. Piston-type wetting-front for GA model

For piston-type wetting-front, $I = H (\theta_s - \theta_0)$. Integrating Equation E.1 for time t, Equation E.2 is obtained. Equation E.2 is the GA model for estimating the depth of penetration by the wetting-front (H). With the input of soil hydraulic parameters in Equation E.2, 'H' at any time 't' can be obtained from trial and error.

$$H = \frac{K_s t}{(\theta_s - \theta_0)} - (h_f - h_s) \log_e \left[1 - \frac{H}{(h_f - h_s)} \right] \qquad \text{(E.2)}$$

HYDRUS is a Galerkin linear finite element model, developed by the United States Salinity Laboratory, for simulating water, heat and solute transport in one-

dimensional variably saturated media. HYDRUS solves the Richards (1928) equation for variably saturated water flow and advection-dispersion equation for heat and solute transport. Richards (1928) equation for flow through vadose zone is a physics-based equation. It is based on Darcy's law combined with the equation of continuity. Richards equation for flow in vertical direction is given by

$$\frac{\partial \theta}{\partial t} = \frac{\partial}{\partial z}\left(K(\theta)\frac{\partial h(\theta)}{\partial z}\right) - \frac{\partial (K(\theta))}{\partial z} \qquad \text{(E.3)}$$

where, θ is volumetric water content and $K(\theta)$ and $h(\theta)$ are unsaturated hydraulic conductivity and suction potential as function of θ, respectively.

Both models are run for an identical set of initial and boundary conditions for comparison. Each model is run for two different soil types: one with very high permeability (sand) and the other with very low permeability (clay loam). Equation E.2 is used to determine the distance traveled by the wetting front (H) from the GA model, which is iterated until the values converge within one percent. The input parameters for Equation E.2 are obtained from literature or assumed where appropriate. K_s and θ_s for sand and clay loam are obtained from Carsel and Parrish (1988) (Table E.1). Water potential at the soil surface (h_s) is assumed to be 7.62 cm (3 inches). Several values of water potential at the wetting-front (h_f) are chosen to cover the practical range of matric potential for each soil type. The practical range of matric potential of each soil type is selected from field data collected by the Oklahoma Mesonet, a network of 76 environmental monitoring stations in Oklahoma. The initial water content (θ_0) for each value of h_f is obtained from compiling HYDRUS, which has a parameter optimization

module to estimate the water retention curve and uses that to get moisture content for any matric potential value.

HYDRUS is compiled for head type boundary at the top surface and free drainage boundary at the bottom surface. The head at top surface is set to 7.62 cm (3 inches), which is the h_s value used in the GA model evaluation. Initial head throughout the soil profile is considered to be constant at h_f, the value used in the GA model evaluation. Also, Van Genuchten's five-parameter model (Van Genuchten, 1980) is used for soil hydraulic properties. Values for the parameters (K_s, θ_s, θ_r, α, and n) are obtained from Carsel and Parrish (1988) (Table E.1).

E.3. Results and Discussion

Tables E.2 and E.3 show the output from the GA model and HYDRUS for the sand and clay loam, respectively for a range suction heads at the wetting front. It is found that the GA model predicts higher values of 'H' than HYDRUS for both sand and clay loam. For sand, the GA model predicts 4.6 to 9.8 times higher value (i.e., deeper penetration) than HYDRUS within 3 days, while for clay loam the prediction is 1.5 to 14.5 times higher within 50 days. It is interesting to note from Tables 2 and 3 that prediction from the GA model gets closer to that of HYDUS when the initial moisture content is higher. This result shows that near the saturation point, the performance of the GA model improves when compared to the output from HYDRUS. Thus, following heavy rainfall events, the GA model might give acceptable result in estimating flow through the vadose zone. However, it should be noted that fine grain soils take longer to reach the saturation point, and a given rainfall event might not be long enough to saturate

the soil. In such cases, field saturated moisture content could be used in Equation E.2, which is usually smaller than the laboratory measured saturated moisture content (Table E.1). Using field saturation value in the GA model would lower the prediction of 'H' (Equation E.2), and thus reduce the error with respect to HYDRUS.

E.4. Conclusion and Recommendation

The GA model over-predicts the flow through the unsaturated soil, compared to HYDRUS for the two soils tested. The prediction by the GA model is higher due to the assumption of complete saturation at the wetting-front (Figure E.1). However, the GA model performance improves for higher initial moisture content. Thus, the GA model may be reasonably used in hydrological analyses after heavy rainfall events. With the advancement of computer processing speed and improved knowledge of soil hydraulic properties, it is not inconceivable that the use of the GA model will be limited in future hydrological analysis.

Table E.1. Unsaturated soil hydraulic parameters of clay loam and sand

Soil Type	θ_r	θ_s	n	α	K_s (cm/d)
Clay Loam	0.095	0.41	1.31	0.019	6.24
Sand	0.045	0.43	2.68	0.145	713

Source: Carsel and Parrish (1988)

Table E.2. Comparison between GA model and HYDRUS for sand

h_f (cm)	θ_0	Time (day)	H		
			HYDRUS (cm)	GA Model (cm)	GA/HYDRUS
-200	0.046	1	310.50	2492	8.0
		2	534.00	4500	8.4
		3	658.00	6450	9.8
-100	0.049	1	315.00	2339	7.4
		2	543.00	4312	7.9
		3	662.00	6246	9.4
-20	0.108	1	414.00	2531	6.1
		2	774.00	4805	6.2
		3	984.00	7055	7.2
-10	0.216	1	784.00	3655	4.7
		2	1532.00	7042	4.6
		3	2196.00	10406	4.7

Table E.3. Comparison between GA model and HYDRUS for clay loam

h_f (cm)	θ_0	Time (day)	H		
			HYDRUS (cm)	GA Model (cm)	GA/HYDRUS
-10000	0.157	1	60.00	720	12.0
		5	199.50	1659	8.3
		10	317.50	2396	7.5
		15	343.50	2982	8.7
		20	358.50	3489	9.7
		50	403.50	5839	14.5
-5000	0.172	1	62.25	533	8.6
		5	209.25	1242	5.9
		10	336.00	1810	5.4
		15	365.25	2268	6.2
		20	382.50	2669	7.0
		50	434.25	4569	10.5
-1000	0.221	1	72.75	289	4.0
		5	251.25	710	2.8
		10	419.25	1076	2.6
		15	467.25	1385	3.0
		20	495.75	1667	3.4
		50	586.00	3113	5.3
-500	0.25	1	81.00	238	2.9
		5	287.25	612	2.1
		10	489.75	952	1.9
		15	559.00	1249	2.2
		20	596.00	1525	2.6
		50	724.00	3002	4.1
-200	0.296	1	103.50	212	2.0
		5	379.50	589	1.6
		10	662.00	961	1.5
		15	790.00	1302	1.6
		20	857.00	1627	1.9
		50	1090.00	3445	3.2

References

Carsel, R. F., and R. S. Parrish. 1988. Developing joint probability distributions of soil water retention characteristics. *Water Resources Research.* 24(5):755-769.

Freyberg, D. L., J.W. Reeder, J. B. Franzini, and I. Remson. 1980. Application of the Green-Ampt model to infiltration under time-dependent surface water depths. *Water Resources Research.* 16(3):517-528.

Green, W. H. and C. A. Ampt. 1911. Studies on Physics I. The flow of air and water through soils, *Journal of Agricultural Science.* IV (Part I):1-24.

Hogarth, W. L., C. W. Rose, T. S. Steenhuis, and J. Y. Parlange. 2001. Historical and recent developments in the mathematical modeling of infiltration in hydrology, *Proceedings of the 21st annual AGU hydrology days.* Colorado State University, Fort Collins, CO.

Ravi, V. and J. Williams. 1998. Estimation of infiltration rate in the vadose zone: compilation of simple mathematical models. EPA/600/R-97/128a. Subsurface protection and remediation division. Ada, OK.

Richards, L. A. 1931. Capillary conduction of liquids through porous medium. *Physics*, I. 318-333.

Simunek, J., K. Huang, and M. Th. Van Genuchten. 1998. The HYDRUS code for simulating the one-dimensional movement of water, heat, and multiple solutes in variably-saturated media. Version 6. Research Report No. 144. U.S. Salinity Laboratory. Riverside, CA.

Van Genuchten, M. Th. 1980. A closed-form equation for predicting the hydraulic conductivity of unsaturated soils. *Soil Science Society of America Journal.* 44:892-898.

Appendix F: Software Availability

The software, NPATH, is available from the author or the Oklahoma Conservation Commission (OCC), who provided the initial funding for this product. Currently, the software is in review by the agency. Following the review, the software is expected to be distributed from OCC's official web page.

Neither the developers of the expert systems nor the University of Oklahoma assume any legal liability or responsibility for the accuracy, completeness, or usefulness of any information, product, or process disclosed in this dissertation.

Author's Contact Address

Abu Noman M. Ahsanuzzaman
Phone: (405) 250-3556 or, (580) 436-8587
Email: noman@ou.edu; ahsanuzzaman@sbcglobal.net